COMPUTER VISION-BASED AUTOMATIC FABRIC DEFECT DETECTION MODELS FOR THE TEXTILE AND APPAREL INDUSTRIES

TONG LE

Ph.D

The Hong Kong Polytechnic University

2017

The Hong Kong Polytechnic University

Institute of Textiles and Clothing

Computer Vision-based Automatic Fabric Defect Detection Models for the Textile and Apparel Industries

Tong Le

A thesis submitted in partial fulfillment of the requirements

for the degree of Doctor of Philosophy

November 2016

CERTIFICATE OF ORIGINALITY

I hereby declare that this thesis is my own work and that, to the best of my knowledge and belief, it reproduces no material previously published or written, nor material that has been accepted for the award of any other degree or diploma, except where due acknowledgement has been made in the text.

_____(Signed)

Tong Le (Name of student)

TO MY FAMILY

For their constant love, support and encouragement

Abstract

Faced with increasingly fierce market competition, textile and apparel enterprises need to control cost and improve the quality of their products in the manufacturing stage. Fabric quality inspection plays an important role in this stage because locating possible fabric defects before cutting is beneficial for reducing raw material waste and ensuring textile product quality. Traditionally, in most textile and apparel companies, fabric quality inspection is performed through a human visual system, which suffers from high labor cost and low effectiveness. Automatic inspection techniques, which can provide intelligent solutions for defect detection without human intervention, are beneficial for improving detection accuracy and efficiency.

Over the past several decades, many computer vision-based defect detection models have been proposed to address the fabric inspection problem. Most existing approaches, such as statistical and structural approaches, rely on feature extractions of fabric defects and normal texture to distinguish possible defects. The difficulty in selecting the appropriate features that can be adapted to different types of fabric texture significantly influenced the effectiveness of these approaches. The primary purpose of this research is to develop effective computer vision-based defect detection models that aims at different types of fabric, such as plain fabric, twill fabric, and striped fabric. Woven fabric with uniform texture is one of the most basic types of fabric, which can be classified as plain fabric and twill fabric according to the fabric weaving structure. On the basis of the analysis of the characteristic of defects in plain and twill fabrics, two distinctive detection models were developed in this research. In addition, another hybrid detection model was proposed for striped fabric, which represents the most basic type of patterned fabric with a single element and is widely used in our daily lives, such as shirts and pants.

Defects on plain fabric can be regarded as uneven edges on a very smooth surface. Thus, an optimal Gabor filter-based detection model was developed for plain fabric inspection. On the basis of a feature analysis of defects, only

two Gabor filters optimized by differential evolutionary algorithm were used to significantly reduce the computational complexity.

With defects regarded as random noise in the image, a defect detection model based on non-local sparse representation was proposed for twill fabric inspection. Through the restoration of non-defective fabric texture on the basis of dictionaries learnt from reference images, defects were successfully segmented from the original inspection fabric images.

To detect the common fabric defects (errors in weaving structure) and pattern defects (repeated pattern variants), a hybrid defect detection model was developed to solve the inspection problem for fabric with a striped pattern. Gabor filters were initially used to detect variants of the repeated pattern and reduce the disturbance caused by the edge of repeated pattern. Sparse representation was adopted to segment the remnant defects in the resultant feature images in the second step.

On the basis of a textile texture database (TILDA) and the amount of real fabric samples acquired from real apparel companies, extensive experiments were conducted to evaluate the performance of the proposed methodologies. Experimental results show that the proposed detection models are effective in detecting various types of fabric defects and are superior to several representative and popular defect detection models.

The results of this research demonstrate that computer vision and artificial intelligence can offer satisfactory performance for the automatic defect detection problems of various types of fabric in the textile and apparel industries. They also reveal that considering the characteristics of different types of fabric texture is of paramount significance to the establishment of a practical fabric inspection model, which is highly sensitive, robust, and efficient.

Acknowledgements

First of all, I would like to express my sincere gratitude to my chief supervisor, Prof. W. K. Wong, for his constructive guidance, advice, and encouragement during this research. His enthusiastic attitude towards research will always motivate me in future endeavors. I also thank my co-supervisor, Dr. C. K. Kwong, for his guidance and many helpful suggestions in this research.

I extend my thanks to my colleagues, Jiajun Wen, Jielin Jiang, Can Gao, and all others for their helps during these three years. I also extend my thanks to my friends, Limei Ji, Yanghong Zhou, and all others for making my stay in PolyU most memorable.

Finally, I am forever indebted to my husband Wei Du, my parents Libo Tong and Ruihua Zhang, my parents-in-law Jun Du and Yidong Xiao. It is their love, support and encouragement which makes this thesis possible.

Contents

List of Figures

List of Tables

Chapter 1

Introduction

1.1 Background

1.1.1 Fabric Inspection in the Textile and Apparel Industries

In the textile and apparel industries, many issues must be considered in the manufacturing stage of production, and fabric quality inspection is one of them. Fabric quality inspection plays an indispensable role in maintaining companies competitive edge in the global market. In weaving mills, fabric quality directly determines the value of the products, and the main and costly raw material of garments influences the cost control of apparel companies. The various types of fabric defects can result in an income loss of $45\% - 65\%$ [1]. The objective of fabric inspection is to locate existing defects and confirm whether the fabric has reached the quality standard.

Fabric quality is affected by yarn quality and loom defects, that is, poor yarns and mechanical faults cause fabric defects. Woven fabric defects can exhibit a variety of forms because of differences in the weaving structures of fabric. At

present, the textile industry has defined more than 70 types of fabric defects [1]. In plain weaving, each weft thread crosses the warp threads by going over one to form a simple flat and smooth criss-cross pattern [2]. Thus, defects on plain fabric are relatively prominent compared with the non-defective fabric structure. Twill weave is regarded as a pattern of diagonal parallel ribs (in contrast with plain weave) formed by floating each weft or filling yarn across the warp yarns in a progression of inter-lacings to the right or left. Therefore, by contrast, defects on twill fabric are normally smaller and less noticeable because of the slightly complicated weaving method. The case of patterned fabrics (e.g., print fabric) is usually significantly more complicated. In addition to the common defects that are likely to be confused with the patterns, defects may occur on the pattern primitive itself or its arrangement. Overall, the diversity of fabric defects makes the fabric quality inspection task greatly difficult and important.

Traditionally, in most apparel companies, fabric inspection still relies on visual checking by trained and experienced operators. However, manual inspection has many limitations, such as low detection accuracy and efficiency. Small defects are difficult to notice, and human errors may occur because of fatigue and inattentiveness, thereby resulting in low success rate of detection. According to some studies [1, 3], the accuracy of human inspection in the textile industry is only approximately $60\% - 75\%$. Moreover, human inspectors usually need to identify the defects on a roll of fabric, which is 1.5 m to 2 m wide and driven with speeds that range from 10 m/min to 50 m/min. Even in the best cases, an expert almost cannot deal with fabrics wider than 1.5 m and moving faster than 20 m/min [4]. Inefficiencies in industrial processes are costly in terms of time, money, and consumer satisfaction. As a result, automatic fabric defect detection techniques are in increasing demand. In automation, fabric defect detection is a quality control process that aims to identify and locate defects. Without manual intervention, the automatic

inspection of an industrial product, which is a prompt, real-time, and accurate modern technology, has gradually become one of the trends of digitizing production to improve product quality and reduce labor cost.

1.1.2 Computer Vision-based Automatic Fabric Inspection

With the advantages of computers and imaging devices, computer vision seeks to develop algorithms that simulate the human visual system and achieve human visual functions. The development of a flexible, efficient, reliable, and integrated real-time vision system for industrial applications is an essential issue in current and future research. Computer vision-based systems have already been proven effective in quality inspections of film, paper, steel roll, and others [5–7]. These objects are classified as uniform materials whose surfaces are even and glossy. The product inspections are usually fulfilled through the contrast between the test object and the reference object owing to the obvious differences between defects and the background. In the textile industry, woven fabric defects refer to any inhomogeneities that appear different from the normal fabric background structure. However, the surface structure of fabric classified as textured material is quite complex because of the diversity of fabric weaving methods. Thus, developing specific defect detection approaches is essentially necessary to effectively address the inspection problem of fabric with different weaving structures.

From the view of computer vision, fabric defect detection is considered a texture analysis problem because fabric surface can be recognized as a two-dimensional (2D) texture that exhibits a high periodicity of sub-patterns. Defects can be considered anomalous arrayed pixels in the image unlike non-defective areas. The aim of an automatic inspection system is to identify the shapes and locations of any possible fabric defect without human intervention. Over the past several decades, with the use of computer vision and pattern

recognition techniques, numerous approaches have been proposed for fabric defect detection.

A majority of studies focused on developing defect detection methods for uniform texture fabric (plain and twill fabric). Gray-level co-occurrence matrix (GLCM) [8], one of the most typical statistical methods, was able to identify fabric defects through an analysis of the gray-level relationship among image pixels. With the advantage of the fact that textile texture is essentially repeated by sub-patterns, template matching approaches [9, 10] provide simple solutions that are easily implemented for fabric defect detection. Fourier transformation [3], wavelet transform coefficients [11], and Gabor filters [12, 13] addressed the fabric defect detection problem in the spectral domain, which can significantly reduce the computational cost. Neural networks (NN) were introduced in fabric inspection as a classifier that could distinguish defects from normal texture [14, 15]. The use of multiple features in defect classification was helpful in increasing detection accuracy. Sparse representation, which was widely used in image denoising, has gained increasing attention in defect detection [16–18]. Defects can be segmented by comparing the original image with its non-defective version, which is estimated through sparse representation.

Most studies only focused on the analysis of the features of fabric defects but not on the structural differences between fabric types. Therefore, the detection models did not show a stable performance on the various types of fabric defect detection problems. For example, GLCM was useful in detecting defects on simple textured materials, such as plain fabric, because the disturbance of the gray-level distribution of such fabric is large enough to be identified. However, the computational cost made the efficiency of this method unsuitable for real-time application in the industrial environment. Although template matching approaches were suited to the inspection of fabric with a regular texture, the detection accuracy was not significantly

increased because of the strict alignment requirements of the methods. In other words, the detection efficiency was also influenced in real-time application in the textile and apparel industries. In the textile and apparel industries, the requirements of the inspection of plain and twill fabric are distinguished. The speed requirement of the plain fabric inspection is high because the appearance probability of defects on plain fabric is significantly lower than that on other types of fabric because of the simple weaving structure. Without considering the advantages of the simple weaving orientation characteristic, the computational cost of most existing detection approaches was large while improving the detection accuracy. By contrast, the blurriness of the boundaries of some defects on twill fabric with diagonal ribs-like weaving structure causes difficulty in accurately locating the defects barely through the feature extractions of defects in either the spatial or spectral domain. Therefore, the primary goal of twill fabric inspection is to ensure detection accuracy. Although NN-based approaches were superior to others in detecting defect classification, the detection accuracy largely depended on the amount of training data (defective fabric samples). However, detection was nearly impossible because of the excessive types of fabric defects, and new ones always emerged. Currently, even for uniform texture fabric, the fabric defect detection problem is still a research difficulty because of the diversity of fabric textures and fabric defects.

In patterned fabric inspection, with fabric printed pattern regarded as the underlying lattice, some motif-based defect detection approaches employed the characteristics of the smallest repeated unit in the fabric image [19, 20]. Learning the distribution of the statistical features of the image motif, which constitutes the underlying lattice of the patterned texture, could amplify the defect information of the defective motif. In theory, motif-based approaches can address the detection of common fabric defects and pattern defects simultaneously. However, the efficiency of these methods in defect detection

of the basic type of patterned fabric with a single element, such as striped fabric, is low because considerable computational work would be wasted in the motif extraction. In fabrics with complex patterns, such as floral patterns, small defects may be missed because of their insignificant influence on the overall lattice of the patterned texture. Therefore, specific analysis of different designed patterns in the inspection of patterned fabric is necessary.

To effectively address the automatic fabric defect detection problem in the textile and apparel industries, the most feasible solution is to develop different detection approaches for different fabric types, according to the specific fabric texture. Therefore, for the first time in this research, the automatic fabric inspection problem will be investigated on the basis of the specific analysis of fabric weaving structure. Three different defect detection models will be developed for plain fabric, twill fabric, and striped fabric. The proposed detection models are expected to achieve high detection accuracy and efficiency.

1.2 Problem Statement

Without effective automatic fabric defect detection, the product quality and productivity of garment manufacturing is significantly influenced. So far, the existing detection models have not obtained satisfactory results in the real environment of the textile and apparel industries despite many studies conducted in the related research area. As discussed in Section 1.1, the existing studies related to fabric defect detection did not consider the difference between the weaving structure of types of fabric, sacrificing detection accuracy (sensitivity) or robustness in attempting to adapt to most fabric types. With the use of computer vision and image processing techniques, this research investigates the automatic fabric defect detection

problem on the basis of specific analysis of fabric weaving structure for the first time, and the analysis is implemented by developing different inspection models for three types of fabric: plain fabric, twill fabric, and striped fabric.

(1) Plain fabric inspection - Owing to the merits of basic criss-cross weaving structure, defects on plain fabric are relatively prominent with respect to the smooth surface texture of background in the image. Moreover, the detection speed requirement is high because the appearance probability of plain fabric defects is significantly lower under the mature weaving technology in today's industry. The problem is that the computational cost of the existing methods is usually excessive, thereby making real-time applications unsuitable in the environment of the industry.

(2) Twill fabric inspection - With the complex structure of twill weaving, defects on twill fabric are normally significantly small and subtle, thereby making the accurate feature extraction of defects difficult. The diagonal rib weaving pattern may also introduce some noise interference in the images, which causes high false alarm rates and influences the robustness of the detection through the use of the existing detection approaches. Therefore, the most challenging problem in this research is simultaneously increasing the detection accuracy and robustness.

(3) Striped fabric inspection - Until now, no existing method has been proposed especially for striped fabric inspection. Unlike uniform texture fabric, in addition to common fabric defects, pattern variants, which refer to the arrangement errors of the primitive unit (stripe), are also important concerns in fabric inspection. Therefore, for striped fabric, investigating a specific detection method that can effectively detect not only common fabric defects but also pattern variants is significant.

1.3 Objectives

This research aims to develop automatic defect detection approaches for plain and twill fabrics and strip patterned woven fabric, which are widely used in our daily lives. On the basis of the specific analysis of each fabric weaving structure, computer vision-based automated defect detection models are proposed for each fabric type. All the proposed detection models are expected to achieve a high detection rate with little false alarm in the specific fabric inspection. The detailed objectives are listed as follows:

(1) This research aims to develop a framework for the defect detection model for plain fabric on the basis of shape and orientation analysis of common defects. With the use of direct feature extraction of plain fabric defects, the proposed detection model is expected to address the detection speed acceleration problem on the premise of high detection accuracy, which means reducing the computational cost of the detection model.

(2) Furthermore, this study aims to investigate and develop a robust defect detection model for twill fabric inspection, which is immune to the disturbance introduced by the special twill weaving texture. The proposed detection model is expected to effectively identify small and subtle fabric defects and to achieve low false alarm rate.

(3) Lastly, this study aims to investigate and develop a hybrid defect detection model for striped fabric on the basis of feature analysis of stripe pattern. The proposed detection model is expected to effectively detect common fabric defects and pattern defects.

1.4 Methodology

This research improves the product quality control of apparel factories by solving automatic fabric inspection problems. According to the distinctive types of fabric structure texture, three different methodologies are developed and described as follows:

(1) Differential evolution-based optimal Gabor filters, which could achieve joint defect localizations in the spatial and spatial frequency domains, were proposed to solve the defect detection of plain fabric. On the basis of the analysis of the particular shape and orientation characteristics of fabric defects, the features of defects were extracted by two Gabor filters (in the horizontal and vertical directions), which could greatly reduce the computational cost. The parameters of the Gabor filters were optimized by differential evolution algorithms to achieve the best discrimination between defects and normal fabric texture.

(2) A defect detection model that consists of image preprocessing, image restoration, and thresholding operation was developed to address the twill fabric inspection problem. The image was initially preprocessed by gray-level transformation to improve the image contrast and make the details of the defects more salient. Defects were labeled by comparing the input image with its estimation, which was restored through sparse representation model based on a learned dictionary. To increase the detection accuracy, the non-local similarities of the fabric structural information were introduced in the sparse coding.

(3) A hybrid defect detection model, which could address the detection of common fabric defects and pattern defects in two steps, was proposed for striped fabric. First, a Gabor filter was optimized to reduce the response of stripe patterns and the corresponding disturbance caused by edge of

stripe patterns. In the following, image restoration-based defect detection techniques were applied in the filtered feature image, which can be treated as uniform texture fabric with remnant defects.

1.5 Significance of this Research

With the use of computer vision-based techniques for fabric inspection, the significance of this research can be summarized in the following four aspects:

(1) A few of the existing detection approaches carefully analyzed the specific characteristics of different fabric types and therefore cannot achieve satisfactory detection results in practical applications. In this research, the fabric inspection problem was addressed based on the analysis of fabric weaving structure for the first time. For plain fabric, twill fabric, and stripe patterned woven fabric, three distinctive automatic detection models were developed, and they effectively improved the overall performance of fabric inspection in the textile and apparel industries.

(2) The three newly proposed distinctive defect detection models solved the problem where a few of the existing approaches can be universally applied to most types of fabric textures and defects. For each specific fabric type, different objectives have been achieved, such as improving the detection efficiency of plain fabric inspection, enhancing detection effectiveness on small twill defects, and solving the detection of two groups of defects on striped fabric.

(3) The optimal Gabor filter-based detection model proposed for plain fabric inspection addressed the computational complexity problem on the premise of high detection accuracy, which makes it applicable for practical application. The sparse representation-based detection model proposed for twill fabric inspection successfully improved detection accuracy and

robustness, especially for the small and blurry defects. Moreover, in this research, a hybrid detection model was specially investigated for striped fabric inspection for the first time, addressing the detection problem of common fabric defects and pattern defects.

(4) In the development of the inspection model for plain fabric, only two optimal Gabor filters were used to extract the features of defects, which improved the feature extraction accuracy and reduced the overall computational cost and the disturbance caused by multi-channel filtering, compared with previous research. In the development of a sparse representation-based detection model for twill fabric, the introduction of non-local similarities of fabric structure information greatly enhanced the detection effect on small defects, and it is superior to the conventional regression representation used in existing studies. The hybrid detection model has taken full advantage of the orientation and frequency features of the stripe pattern, which makes it significantly more effective than motif-based models in industrial applications.

1.6 Structure of this Thesis

The structure of this research can be summarized as follows:

Chapter 2 provides a comprehensive literature review related to automatic fabric defect detection. The existing methods are classified into several categories: statistical, structural, model-based, spectral, learning-based, motif-based, and hybrid detection approaches.

Chapter 3 demonstrates the research methodology in detail, including the concepts and principles of Gabor filters, differential evolution, sparse representation and dictionary learning.

Chapters 4, 5, and 6 investigate the three distinctive defect detection models

for plain fabric, twill fabric, and striped fabric, respectively. The framework of these three models are elaborated in detail. With the use of TILDA database and real fabric samples collected from apparel companies, extensive experiments are conducted to show the effectiveness of the proposed detection models. Moreover, the performance of the proposed models is compared with some representative models.

Chapter 7 summarizes the contributions and limitations of this research. Suggestions for future studies are also provided.

Chapter 2

Literature Review

With the increasing competition in the fashion market, all textile and apparel companies must enhance their competitiveness to maintain their competitive edge in the global market. As a result, automatic fabric inspection techniques used to ensure high-quality products are desperately expected in the textile and apparel industries. They are also beneficial for improving manufacturing productivity and reducing labor cost. Fabric defect detection has been a widely considered research topic for many years. In the past several decades, to achieve better performance, many intelligent detection approaches have been proposed for fabric inspection. On the basis of the analysis of previous surveys on fabric defect detection [1, 21], in this research, the existing defect detection approaches are classified into six categories: statistical, spectral, structural, model-based, learning-based, and hybrid approaches. For the rest of this chapter, each class of approaches is reviewed in detail.

2.1 Statistical Approaches

In the statistical approaches, first-order statistics (e.g., mean and variance) and second-order statistics (e.g., autocorrelation function and co-occurrence

matrices) are used to represent the textural features in texture discrimination. The statistics of non-defective regions are assumed to be stationary, and these regions cover the greatest portion of the images as the background. The defective area is identified as the region that has a distinct statistical behavior from the image background. For example, bi-level thresholding, morphological filters, and gray-level intensity-based approaches distinguish these two areas by detecting the boundaries of image intensity change, whereas fractals and co-occurrence matrices label the pixels that break a specific relationship as defects.

2.1.1 Defect Detection based on Bi-level Thresholding

Bi-level thresholding, which segments high-contrast defects directly through the analysis of gray-level discrimination in an image, is the simplest statistical method for fabric inspection. A high-contrast defect is assumed to cause a significant intensity change in the image, thereby allowing the resultant intensity mount or valley to be identified by thresholding operations.

In [22], two adaptive point-to-point threshold limits, which were determined by first-order statistical parameters of the non-defective fabric images, were adopted to obtain the binary feature image. Thereafter, local averaging was applied to remove the noise caused by non-uniform illumination. In this study, the detection of four basic types of defects, such as horizontal and vertical defects, spots, and wrinkles, was solved.

[4] also adopted bi-level thresholding to address the fabric defect detection problem. To overcome the uneven illumination problem, thresholding limits were computed within a small window of the local area and applied variably to the entire image. However, the proposed methods were applied to some representative defects only, such as the warp float, broken pick, and hole,

which are composed of more than 16 pixels in the image.

The main advantages of bi-level thresholding-based defect detection are low computational cost and easy implementation. However, the detection accuracy of such techniques largely depends on the contrast between the defects and the normal fabric texture. Normally, bi-level thresholding would fail to detect defects that did not alter the average intensity of the image.

2.1.2 Defect Detection based on Mathematical Morphology

Mathematical morphology (MM) is a technique for extracting image components, such as boundaries, skeletons, and convex hulls, by using geometrical structural elements. Basic morphological operators include erosion, dilation, opening, and closing. The geometric representation and description of defects could be well extracted by MM-based detection approaches, which are beneficial for fabric defect classification.

In [23], Fourier transform operations followed by morphological operations were applied for fabric defect detection. Filtered by spatial filters in the optical domain, only the aperiodic image structure was processed by morphological operations, which were conducive to reducing information loss caused by frequency transformation.

In [24], on the basis of the non-defective fabric texture extracted by a trained Gabor wavelet network, the linear structure element was designed for several morphological operations. After processing by an opening and two closing operations, only defective areas remained in the detection results. Defective samples scanned from a defect handbook [25] were used as subjects of the experiments, the results of which revealed that morphological operations were useful for the robustness of the detection model in terms of low false alarm rate. Morphological processing could also be used to adjust the uneven

illumination of images [26]. Erosion and dilation operations were applied on top-hat and bottom-hat filtered images, respectively.

In [27], for denim fabric inspection, morphological operation was adopted to remove the noise in the linear filtered images to reduce the false alarm rate of the detection model. In this study, the effectiveness of the proposed model was evaluated through the detection of five types of defects.

MM was originally developed for binary images. Therefore, [28] applied morphological operations on the bit plane of the images, in which the boundary of the object is more prominent. A series of weighted morphological operations was applied on the lower-order bit planes, which carry more subtle image details.

The main features of the morphological operation-based detection model are its simplicity and effectiveness in reducing false alarm rate by eliminating small discrete points in the results. However, the detection accuracy of tiny defects is also significantly influenced. Moreover, in the binary feature image, distinguishing between the defects and noise is difficult, thereby making the selection of structural element size a challenging task.

2.1.3 Defect Detection based on Gray-level Intensity

Bollinger bands, which were originally proposed for financial technical analysis [29], could enhance the pattern of a trend for a certain period. The principle of Bollinger bands is that periodic upper and lower bands are generated by rows (columns) of the patterned fabric image. Therefore, a defective region causes a prompt and a large variation in the standard deviation of Bollinger bands. In [30], for each row and column in the image, the upper and lower Bollinger bands were calculated based on the mean and variance of the gray-level intensities of the corresponding row and column in

the image. The optimal thresholding limits were obtained from the average of the Bollinger bands of all non-defective reference images. The performance of the proposed method was evaluated through the detection of some obvious defects on dot-patterned, star-patterned and check-patterned fabric samples. For plain and twill fabric inspection, a directional Bollinger bands method was proposed in [31]. Instead of global statistic features, moving average and standard deviation were used to extract the features of defects. Nevertheless, the Bollinger bands computation was applied in four directions for each testing image, significantly increasing the computational cost of the detection model.

Sum and difference histograms (SDH) were developed as an alternative to the usual GLCM, which has a high computational cost [32]. SDH, which is defined as the probabilities of the intensity sum and difference of two pixels, could achieve classification results that are nearly as accurate as those of GLCM. In addition, it could reduce the overall computation time and memory storage requirement. In [33], seven features (e.g., energy, contrast, and entropy) were first extracted from SDH and then processed by a gradient-based searching strategy to detect possible fabric defects.

For the density inspection of yarn-dyed fabric, a mathematical statistics-based two-step detection model was proposed in [34]. In the approximate measurement, yarn density was estimated by counting the peak of the projection curve of the whole image into HSV (Hue, Saturation, Value) mode. Thereafter, the precise measurement was based on the projection curve of the sub-images obtained based on the estimated yarn density. The fabric yarn density was precisely calculated from the probability distribution map of peaks generated from the projection curve of all sub-images.

However, through the aforementioned approaches, the identification of a defective area largely depends on the variation of gray-level value distribution.

In addition, more than one statistical feature is usually needed to achieve better detection results. Therefore, these approaches could not be universally applied to most fabric types and defects.

2.1.4 Defect Detection based on Fractals

Fractals introduced in [35] are capable of characterizing the geometric structures such as coastal lines, mountains, and trees in natural images. In texture analysis applications, fractals are highly useful in representing not only the roughness but also the affine self-similarity of the texture, which can be used to distinguish between smooth and rough regions.

[36] applied estimated fractal dimension (FD) features in fabric inspection. The defect decision depends on the variation of FD. Moreover, the differential box counting method was adopted to reduce computational complexity and enhance the efficiency of the detection model. However, only limited types of defects were involved in the experiments, and the false alarm rate was as high as 28%.

In [37], a Fourier-domain maximum likelihood estimator was derived to estimate the fractal parameter, which could be used in subsequent defect segmentation. Thereafter, the flexibility of the proposed detection method was validated through geometric transformation tests such as rotation, size rescaling, and gray-level shift. However, only three classic types of obvious defects (i.e., stain spot, hole, and warp drop) were detected.

Later, [38] compared the four fractal features-based defect detection method with the single fractal-based method in [37]. It claimed that even different textures may have similar fractal features that are difficult to discriminate. Under different measuring scales, four fractal features were extracted and combined with support vector data description (SVDD) for defect classifi-

cation. In addition to fractal dimension, topothesy, known as an additional fractal feature, was also useful in fabric inspection [39]. However, only four types of defects were subject to the fabric inspection experiments.

The ability to characterize roughness and self-similarity makes fractals effective in detecting the most common defects on smooth surfaces such as plain fabric. However, to improve the detection rate, a certain computational cost is required by extracting additional fractal features, which are unsuitable to applications in the environment of industries.

2.1.5 Defect Detection based on Co-occurrence Matrix

Co-occurrence matrix, which describes the 2D spatial relationship of co-occurring values, is usually applied to measure the texture of fabric images. Various metrics of the matrix can be taken to obtain a useful set of features, such as energy, mean, and variance, which can represent specific characteristics of fabric texture. GLCM has been widely used for texture analysis of wood and fabric [40].

In [8], after decomposition into several sub-bands, the image was divided into non-overlapping patches. Co-occurrence features were extracted from each of the image patches and then used to classify the image patch as defective or non-defective. In [41], under different combinations of the distance between the pixel pair d and the angular relation θ, several GLCM were computed to represent the fabric texture. Therefore, four features (energy, homogeneity, contrast, and correlation) of every GLCM were applied to label the testing image as defective or non-defective according to the dissimilarity between its GLCM features and that of non-defective samples. The performance of the proposed method was evaluated offline through samples collected from websites.

For yarn-dyed fabric defect detection, GLCM, together with autocorrelation function, which is able to extract the minimum repeat unit of the fabric texture pattern, was used to increase the accurate defect detection rate [42]. First, the input image was divided into several non-overlapping patches according to the pattern unit size calculated through autocorrelation function. Second, the Euclidean distance between the GLCM of each patch and that of the template pattern unit was computed to distinguish the defective image patch.

Although second-order statistics are invariant to intensity transformation and are capable of providing more accurate texture information of the image, they require high computational cost, which significantly influences the efficiency of the detection model in industry applications. Furthermore, detection models based on co-occurrence are mainly used to classify the input image as defective or non-defective according to the second-order statistical feature. Therefore, these detection models were unable to correctly detect the accurate location and shape of the defects.

2.2 Structural Approaches

In structural approaches, with the advantage of replicated fabric structure by texture primitives, texture analysis is performed by extracting the texture elements and inferring their replacement rules [43]. Normally, the defects can be distinguished by comparing the inspection image with a template image that represents the non-defective fabric texture. Only a few structural approaches have been proposed because strict standards of the image alignment problem and texture consistency are required in image comparison.

In [44], a texture blob-based detection method was developed for fabric inspection. Texture blobs in different sizes and orientations could uniquely characterize the basic structural elements of the inspection fabric texture.

With the occurrence of local intensity changes caused by fabric defects, the attributes of the blobs would vary. Therefore, defective areas could be distinguished through a comparison of the features of blobs extracted from the non-defective fabric texture and the inspection fabric samples.

[45] first proposed a traditional image subtraction method for defect detection on lace, which comprises a fine and complex pattern of threads. The prototype image, which represents the reference pattern, was extracted from a binary image through correlation function. Closed-loop feedback correction was applied to distinguish real defects from false alarms in the second step because inherent distortions in the lace result in false alarms in direct comparison.

In [10], patterned jacquard fabric defect detection was accomplished by comparing the inspection image with a Golden image, which is subtracted from the non-defective reference image and refers to its pattern unit. The Golden image subtraction is performed from the first pixel of the first row to the end of the last row, similar to a convolution filter. However, the validation of this method is limited only to the fabric defects of holes and thick bars.

Image decomposition, which was optimized through the largest correlation between a non-defective reference image and the inspection image, was applied in patterned fabric defect detection [46]. A fabric image was decomposed into a cartoon structure, which represents the defective object, and a texture structure, which represents the repeat pattern of the fabric. The performance of the proposed method was evaluated on dot-, star-, and box-patterned fabric samples.

Although structural approaches were generally effective in the inspection of fabric with a regular patterned texture, the detection accuracy largely depends on the choice of matching template and alignment render. Moreover, because of the weaving process, many stochastic variations appear in the real fabric samples, and they lead to a high false alarm rate and low efficiency of real-

time applications.

2.3 Model-based Approaches

As a real texture, fabric is regarded as a mixture of stochastic and deterministic components. Texture analysis can be addressed by exploiting the relationships among pixels in the image. Several probabilistic models of the textures have been used for fabric inspection. Autoregressive (AR) model and Markov random field (MRF) are the two common techniques applied in exploiting the relationships among pixels in a textural image. The linear dependence among different pixels in a textural image can be exploited by the AR model. MRF stresses that pixel intensity in an image depends on the neighboring pixels only, and it can combine statistical and structural information in pattern recognition.

A one-dimensional (1D) AR-based detection method was proposed in [47]. Regarded as a 1D series of gray-level fluctuations, the acquired image was treated as a 1D stochastic process. According to the extracted AR coefficients, the pixels, whose gray-level values were predicted to be different from the originals, would be classified as defective. In [48], an unsupervised textured image segmentation algorithm was proposed by using a 2D quarter plane autoregressive model, the parameters of which were first estimated with a probabilistic criterion. Thereafter, the label of distinctive texture was obtained from a maximum a posteriori estimation by using a simulated annealing method.

MRF, which depicts the intensity dependence between neighboring pixels, was able to capture the local contextual information in an image. The proposed detection approach in [49] attempted to model the normal fabric texture by determining the parameters of a predefined MRF model. A

Gaussian MRF (GMRF) was first trained to fit small image patches obtained from non-defective fabric samples. Thereafter, the statistical features were extracted from GMRF and were used as the inputs of the defects classifier. [50] addressed the fabric defect detection problem by using the wavelet-domain hidden Markov tree (HMT) model. The HMT for the wavelet-transformed defect-free template image is modeled using the expectation-maximization (EM) algorithm. Thereafter, the log-likelihood map (LLM) derived from the coefficients of HMT was constructed and used as the measurement of defective samples.

The abovementioned detection approaches are sensitive to small defects owing to their ability to characterize micro-textures according to the local dependence among different pixels in the image. However, they are insensitive to the translation of patterns of the fabric texture because of the lack of depiction and estimation of the global trend of fabric texture and pattern.

2.4 Spectral Approaches

A woven fabric texture is composed of the repetition of some basic texture primitives, which are determined by the specific weaving pattern. With a deterministic rule of displacement of the texture primitives, the fabric surface texture exhibits a high periodicity of sub-patterns, which permits the use of spectral features for the detection of defects. Psychophysical research has also indicated that human visual system analyzes textured images in the spatial frequency domain [21]. Spectral techniques have been the most widely used approaches in fabric defect detection [51–55] because textural features extracted in the frequency domain are less sensitive to noise and intensity variation than in the spatial domain. In general, the techniques involved

in spectral approaches are Fourier transform (FT), wavelet transform (WT), and Gabor transform (GT), which are described in detail in the following subsections.

2.4.1 Defect Detection based on FT

Owing to the high periodicity of weaving patterns, the spatial periodicity of a woven fabric image can be transferred to spatial frequency by fast FT. The spatial domain is usually noise sensitive and arduous in locating defects, while FT uses the frequency domain to characterize the defects. Texture pattern can be extracted by analyzing the frequency spectrum of fabric sample images, although the occurrence of defects changes the corresponding intensity of the frequency spectrum.

In [56], a combination of discrete Fourier transform (DFT) and Hough transform [57] was used for fabric and machined surface inspection. The high-energy frequency components shown in the DFT of the original image were detected by 1D Hough transform and removed to reconstruct a uniform texture image through inverse DFT. The normal fabric texture could be eliminated, and only defects remain in the resultant image.

Later, in [3], on the basis of the 3D frequency spectrum, fabric defects were extracted by detecting the abnormal values in two central spatial frequency spectrums. Subsequently, the classification of defects was based on seven characteristic parameters extracted from the Fourier spectrum. In practice, the defect classification is helpful in determining the problem in the production.

However, the DFT-based approaches are not effective for those fabric images in which the frequency components associated with the homogenous and defective images are highly mixed together in the spectral domain. This ineffectiveness is due to the difficulty in manipulating the frequency components

associated with homogenous regions without affecting the corresponding components associated with the defective regions.

The power spectrum generated from FT provides rich structural information on fabric texture, which was applied in fabric inspection [58]. Warp and weft yarn periodicities are associated with the power spectrum peaks on the principal horizontal and vertical lines, respectively. The Fourier power at the origin reflects the average brightness (DC) of the image. Therefore, DC-suppressed Fourier power spectrum (DCSFPS) was computed to obtain the boundaries of fabric texture, which represent the weave pattern. In this studies, 27 statistical features obtained from DCSFPS along with fabric cover factor, which represents fabric performance features (e.g., wear resistance, permeability, and flexural rigidity), were used as the inputs to an NN for defect classification. The effectiveness of the proposed method was evaluated on two types of fabric inspection.

The application of Fourier analysis in fabric defect detection is invariant to rotation, translation, and rescaling, and is able to measure the coarseness of fabric texture. However, it is unsuitable for detecting local defects because of the difficulty in quantifying the contribution of each spectral component of the infinite Fourier basis. Furthermore, without the support in the spatial domain, the location of defects cannot be effectively confirmed.

2.4.2 Defect Detection based on WT

In the recent past, multi-resolution analysis has received considerable attention as a textural feature extractor. WT is a multi-resolution analysis method that can decompose the inspection image into a hierarchy of sub-images with varying spatial resolutions. Unlike FT, WT is a time-frequency function that consists of small waves of varying frequencies and limited

duration. WT provides conjoint analysis of textured images in the spatial and spectral domains. Multi-channel modeling is capable of extracting the intrinsic characteristics of a textural image at different scales, which makes it well suited to the texture analysis problem. Wavelet-based defect detection can be achieved by examining the significant features of these decomposed images at every scale.

With the inspection image decomposed with a family of real orthogonal wavelet bases, wavelet packets were used to detect surface defects in [59]. Shift-invariant features were computed from the wavelet packet coefficients of a set of dominant frequency channels, which depict the significant textural information of the image. Thereafter, the defects were identified by an NN classifier on the basis of the computed features.

In [52], a multi-resolution approach based on wavelet transform and an image restoration technique was proposed for textural surface inspection. At each level of standard wavelet decomposition, a smooth sub-image and three detailed sub-images, which contain fine structures with horizontal, vertical, and diagonal orientations, were obtained to represent the reference textural structure. Therefore, in the reconstructed image, the normal fabric texture was removed, and only local anomalies were enhanced. Later, through the analysis of the energy distribution of wavelet coefficients, an automatic wavelet band selection procedure was developed to obtain the optimal image reconstruction parameters, in order to improve the detection accuracy [60].

Discriminative detection models based on adaptive wavelet bases could be designed for specific fabric inspection problems. In [61], the performance of six WT-based defect detection methods was evaluated on the classification of 466 defective and 434 non-defective samples. Results revealed that the wavelet designed by the discriminative feature extraction (DFE) method obtains the most accurate defect classification. Instead of empirically

selecting a wavelet from the standard wavelets, the adaptive wavelets were designed to discriminate between defective and non-defective samples.

In [62], to achieve the adaptive wavelet bases for fabric defect detection, the wavelet coefficients were optimized according to a cost function to represent the texture of normal fabric. Therefore, processed by the adaptive WT, a simple thresholding operation would be able to discriminate the difference between the wavelet filtered responses of defective and non-defective areas in the image.

[63] applied the visual attention mechanism of the wavelet domain to address the dynamic detection of fabric defects. According to the theories of visual attention mechanism [64], human attention is likely to be attracted by a salient object, and a combination of feature maps extracted from a specific location can form a better representation of the inspection object. In [63], feature images extracted from the reference images were first decomposed into a set of feature sub-maps by wavelet decomposition. Thereafter, the center-surround operator was adopted to enhance the difference among sub-maps to form a feature saliency map used to reflect the features of possible defects. The experiments revealed that the concept of visual saliency is useful in distributing computing resources reasonably and improving the effectiveness of the fabric defect detection.

WT provides multi-resolution analysis of images, which allows it to detect fabric defects of any size, especially some local defects. In addition, the optimal wavelet bands are adaptive to the fabric texture of different coarseness. However, when the detection model is highly accurate, more wavelet bands must be optimized, thereby increasing the computational cost significantly.

2.4.3 Defect Detection based on GT

GT is a special case of short-term FT. With its merits of optimal joint localization in the spatial and frequency domains [65], 2D GT has become a popular technique for various applications, such as boundary detection [66, 67], texture analysis [68], and palm vein recognition [69, 70]. Consequently, owing to its small bandwidth in the spatial and frequency domains, GT is regarded as a promising method for fabric defect detection. The parameters of a Gabor filter can be selectively tuned to discriminate a known category of defects. In general, the existing defect detection models based on GT can be classified into two categories: models based on a Gabor filter bank and on optimized Gabor filters.

Some researchers have proposed fabric inspection models based on a Gabor filter bank, which consists of more than ten filters that essentially cover the frequency domain. In [12], a set of twenty-four Gabor filters was generated at four scales and six orientations to detect the possible defects that may appear on the fabric. This method was based on the idea of multi-resolution analysis, in which the detection of defects in any orientation and size can be ensured by multiple Gabor filters. Features of defects were represented by combining the outputs of all Gabor filters, the parameters of which were predefined empirically. Although the implementation of this detection model is quite easy, filtering by a Gabor filter bank can generate a large amount of data, which might cause a disturbance to the texture discrimination problem [71].

Thereafter, [72] applied feature selection on a predefined Gabor filter bank to build a more compact filter bank that was able to produce low dimensional feature representation with improved sample-to-feature ratio. However, the performance of this approach primarily depends on the parameter settings of the original Gabor filter bank. In [73], principal component analysis (PCA)

has been performed on the outputs of a Gabor filter bank, to reduce the dimension of feature vectors. Thereafter, the Euclidean norm of the local features was calculated to distinguish defective areas. The performance of the proposed detection model was evaluated on two types of fabric textures, which were selected from TILDA [74].

Some detection approaches based on optimized Gabor filters have also been developed in recent years. These approaches usually employed only one or several Gabor filters, the parameters of which were optimized toward specific objectives. In [13], fabric defect detection was considered the problem of segmenting a known non-defective texture from an unknown defective texture. Along four directions, Gabor filters were optimized in a semi-supervised mode to generate high response to non-defective fabric areas. In the experiments, 35 different flawed homogeneous textures were used to evaluate the effectiveness of the proposed method.

To alleviate the computational cost and the limitation of the rotation sensitivity of 2D Gabor filters, [75] proposed processing 1D ring-projection transformed image signal with a 1D Gabor filter. The average value of the pixels covered by the ring projection was used to substitute the original image intensities, which might possibly cause the loss of defect features. The 1D Gabor filter was optimized to have the minimum responding energy toward normal fabric texture through the use of an exhaustive searching algorithm. However, insufficient experiments have been conducted to evaluate the effectiveness of the proposed method.

For slub extraction in woven fabric, the parameters of a Gabor filter were obtained in the frequency domain according to the frequency characteristics of slubs. The central frequency of the Gabor filter was designed by comparing the frequency spectra of slub yarn with a slub-free image in the frequency feature space. The orientation of the Gabor filter was set perpendicular to the

slubs. However, only obvious defects would change the distribution of the peaks in the frequency spectrum of the images, such that the effectiveness of the proposed method is limited.

[76] proposed a defect detection system based on a non-linear network called Gabor wavelet network (GWN) because the transfer function is a Gabor wavelet function. Non-defective images were employed as the template images of GWN. Characteristic parameters of the non-defective texture were acquired by training the GWN to minimize an error function, and then they were used to design the optimal parameters of the Gabor filters for fabric inspection.

Similar to the previous studies, [77] used a non-defective fabric sample as the template image to optimize Gabor filters at seven scales through the genetic algorithm with the similar optimization objective in [76]. Thus, a set of optimal Gabor filters were tuned to match the desired features under different resolutions.

Two-step detection was once proposed for fabric stain release [78]. After filtering by a Gabor filter bank initially, the histogram of the input image was analyzed to predict the presence of possible defects. The most suitable Gabor filter, whose parameters best matched the features of possible defects, was selected in the coarse segmentation stage and iteratively refined in the fine segmentation stage. However, only global defects, such as stain a that covers the main area, could be detected by the proposed detection model because local (small) defects would be neglected through histogram analysis.

In [79], defect detection was addressed by adopting an elliptical-ring Gabor filter, the parameters of which, such as aspect ratio, center, and support of the filter, were optimized by a simulated annealing algorithm. Ring Gabor filter is the modification of a classical Gabor filter, fulfilling the texture discrimination task in terms of higher accuracy with the ring-like filter pass field.

In general, fabric defect detection approaches based on a Gabor filter bank have two main drawbacks: (1) They usually have high computational cost, which is vital to the real-time inspection system; and (2) Without automatic parameter adjustment, the empirical parameters cannot efficiently handle the different situations of the defect detection problems.

Moreover, in the abovementioned studies, Gabor filters were optimized in accordance with the features of non-defective fabrics. These optimal Gabor filters would be good at determining the features of normal fabric textures. However, without any prior knowledge about the common defects, these filters may not perform well in detecting subtle defects that have not significantly altered the spectral features of normal fabric. Therefore, building the optimization model for Gabor filters is crucial for the defect detection results.

Finally, in [80], the optimal parameters of the Gabor filter were acquired by exhaustive searching in the theoretical region. This method was time consuming, and it is not suitable for real-time operation. In [13], the Gabor filters were optimized by sequential quadratic programming (SQP). SQP is a gradient-based optimization method, the optimization results of which mainly depend on the initial values of the variables. In [76], the training process of GWN was conducted through the Levenberg-Marquardt algorithm, which is also a gradient-based optimization algorithm. [79] adopted simulated annealing (SA) algorithm, which is a stochastic optimization algorithm, for Gabor filter optimization. Compared with gradient-based optimization algorithm, SA has increased the probability of achieving the global optimal solution by accepting some worse solutions with an adaptive probability in the optimization. However, because only a single individual is employed in the optimization, the performance of this algorithm is not stable. Moreover, it requires a high computational time.

2.5 Learning-based Approaches

2.5.1 Defect Detection based on NN

NNs are among the best classifiers used for defect identification because of their ability in analyzing the relationships among multiple features and to describe complex decision regions.

In [81], fuzzification technique (fuzzy logic) and a back-propagation NN were combined to achieve the classification of eight types of fabric defects and some non-defective samples. Four input features (the ratio of projection lengths in the horizontal and vertical directions, the gray-level mean and standard deviation of the image, and the neighboring gray level dependence matrix) were selected as the inputs to the NN. The fuzzification process was useful in increasing the separability of classes in the feature space, thereby improving classification accuracy.

[22] proposed a three-layer back-propagation artificial NN for fabric defect classification. Only five hidden nodes were used to control the overall computational cost. The outputs of the third layer indicated the general classes of the possible defect types. Similarly, a low-cost solution using feed-forward NN for fabric inspection was detailed in [15, 82]. PCA by singular value decomposition was applied to reduce the dimension of feature vectors which were generated from the gray-level arrangement of neighboring pixels of every pixels in the image. Twill and plain fabric samples with commonly occurring defects gathered from the loom were used in the experiments. In [83], neighborhood-preserving cross-correlation feature vectors together with probabilistic NN were used for the inspection of textile fabrics.

The main advantages of NN-based detection approaches are that they can analyze and generalize multiple features of the inspection fabric samples

to improve the defect classification results. However, the robustness of the network largely depends on the amount of training data (defective fabric samples). The large number of training samples brings excessive computational cost to the detection system, influencing detection efficiency. Moreover, the new type of fabric defect constantly appears in the industry, making the collection of all types of training samples impossible.

2.5.2 Defect Detection based on Sparse Representation

The fabric defects that appear as anomalous areas can also be regarded as noise in the image. Therefore, with the use of image denoising techniques, some defect detection models have been presented [16–18, 84, 85]. Through sparse representation with a dictionary, the corresponding normal fabric texture could be estimated according to the input defective samples. Hence, the defective areas could be enhanced in the residual image, which is the result of subtracting the estimated image from the input image.

In [16], on the basis of sparse coding, an over-complete dictionary was trained from the inspection image itself, considering the fabric defect was small. For a specific fabric type, each column of the image was considered the training data of dictionary learning, which is beneficial for defect detection by finding abnormal pixels in a 1D signal. However, to adapt to linear defects, the algorithm was not only implemented on the original image but also on its rotated version, thereby increasing the computation cost of the system significantly. Moreover, the sparse representation was based on the basic regression model, which is unsuitable for eliminating scattered noise (e.g., spot defects).

Later, in [17], after image restoration was performed by the regression model, Euclidean distance and correlation coefficient between the original image and

its approximation were selected as the features in training an SVDD classifier, which was adopted for discriminating novelty from normal samples. Similar to NN-based approaches, a defect classifier could significantly improve the robustness of fabric inspection. However, on the one hand, the problem also lies in the difficulty in collecting enough defective fabric samples. On the other hand, only two statistical features were used as the classification norm, which cannot ensure the detection of small defects.

To overcome the computation problem, the projections of a fabric image on all vectors of a small-scale dictionary, which was trained from non-defective samples, could be considered the features in defect detection [18, 85]. A Gabor filter, whose parameters were trained according to the features of normal fabric texture, was introduced as preprocessing in the detection model. Although the complexity of the input image signal and the influence of noise could be greatly reduced after preprocessing, this method is not ideal for improving detection accuracy. When defects are small and mixed with noise, the contrast between defects and fabric texture background is reduced after Gabor filtering as well. Consequently, the defect detection rate is greatly influenced.

Overall, sparse representation-based approaches were more universally applicable to most types of fabric defects because they did not rely on the feature extraction of defects. As long as the dictionary and sparse coding model are reasonably chosen, even small defects are likely to be identified through image restoration. However, the computational cost of sparse coding is usually high. Thus, these approaches are more suitable for fabrics with complex textures in the industry.

2.6 Motif-based Approaches

Patterned fabric surface can be regarded as a 2D patterned texture, which is composed of underlying repeated units (lattice). The lattice can be further decomposed into a lower level of elements called motifs. Usually, the lattice is generated by a motif with at least one of the symmetry rules including translational, rotational, reflectional, and glide-reflectional symmetry [86, 87].

In [19], the underlying lattice of fabric texture was first extracted to identify the representative motif of the non-defective patterned texture by a crystallography-based pattern extraction model [88]. An energy-variance (E-V) space was designed based on the energies of moving subtraction and variance between any two motifs to illustrate the distribution of their statistical behaviors. Therefore, the decision boundaries for defective and non-defective motifs were determined by the subsequent feature classification based on a max-min decision region (MMDR). The performance of the proposed detection model was evaluated on a pattern texture that consists of parallelogram, rectangle, and triangle motifs. Later, the effect of the shape transform of irregular motifs on defect detection accuracy was studied in [89]. Before the E-V space of the motif feature was computed, all motifs were transformed to rectangular shapes.

To improve the detection accuracy through MMDR in the E-V space, [20] applied ellipsoidal decision region (EDR). The E-V values of non-defective fabric samples were assumed to obey a 2D Gaussian mixture model (GMM), on the basis of which the E-V values could be clustered into several classes by K-means clustering. Thereafter, the boundaries of the ellipsoid decision region were determined by finding the convex hull of each cluster. Finally, the ellipsoid region with constant eccentricity could enhance the detection performance on the ambiguous points, which were originally on

the boundaries of MMDR.

With the use of lattice and motif, these approaches provided solutions for the simultaneous detection of two types of defects: common fabric defects and pattern variants. However, because the detection decision boundaries were all determined according to the features of motifs, the performances of these approaches in detecting common defects are unsatisfactory. The influences of small common defects on the features of motifs are not large enough.

2.7 Hybrid Approaches

A majority of the aforementioned approaches focus on analyzing the defect detection problem from only one aspect, such as the statistical behavior in the spatial domain, structural information of the texture, or the corresponding frequency component. Thus, to improve the detection performance and avoid the drawback of adopting a single method, some hybrid approaches have also been proposed for fabric inspection, especially for some complex texture discrimination, such as jacquard and patterned fabric.

In [90], wavelet preprocessed Golden image subtraction (GWIS) was proposed for pattern fabric defect detection. WT was used as an image denosing tool [91] because white Gaussian noise caused by the dirt in the real fabric yarns was enhanced through histogram equalization, which was applied to highlight the detail of the fabric texture. Thereafter, Golden image subtraction was applied in representing the repeated pattern unit in the non-defective fabric image and in detecting the possible defects that might distort the extracted reference unit.

A method that combines the optimal Gabor filter and local binary patterns (LBP) was developed for multi-texture segmentation [92]. LBP was selected as a complementary tool for feature extraction from the image filtered by a

single Gabor filter, which was optimized by the immune genetic algorithm. Finally, K-nearest neighbor was adopted to determine the boundaries between different textures.

To address the problem of defect detection and defect classification, a fabric inspection system, which consists of Gabor filters, LBP, and Tamura method, was developed in [93]. A Gabor filter bank was generated to segment defects from the regular fabric texture in the feature space. Thereafter, Tamura, which could measure the regularity and roughness of texture, was adopted in defect classification together with LBP.

Hybrid approaches normally contain two or more techniques that address different problems in the system. Each technique has its own merits, and thus, the system generally has high accuracy and robustness. However, a complex system structure can also lead to a large computation amount. Thus, hybrid approaches are usually applied to composite problems.

2.8 Summary

On the basis of the abovementioned literature review, the following conclusions can be made:

(1) Although many studies have been conducted to address the fabric defect detection problem, few of the existing approaches considered the characteristics of specific weaving textures, which makes them inapplicable for implementation in the real environment of the industry.

(2) In the inspection of plain fabric, because of the lack of analysis of the specific characteristics of plain weaving and plain fabric defects, the efficiency (computational complexity) of the existing approaches in practical application has not been solved well. Effective methodologies are desired to

cope with the fabric inspection problem in a manner closer to reality.

(3) The case where some twill fabric defects are small and of low contrast has not been investigated in existing studies, which do not satisfy the detection accuracy of twill fabric inspection. Corresponding methodologies are desired to improve the performance of twill fabric defect detection in the industry.

(4) None of the existing defect detection approaches are proposed for striped fabric. Through the idea of hybrid detection approaches, common fabric defects and pattern defects on striped fabric are expected to be identified in two steps.

In summary, the performances of the existing approaches on plain fabric inspection, twill fabric inspection, and striped fabric inspection are not satisfied, leaving much room for further research explorations. The current study investigates the fabric inspection problem closer to reality, in which three different defect detection approaches are proposed, taking the advantages of specific characteristics of fabric weaving texture and defects. The detection accuracy, robustness, and efficiency are significantly improved.

Chapter 3

Research Methodology

A detailed review of the up-to-date achievements in the field of automatic fabric inspection was given in Chapter 2. Most studies focused on the feature extraction of fabric defects, neglecting the structure differences among the weaving textures of different types of fabric. However, so far, the existing detection methods have had a limited effect on industrial applications despite the widely accepted fact that effective automatic fabric defect detection is helpful in improving the performances of production cost control.

In this chapter, first, the methodologies in investigating the automatic fabric inspection models are clearly stated. Then, the Gabor filters and sparse representation, which are adopted as the basis of the methodologies for automatic fabric inspection, are presented.

3.1 Solution Mechanisms

According to the discussions in the previous chapters, the inspection of most types of fabric through using only one detection approach is difficult because the characteristics of fabric texture and defects vary with different weaving

methods. Therefore, in this research, three distinctive fabric defect detection models are developed for the inspection of plain, twill, and striped fabrics.

(1) Plain fabric is the most basic fabric type. The smooth surface of plain fabric means that plain fabric defects are more prominent than others compared with non-defective fabric areas. Moreover, the orientation of most plain fabric defects (e.g., slub, broken yarn, and missing yarn) are usually limited in either the horizontal or vertical direction because of the simple crisscross weaving pattern.

(2) Twill fabric texture is slightly more complex than that of plain fabric. The surface of twill fabric is associated with diagonal parallel ribs, which cause twill defects to mix easily with the weaving pattern, and the features of defects are blurry in the image.

(3) Stripe is the one of the most basic elements in patterned fabric, which is widely used in fashion apparel (e.g., business shirts and pants). Spectral features (e.g., central frequency and frequency spectrum) are the dominant characteristics of striped fabric. The greatest challenge is that common fabric defects are usually confused with pattern defects.

On the basis of the abovementioned description, the inspection model for woven fabric is proposed and shown in Fig. 3.1. As shown in this figure, the inspection of each fabric type involves two stages, namely, the offline training stage, which aims to obtain the optimal parameters for the subsequent inspection, and the real-time inspection stage, in which the inspection images are labeled as defective or non-defective. To achieve the research objectives stated in Chapter 2, digital imaging, pattern recognition, and optimization techniques are applied in this research. The details of the research methodology are described in the remainder of this section.

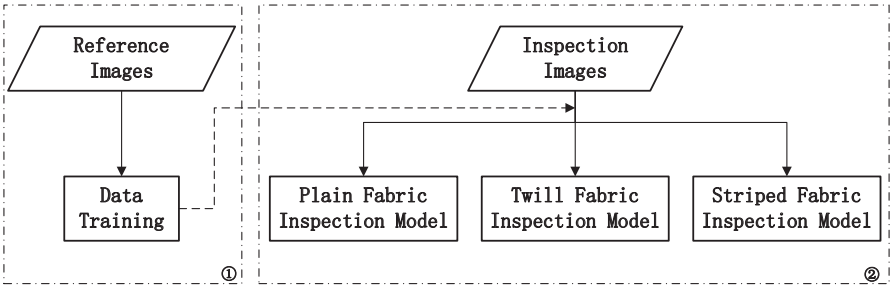

Figure 3.1: Inspection model for woven fabric: ① offline training stage; ② real-time inspection stage.

3.1.1 Research Methodology for Plain Fabric Inspection

Gabor filters, one of the most popular techniques, are suitable for object extraction from a smooth background (e.g., plain fabric). A Gabor filter is also known as a good edge detector because of its joint localization in the spatial and spatial frequency domains. The prominent characteristics of plain fabric defects are their linear shape and fixed orientations. Therefore, Gabor filters are selected as the core technique in developing the defect detection model for plain fabric.

(1) Phase I - Parameter optimization of Gabor filters

A number of parameters of a Gabor filter provide enough freedom to design filters with various shapes, orientations, and frequency characteristics. Therefore, to achieve the best feature extraction of fabric defects, the optimization of Gabor filter parameters is the critical issue in the training stage of the Gabor filter-based detection model. Through the use of some typical defective samples as reference images, a fitness function is designed to achieve the best discrimination between defects and normal fabric texture.

(2) Phase II - Fabric defect detection based on optimal Gabor filters

Plain fabric defects normally lie in only two directions: weft and warp. Thus, only horizontal and vertical optimal Gabor filters obtained in phase I are

used to extract the features of defects. Combined with the thresholding and feature fusion operations, the optimal Gabor filters can successfully segment the possible defects from the original image background.

3.1.2 Research Methodology for Twill Fabric Inspection

Owing to their sensitivity to small aberrations in the image, denoising techniques have shown their potential in addressing the detection of small and blurry defects, such as defects on twill fabric. Considered stochastically distributed noise, fabric defects can be detected by reconstructing the non-defective fabric texture. Sparse representation, which can estimate the input signal based on related dictionaries, is adopted to address the inspection problem of twill fabric defects.

(1) Phase I - Adaptive dictionary learning

The selection of dictionary influences the accuracy of normal fabric texture restoration, which in turn will affects the false alarm rate of the detection model. In the training stage, non-defective fabric samples are used to learn several sub-dictionaries, which can be adaptively selected in the subsequent image estimation and provide related structural information for sparse coding.

(2) Phase II - Fabric defect detection based on sparse representation

With the adaptive dictionary learned in phase I, sparse representation should estimate the non-defective version of the inspection images. Therefore, possible defects can be eliminated. To increase estimation accuracy, non-local similarities of the fabric structural information are considered in sparse coding.

3.1.3 Research Methodology for Striped Fabric Inspection

Unlike in fabric of solid color, two groups of defects exist in striped fabric: common fabric defects and repeat pattern variation. In addition, the edges of stripe patterns usually cause disturbance in the extraction of common defects. Therefore, a hybrid detection model, which can solve the disturbance problem and address the detection of these two groups of defects in two steps, is necessary.

(1) Step I - Reduction of disturbance caused by stripe patterns

The frequency of the stripe pattern is the most prominent component in the frequency spectrum of striped fabric image. Thus, a Gabor filter in the perpendicular direction to the stripe optimized according to the filter response of non-defective fabric samples can successfully eliminate the stripe pattern, while remaining pattern variations and common defects. Preprocessing with pattern removal can significantly reduce such disturbance.

(2) Step II - Detection of common fabric defects

Common fabric defects are usually mixed with the repeat pattern on the patterned fabric. After the repeat pattern removal is performed, inspection procedures for fabric in solid color are useful for detecting remaining defects in the filtered images. Although the optimal Gabor filters suppress only the frequency response of the repeat patter, filtered by Gabor filters, part of the detailed information of the rest of the fabric texture may have a slight degree of loss. Therefore, an image restoration-based detection model is suitable for the inspection of the feature image of striped fabric.

The details of the abovementioned defect detection models will be introduced in Chapters 4, 5 ,and 6.

3.2 Gabor Transform

GT, which is a special case of windowed FT, was proposed for extracting the local information of the input signal [94]. A 2D GT function consists of an oriented complex sinusoidal wave modulated by a Gaussian envelope [65]. A complete but non-orthogonal basis can be formed by a set of Gabor wavelets. The impulse response formulation in the spatial domain is shown as follows:

$$f(x,y) = \frac{1}{2\sigma_x\sigma_y} exp[-\frac{1}{2}(\frac{x'^2}{\sigma_x'^2} + \frac{y'^2}{\sigma_y'^2})] \cdot exp(2\pi j f_0 x'), \tag{3.1}$$

where f_0 represents the central frequency of the span-limited sinusoidal grating. σ_x and σ_y, which are the standard deviations of the Gaussian function, are the smoothing parameters of Gabor transform. These two variables are regarded as the shape factors of the Gaussian surface, which determine the coverage size of Gabor transform in the spatial domain. When σ_x equals σ_y, the Gaussian surface is a circle. Usually, parameter σ_y is represented as $\lambda\sigma_x$ such that the shape of the Gaussian surface could be adjusted by changing coefficient λ. Here, (x', y') is (x, y) rotated by θ:

$$\begin{bmatrix} x' \\ y' \end{bmatrix} = \begin{bmatrix} \cos\theta^i & -\sin\theta^i \\ \sin\theta^i & cos\theta^i \end{bmatrix} \begin{bmatrix} x \\ y \end{bmatrix}. \tag{3.2}$$

In the spatial frequency domain, the Gabor transform acts as a bandpass filter and its Fourier transform is given by

$$F(u,v) = exp[-\frac{1}{2}(\frac{(u-f_0)'^2}{\sigma_u'^2} + \frac{v'^2}{\sigma_v'^2})], \tag{3.3}$$

where

$$\sigma_u = \frac{1}{2\pi\sigma_x} \quad \text{and} \quad \sigma_v = \frac{1}{2\pi\sigma_y}.$$

The half-peak bandwidth B is another important term that is used in

specifying the Gabor filter

$$B = log_2 \frac{\sigma_x f_0 \pi + \sqrt{\frac{ln2}{2}}}{\sigma_x f_0 \pi - \sqrt{\frac{ln2}{2}}}. \tag{3.4}$$

According to [65], the half-peak bandwidth is approximately 1-1.5 octaves along the preferred orientation. The bandwidth determines the value of σ_x whose value should not be specified directly but changed through frequency bandwidth B. In this context, a small bandwidth corresponds to a large σ_x. Owing to the small bandwidth of a Gabor filter in both spatial and spatial frequency domains, this filter is widely used in texture analysis as the bandpass filter. From the aforementioned definition of Gabor parameters, the properties of a Gabor filter are mainly governed by parameter set $\{f_0, \sigma_x, \sigma_y, \theta, B\}$. GT could provide a good description of local structural information with the various selections of spatial frequency and orientation.

From Eq. (3.1) we know that the Gabor filter f forms a complex-valued function that consists of real and imaginary parts, as shown in Eqs. (3.5) and (3.6), respectively. The real part of the Gabor filter that acts as a proven blob detector is even symmetric, while the imaginary part of Gabor filter acting as a proven edge detector is odd symmetric [66, 95]. For convenience, in the rest of this research, the real part of the Gabor filter is expressed as the real Gabor filter, and the imaginary part of Gabor filter is expressed as the imaginary Gabor filter.

$$f_e(x, y) = \frac{1}{2\sigma_x \sigma_y} exp[-\frac{1}{2}(\frac{x'^2}{\sigma_x'^2} + \frac{y'^2}{\sigma_y'^2})] \cdot \cos(2\pi j f_0 x'), \tag{3.5}$$

$$f_o(x, y) = \frac{1}{2\sigma_x \sigma_y} exp[-\frac{1}{2}(\frac{x'^2}{\sigma_x'^2} + \frac{y'^2}{\sigma_y'^2})] \cdot \sin(2\pi j f_0 x'). \tag{3.6}$$

For a given image $i(x, y)$ and a $k \times k$ Gabor filter mask, the Gabor-filtered output is obtained by convolution operation. Feature image $G(x, y)$ that represents the local energy measures of the filtered image is obtained by computing the square nonlinear operator $\| \cdot \|_2$, as shown in Eq. (3.7). Feature image $G(x, y)$ strongly depends on the choice of parameters f_0 along with σ_x, σ_y, and θ, which provide enough freedom to design filters of various shapes, orientations, and frequency characteristics.

$$G(x, y) = \sqrt{G_e(x, y|f_0, \sigma_x, \sigma_y, \theta)^2 + G_o(x, y|f_0, \sigma_x, \sigma_y, \theta)^2}, \tag{3.7}$$

where

$$G_e(x, y|f_0, \sigma_x, \sigma_y, \theta) = \sum_{m=-k}^{k} \sum_{n=-k}^{k} i(x + m, y + n) f_e(m, n|f_0, \sigma_x, \sigma_y, \theta), \tag{3.8}$$

$$G_o(x, y|f_0, \sigma_x, \sigma_y, \theta) = \sum_{m=-k}^{k} \sum_{n=-k}^{k} i(x + m, y + n) f_o(m, n|f_0, \sigma_x, \sigma_y, \theta). \tag{3.9}$$

In [96], taking Eq. (3.1) as the mother Gabor wavelet, a class of self-similar Gabor wavelets was generated by appropriate dilation and rotation for texture analysis

$$f_{pq}(x, y) = \alpha^{-p} f(x', y'), \tag{3.10}$$

where

$$x' = \alpha^{-p}(x \cos\theta_q + y \sin\theta_q),$$

$$y' = \alpha^{-p}(-x \sin\theta_q + y \cos\theta_q),$$

$$\alpha > 1; \quad p = 1, 2, ..., S; \quad q = 1, 2, ..., L.$$

Integer subscripts p and q represent the index of scale (dilation) and orientation (rotation), respectively. S is the total number of scales and L is the

total number of orientations in the self-similar Gabor filters bank. The angle for each orientation is given by

$$\theta_q = \frac{\pi(q-1)}{L}, \qquad q = 1, 2, ..., L. \tag{3.11}$$

Therefore, a Gabor filter bank, which essentially covers the spatial frequency domain, could be constructed for unsupervised fabric defect detection by defining the number of scales and orientations.

By contrast, if the best combination of Gabor filter parameters could be defined to represent the features of the object to be detected, then only one or a small number of Gabor filters could be effectively used to solve detection problems. For example, in [13, 76], Gabor filters were optimized according to the filtering response of non-defective fabric texture. This step distinguished defects from the background in the filtered images.

3.3 Sparse representation

According to the sparsity of the observed object, sparse representation was proposed for describing nature images from their primary feature elements [97]. The set of basic elements is known as the "dictionary", most coefficients of which are required to be zero in sparse coding. Sparse representation has been widely applied in image restoration, face recognition, and image classification [98–100].

Mathematically, the sparse representation model assumes that for an input image $\mathbf{y} \in \mathbf{R}^N$, we can have its corresponding estimation $\mathbf{x} \approx \mathbf{\Phi}\boldsymbol{\alpha}_{\boldsymbol{y}}$, where $\mathbf{\Phi} \in \mathbf{R}^{N \times M} (N < M)$ denotes an over-complete dictionary, and most of the coefficients in $\boldsymbol{\alpha}$ are close to zero. With the sparsity prior, an approximation of $\mathbf{x}$ from a given image $\mathbf{y}$ with respect to dictionary $\mathbf{\Phi}$ could be solved by the

most commonly used solution model [101]:

$$\boldsymbol{\alpha_y} = arg\min\{\| \mathbf{y} - \boldsymbol{\Phi} \circ \boldsymbol{\alpha} \|_2^2 + \lambda \| \boldsymbol{\alpha} \|_0\}, \tag{3.12}$$

where λ denotes the regularization parameter that controls the balance between sparse approximation of $\mathbf{x}$ and sparsity of $\boldsymbol{\alpha}$. The l_2-norm $\| \cdot \|_2$ is computed to ensure that the error between the original image and its estimation is as small as possible, which represents image restoration accuracy. The l_0-norm $\| \cdot \|_0$ is a pseudo-norm that counts the number of non-zero entries in $\boldsymbol{\alpha}$, which is known as sparse regulation term. However, the regulation is usually relaxed to the convex l_1-minimization, because l_0-minimization is an NP-hard optimization problem.

Dictionary learning and sparse coding are two key issues in solving the image sparse representation. Sparse coding aims to find sparse representation coefficients based on the input signal and a known dictionary. In the past decade, several algorithms were proposed to solve the sparse representation problem stated in Eq. (3.12). Matching pursuit (MP) [102] and the orthogonal matching pursuit (OMP) [103] are the simplest algorithms. However, their searching strategies are greedy and time consuming. Basis pursuit (BP) [104] is another well-known pursuit approach, which replaces the non-convex l_0 norm with convex l_1 norm to achieve more sparse solutions.

Generally, the dictionary selected can be an over-complete and unspecified set of functions, such as steerable wavelets, contourlets, and short-term Fourier transforms. The main advantage of such dictionaries is that it leads to simple and fast algorithms for sparse coding. However, the success of such dictionaries in the application depends on how related they are to the image local structure and how suitable they are to describe sparsely input images. Recently, learning dictionaries from referencing images have attracted attention in image sparse representation research, as these methods

could better characterize image structures [98, 105, 106]. Method of optimal directions (MOD) [107] and K-SVD [105] are the two representativesof over-complete dictionary learning algorithms. K-SVD, which alternatively updates the dictionary and coefficients, has been more widely used in various applications. Moreover, according to specific situation, PCA could perform well in learning a complete dictionary.

3.4 Summary

This chapter presents the basic solution framework of the automatic fabric inspection problem investigated in this research. Analysis was conducted on the characteristics of fabric defect detection cases for three different types of fabrics. Moreover, corresponding research methodologies are clearly stated. Finally, on the basis of core techniques in the research methodologies, the basic knowledge of Gabor transform and sparse representation are briefly introduced.

Chapter 4

Differential Evolution-based Optimal Gabor Filters Model for Plain Fabric Inspection

Following the solution mechanism presented in Chapter 3, three automatic defect detection models for three types of woven fabric are investigated. As uniform texture fabrics are divided into plain and twill fabric according to the weaving structure, this chapter will first investigate the defect detection problem for plain fabric.

4.1 Framework of Plain Fabric Inspection Model

Fabric defects could be viewed as abnormal structures on fabric surface. Fig. 4.1 shows several typical defective samples of plain fabric. In the gray-level image, compared with defects, the gray-level variation of non-defective area is low such that it could be recognized as a continuous and homogeneous area. By contrast, defects on the fabric surface (appearing as the discontinuous area) could be identified as edges in the image. Hence, Gabor filters, which are

effective edge detectors, can efficiently solve the defect detection problem. As an imaginary Gabor filter proved useful in detecting edges that are in the perpendicular direction to the Gabor filter parameter, the real Gabor filter, which acts as a good blob detector, proved useful in fabric defect detection [66], especially for defects that appear as knots [108]. Therefore, in the defect detection model for plain fabric, the combination of real and imaginary Gabor filters is used to detect defects, which guarantees the best detection results.

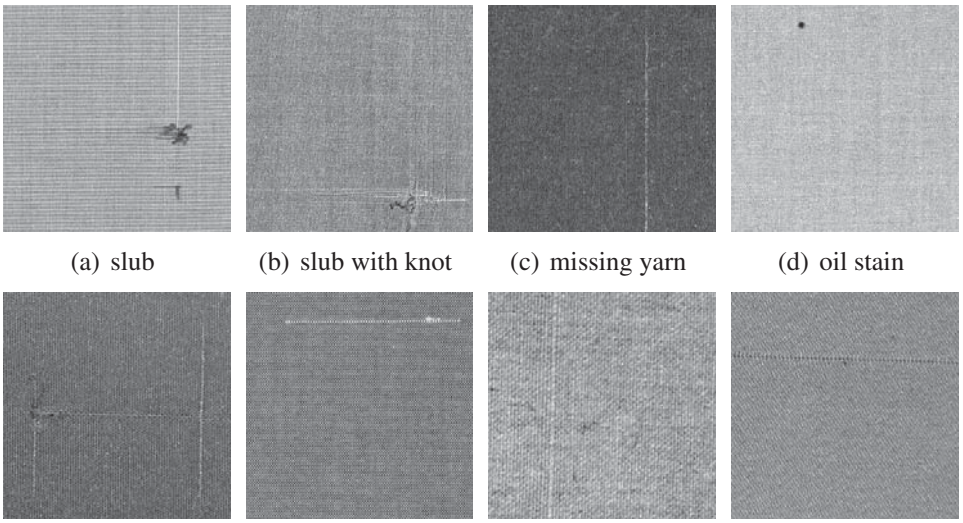

(a) slub (b) slub with knot (c) missing yarn (d) oil stain

(e) chapped pick (f) chapped pick (g) dyed yarn (h) broken pick

Figure 4.1: Gray-level images of defective fabric samples.

As a result of the criss-cross weaving structure of plain fabric, common defects, such as slub, double pick, chapped weft, and thick yarn [109], appeared as vertical and horizontal lines. Even the defects of knot and spot are regarded as abnormal structures constructed by lines. Consequently, Gabor filters optimized only in the horizontal and vertical directions were applied in the proposed defect detection model. These filters are effective and efficient for segmenting fabric defects from a non-defective fabric background. On the one hand, instead of employing a Gabor filter bank, this method can dramatically reduce computational cost. On the other hand, Gabor filters in these two orientations are more pertinent to fabric defects, which avoid any false alarm. Moreover, [110] stated that increasing the number of orientations and central frequencies has no significant effect on texture

analysis. The proposed horizontal and vertical optimal Gabor filters could then directly accentuate the response of defective texture, while attenuating other areas. Consequently, defective and non-defective areas are mapped into two distinctive feature spaces.

On the basis of the above discussion, a defect detection model based on CoDE-optimized Gabor filters is developed to handle the plain fabric inspection problem. Defects can be featured first in the filtered image by only two optimal Gabor filters and then segmented by solving a simple thresholding problem. Fig. 4.2 shows the flowchart of the proposed defect detection model. The real-time detection model consists of three operations, namely, optimal Gabor filtering, thresholding, and image fusion. The details of each operation are discussed in the next two sections.

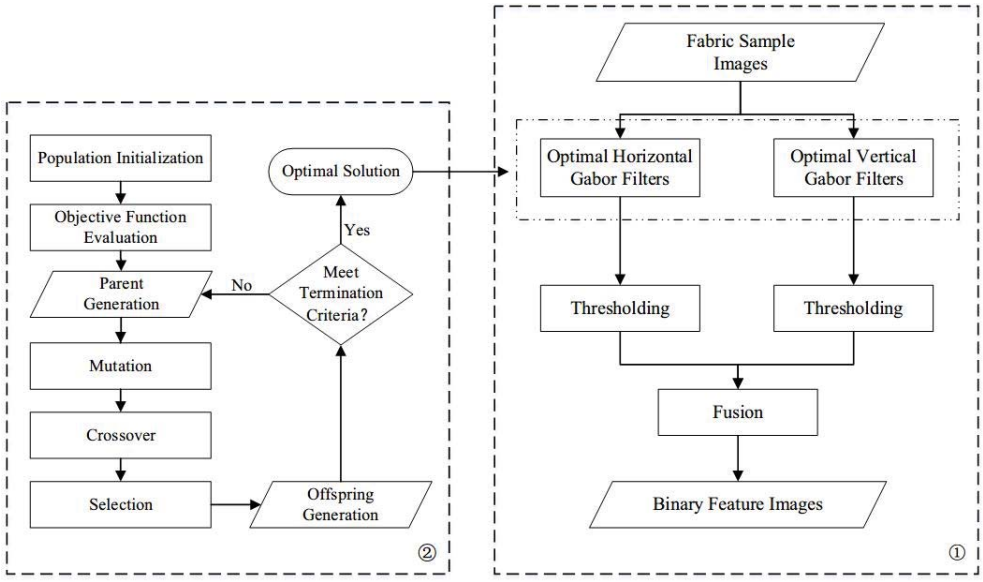

Figure 4.2: Flowchart of the plain fabric inspection process: ① detection model; ② Gabor filter optimization process.

4.2 CoDE-based Optimal Gabor Filters

Gabor filter optimization is conducted offline before fabric inspection. In optimization, several typical defective samples together with non-defective

fabric samples are utilized as training images. Unlike the unsupervised system in [12] and semi-supervised system in [13], with a priori knowledge of the orientation and size of a most common defect sample, the Gabor filter optimization could be regarded as a supervised process. It is a good practice to define the optimization objective by adopting supervised models. The best texture discrimination is easier to obtain when both features of defective and non-defective samples are utilized in the objective function. The complicated texture analysis problem could be converted into a simple binary thresholding problem when features of the two texture exhibit small intra-class scatter and large inter-class separation.

4.2.1 Optimization Objective Function Design

In Gabor filter optimization, for every type of plain fabric, a non-defective fabric image $i_f(x, y)$ and a defective image $i_d(x, y)$ are needed. The feature images obtained by using Eq. (3.7) are represented by $I_f(x, y)$ and $I_d(x, y)$. Each of these two feature images is divided into P non-overlapping patches of $l \times l$ pixels. Then the average value and variance of each patch are obtained by

$$\mu_p = \frac{1}{l \times l} \sum_{i=1}^{l} \sum_{j=1}^{l} I_p(x, y), \tag{4.1}$$

$$\sigma_p = \sqrt{\frac{1}{l \times l} \sum_{i=1}^{l} \sum_{j=1}^{l} (I_p(x, y) - \mu_p)}. \tag{4.2}$$

Among all patches of each feature image, the maximum average value μ_{max} and the minimum average value μ_{min} are determined. As described in Section 4.1, the response of the defective texture will be accentuated in the feature image when the input image is filtered by an optimal Gabor filter.

Consequently, among all patches of $I_d(x, y)$, the patch with the maximum average value μ_{max} should be a defective one, while the patch with the minimum average value μ_{min} should be a non-defective one. Therefore, to realize the best discrimination between defective and non-defective area, the fitness function is defined as

$$S_1 = \frac{\mu_{d_{max}} - \mu_{d_{min}}}{\mu_{d_{min}}}, \tag{4.3}$$

where $\mu_{d_{max}}$ and $\mu_{d_{min}}$ represent the maximum and minimum average values of patches derived from the defective sample image. S_1 is derived from Fisher distance, the largest value of which produces the best texture segmentation result [78]. To ensure that as few pixels in non-defective areas as possible are classified as defective pixels, on average, the response of this area should be as low as possible. Furthermore, to improve the robustness of the defect detection model, the variance of the filtered image should be as low as possible. As a result, the final objective function adopted is

$$\text{maximize} \quad J = \frac{S_1}{\mu_f \sigma_f} = \frac{\mu_{d_{max}} - \mu_{d_{min}}}{\mu_{d_{min}} \mu_f \sigma_f}, \tag{4.4}$$

where μ_f and σ_f are the average value and variance, respectively, of the filtered non-defective sample. The performance of Gabor filters could be evaluated according to energy response of defective and non-defective textures. Compared with the works in [12], aside from maximizing the difference between defects and normal fabric texture, the response of non-defective texture could be limited in the feature image by minimizing μ_f and σ_f. Consequently, the possibility of false alarm is greatly reduced. Moreover, unlike the semi-supervised detection models in [77] and [79], the proposed model could achieve a relatively high detection rate by employing non-defective and defective fabric samples as reference images.

In Eq. (4.4), the difference value between $\mu_{d_{max}}$ and $\mu_{d_{min}}$ controls the discrimination degree between defective and non-defective areas. Meanwhile, this method is effective in improving the robustness and reducing the false alarm of the proposed defect detection model by applying the first-order statistics of filtered non-defective image in the definition of the final optimization fitness.

4.2.2 Gabor Filter Optimization by CoDE

Given that the proposed optimization objective function contains many local optimal solutions, obtaining the optimal Gabor filter through adjusting the filter responses of reference images is a complicated optimization problem. The sequential quadratic programming (SQP) and the Levenberg-Marquardt algorithm used in [13] and [76] are gradient-based optimization methods, optimization results of which mainly depend on the initial values of variables. In [79], simulated annealing (SA) algorithm, which is a stochastic optimization algorithm, employs only a single individual. This feature makes the optimization result unstable. The evolutionary algorithm CoDE, which has shown superior performance in solving multi-modal problems [111], is selected as the optimization algorithm in this research. In the following, the optimization process is illustrated in detail.

As described in Chapter 3, a Gabor transform function has five parameters, which are f_0, σ_x, σ_y, B, and θ, three of these need to be optimized, namely f_0, σ_x, and σ_y, because of the following reasons: (1) As the Gabor filter optimization largely depends on the features of fabric defects, f_0 denoting the scale of defect is selected as the first variable in the optimization. (2) Smoothing parameters σ_x and σ_y play significant roles in the performance of Gabor filters [110]. These parameters determine the shape of a Gabor filter that is related to the arrangement of texels in a specific fabric texture.

Accordingly, frequency bandwidth B, which determines the value of σ_x, is selected as the second variable in the optimization as well. (3) Shape factor λ is selected as the third variable because the value of σ_y is determined by λ together with σ_x. In real fabric samples, the widths of the warp and weft yarns are not always the same. Therefore, the shape of optimal Gabor filters has to be adjusted adaptively by optimizing smoothing parameters σ_x and σ_y, respectively, instead of predefining the ratio. The last parameter θ is set as 0° and 90°, because only two optimal Gabor filters are designed along the orientation of fabric defects in the proposed defect detection model. To sum up, central frequency f_0, frequency bandwidth B, and shape factor λ constitute the decision vector during optimization. The optimal Gabor filter is composed of parameters that maximize objective function J. In the model, J is used to optimize Gabor filters horizontally and vertically.

The specific optimization process is described below:

(1) Representation: The first step of the optimization process is to encode solutions into decision vectors. For the fabric defect detection problem, the decision vector has three dimensions, which are f_0, B, and λ. The target is to find the optimal combination of f_0, B, and λ according to the objective function.

(2) Population initialization: For the initialization of the population, we randomly assign the real number in the specific range to each dimension of the chromosomes. Two of the variables (B and λ) are continuous, while the remaining f_0 is discrete. To apply CoDE, which is a continuous evolutionary algorithm, in our problem, we initialize the chromosome with real numbers at first, while rounding down the dimension representing f_0 when we evaluate the population based on the objective function.

(3) Mutation, crossover and selection: After the initialization process, the population needs to undergo mutation and crossover operations. CoDE is

employed as the optimization algorithm in our problem, which has three selected trial vector generation strategies and three parameter settings to generate the trial vector. The three trail vector generation strategies are "rand/1/bin", "rand/2/bin", and "current-to-rand/1". While the three control parameter settings are $[F = 1.0, C_r = 0.1]$, $[F = 1.0, C_r = 0.9]$ and $[F = 0.8, C_r = 0.2]$. At every generation, for individual X_i in the current population, three candidate trial vectors U_{i1}, U_{i2}, and U_{i3} are obtained by using three trial vector generation strategies. Each strategy has a control parameter setting that is randomly chosen from the three parameter settings (see Eqs. (4.5) - (4.7)). We evaluate these three trial vectors according to the objective function, and choose the best trial vector (denoted as U_i) from U_{i1}, U_{i2}, and U_{i3}. U_i will enter the next generation if it is better than X_i. The evolution process will not stop until predefined criteria are met.

"rand/1/bin"

$$u_{i,j,G} = \begin{cases} x_{r1,j,G} + F \cdot (x_{r2,j,G} - x_{r3,j,G}), & \text{if rand} < C_r \text{ or } j = j_{rand}, \\ x_{i,j,G}, & \text{otherwise.} \end{cases} \tag{4.5}$$

"rand/2/bin"

$$u_{i,j,G} = \begin{cases} x_{r1,j,G} + F \cdot (x_{r2,j,G} - x_{r3,j,G}) & \\ +F \cdot (x_{r4,j,G} - x_{r5,j,G}), & \text{if rand} < C_r \text{ or } j = j_{rand}, \\ x_{i,j,G}, & \text{otherwise.} \end{cases} \tag{4.6}$$

"current-to-rand/1"

$$\overrightarrow{u}_{i,G} = \overrightarrow{x}_{i,G} + \text{rand} \cdot (\overrightarrow{x}_{r1,G} - \overrightarrow{x}_{i,G}) + F \cdot (\overrightarrow{x}_{r2,G} - \overrightarrow{x}_{r3,G}). \tag{4.7}$$

4.3 Defect Detection based on Optimal Gabor Filters

During real-time defect detection, inspection fabric images are filtered by the optimal Gabor filters horizontally and vertically. As shown in Fig. 4.3, it is impossible to segment the defects barely from the original gray-level information. However, filtered by the horizontal and vertical Gabor filter obtained by the previous procedure in last section, defects can be efficiently highlighted from the gray value of the output feature images shown in Figs. 4.3(c) and 4.3(d).

(a) original inspection image

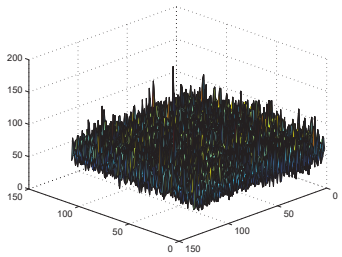

(b) 3D visualized gray-level intensities of original image

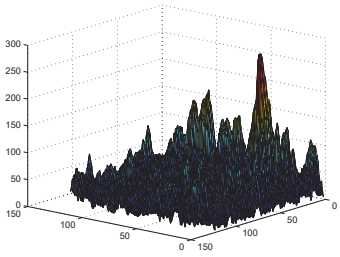

(c) 3D visualized gray-level intensities of horizontally filtered image

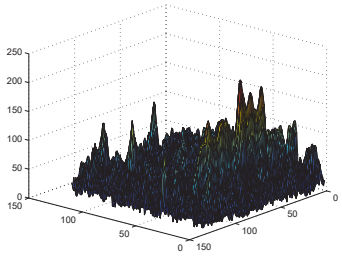

(d) 3D visualized gray-level intensities of vertically filtered image

Figure 4.3: Example of optimal Gabor filtering effect.

4.3.1 Adaptive Thresholding

According to the objective function introduced in Section 4.2.1 and the filtering results shown in Fig. 4.3, the local energy of feature image will

be at the minimum when the optimal Gabor filter covers a homogeneous area and, conversely, at the maximum for an inhomogeneous area. As a result, a simple statistic technique that follows the spectral filtering could distinguish defective pixels from homogeneous pixels in the feature image. Thresholding technique is applied to the filtered image that resultes from the optimal Gabor filter. Before thresholding operation, all filtered images are first normalized by using:

$$f_s(x,y) = \frac{f(x,y) - \min(f(x,y))}{\max(f(x,y)) - \min(f(x,y))}. \tag{4.8}$$

In the normalization of the filtered image, the maximum and minimum gray-level intensities $max(f(x,y))$ and $min(f(x,y))$, respectively, should be selected from the whole range of gray-level intensities of the filtered defective and non-defective images. Otherwise, the comparability between two images will be lost.

Thresholding limits are derived from the feature image of a non-defective reference sample, which is filtered by the optimal Gabor filters. The gray-level intensity of the feature image is denoted as $R(x,y)$. The upper and lower thresholding limits are

$$\psi_{upper} = \max_{x,y \in W} |R(x,y)|, \tag{4.9}$$

$$\psi_{lower} = \min_{x,y \in W} |R(x,y)|, \tag{4.10}$$

where W is a window centered at the feature image. Then, the two thresholding limits ψ_{upper} and ψ_{lower} are obtained within window "W" from the feature image of a non-defective sample. The window size is obtained by removing 10 pixels from each side of the image $R(x,y)$ to avoid the distortion

effects caused by the borders of image [12].

It is assumed that the response of defective texture drops out the range which is determined by thresholdings obtained from non-defective samples. Hence, the binary image $B(x, y)$ which represents the features of defects could be obtained by

$$B(x,y) = \begin{cases} 1, & \text{if } G(x,y) > \psi_{upper} \text{ or } G(x,y) < \psi_{lower}, \\ 0, & \text{otherwise.} \end{cases} \tag{4.11}$$

4.3.2 Binary Image Fusion

After threshold processing, two binary feature images are obtained, which represent the feature of defects horizontally and vertically, respectively. Given that these two feature images are the filtered results in a pair of perpendicular directions, they are not cross-correlated with each other. Thereafter, the final step of the proposed detection model is to fuse these two binary feature images to illustrate the whole defect detected by the optimal Gabor filters, as shown in Fig. 4.2. The final detection result is obtained by combining the binary feature outputs of the horizontal and vertical optimal filters with "OR" operation

$$B = B_h \vee B_v, \tag{4.12}$$

where B is a binary image that denotes the final detection result. B_h and B_v are the binary feature outputs of horizontal and vertical optimal Gabor filters, respectively. Symbol "$\vee$" denotes logical operator "OR".

4.4 Experiment Results and Discussion

In this section, the performance of the proposed plain fabric defect detection model is evaluated by using a database that comprises 91 non-defective and 91 defective fabric samples acquired from an apparel factory in Mainland China and scanned from the fabric defect handbook [25]. These fabric samples contained common types of defects that always appear in the textile industry. First, the experimental setup is introduced in detail. Second, the experiments are conducted from two aspects, namely, (1) the proposed detection model is applied for defect detection of the fabric database and (2) with the same fabric samples, the performance of the proposed defect detection model is compared with the other four popular models.

4.4.1 Experimental Setup

Images used in the experiments are acquired in two ways. Images of real defect fabric samples were captured with a digital camera under day light and flashlight. All images are of 256×256 pixels. Images from the fabric defects handbook were scanned with 300×300 dpi. The defective plain fabric samples mainly consist of slub, burl mark, broken end and broken pick. Table 4.1 gives specific information related to images used in the experiments. All detection models used in the experiments are realized under the image processing toolbox of MATLAB prototyping environment. Experiments are conducted on a personal computer with a Win8 operating system and an Intel core i7 processor. The performance of the defect detection model is visually assessed with binary feature images. In this research, the following four measurements (expressed as percentages) are employed to evaluate the performance of defect detection models:

$$Precision = \frac{\text{TA}}{\text{TA+FA}}, \tag{4.13}$$

$$Sensitivity = \frac{\text{TA}}{\text{TA+FN}}, \tag{4.14}$$

$$Specificity = \frac{\text{TN}}{\text{TN+FA}}, \tag{4.15}$$

$$Accuracy = \frac{\text{TA+TN}}{\text{TA+TN+FA+TN}}, \tag{4.16}$$

where correct detection with good localization is recoded as true alarm (TA). Hence white pixels in the detection result cover only the defective area from the original image. False alarm (FA) means that white pixels appear in the detection result of a non-defective sample. True normal (TN) is recorded if no white pixels appear in the detection result of a non-defective sample. Conversely, false normal (FN) is recorded when no white pixels appear in the detection result of a defective sample.

Table 4.1: Properties of testing images

	Real fabric samples	**Defects handbook samples**
Device	Canon 600D	Scanner
Light	camera flashlight	–
Resolution	256×256	256×256
dpi	72	300×300

The selected Gabor filters will slide over the entire image on a pixel-by-pixel basis such that the corresponding energy of every pixel in the image could be determined. To compromise between detection rate and computational cost, the size of the Gabor filter mask was set as 7×7 [12]. The population size of CoDE is 50. Theoretically, the value range of parameter f_0 should be 0 to 1 Hz. However, according to the specific optimization problem in this paper,

the value range of f_0 is constrained to $[\frac{1}{N}, 0.5]$, where N is the size of the reference image. The constraint is not mandatory, but it helps increase search efficiency of the optimization algorithm. The value ranges of other parameters in the Gabor filter optimization are listed below.

Table 4.2: Value ranges of parameters

	f_0	B	λ
Value range	$[0, \frac{N}{10}]$	$[0.5, 1.5]$	$[0.5, 2]$

4.4.2 Performance Evaluation of the Proposed Defect Detection Model

The inspection of plain fabric was performed in accordance with the flowchart shown in Fig. 4.2. Typical detection results are shown in Figs. 4.4, 4.6, and 4.8. The images in the first column are the original defective images. The images in the second and third columns are the filtered outputs of the horizontal and vertical optimal Gabor filters, respectively. The images in the fourth column show the final binary detection results after thresholding and the image fusion in the second and third columns. The proposed detection model could successfully segment the defects of various shapes, sizes, and positions. Table 4.3 summarizes the overall testing results by using the proposed defect detection model on plain fabric inspection. The four measurements provide the evaluation of the detection model from different aspects. *Precision* indicates the percentage of correct alarms during detection. *Sensitivity* indicates the percentage of defective samples that are correctly detected. *Specificity* is the percentage of non-defective samples that are correctly classified as normal. *Accuracy* indicates the percentage of correct classification of all testing samples.

Fig. 4.4 shows the detection results of four defect samples on a piece of light blue plain fabric. These defects are snags, oil stain, and spot. Fig. 4.4(a) is

Table 4.3: Performance evaluations of the proposed defect detection model

	Precision	**Sensitivity**	**Specificity**	**Accuracy**
Performance	93.5%	95.6%	93.3%	94.4%

selected as the reference image in the Gabor filters optimization of the defect detection model. The horizontal and vertical optimal Gabor filters obtained by CoDE are shown in Fig. 4.5. For the sake of clear illustration, the size of filter mask is set as 19×19 in Figs. 4.5 and 4.7. The last column of binary feature images shows detection results. It is noticed that all defects are correctly detected and located, though there is a tiny false detection in the first fabric sample, which can be eliminated if learning schemes are included in the detection model later. Moreover, even though the defect sample used in the Gabor filter optimization process is a broken yarn with snag, defects of oil stain and spot in the third and fourth fabric samples, respectively, are well detected. These results indicate that the proposed defect detection model is effective for structural fabric defects, which alter the textural property of an image, and for tonal fabric defects, which change the tonal property rather than the fabric structure.

In Fig. 4.6, the two defect samples were obtained from a piece of white plain fabric. The images taken by a digital camera are underexposed because the white background of the fabric is too bright. These two defects are different shapes of color stain. However, by applying the proposed defect detection model, both defects were segmented from the fabric texture background by the same optimal Gabor filters, as shown in Fig. 4.7. These experimental results further verify the effectiveness of the proposed model for detecting various types of fabric defects. In addition, the optimal Gabor filtering operation in the proposed detection model is even robust to various illumination conditions as long as the contrast between defective and non-defective area is satisfied. Fig. 4.8 presents more detection results on plain fabric. Given that the weaving structure of plain fabric leads to a smooth

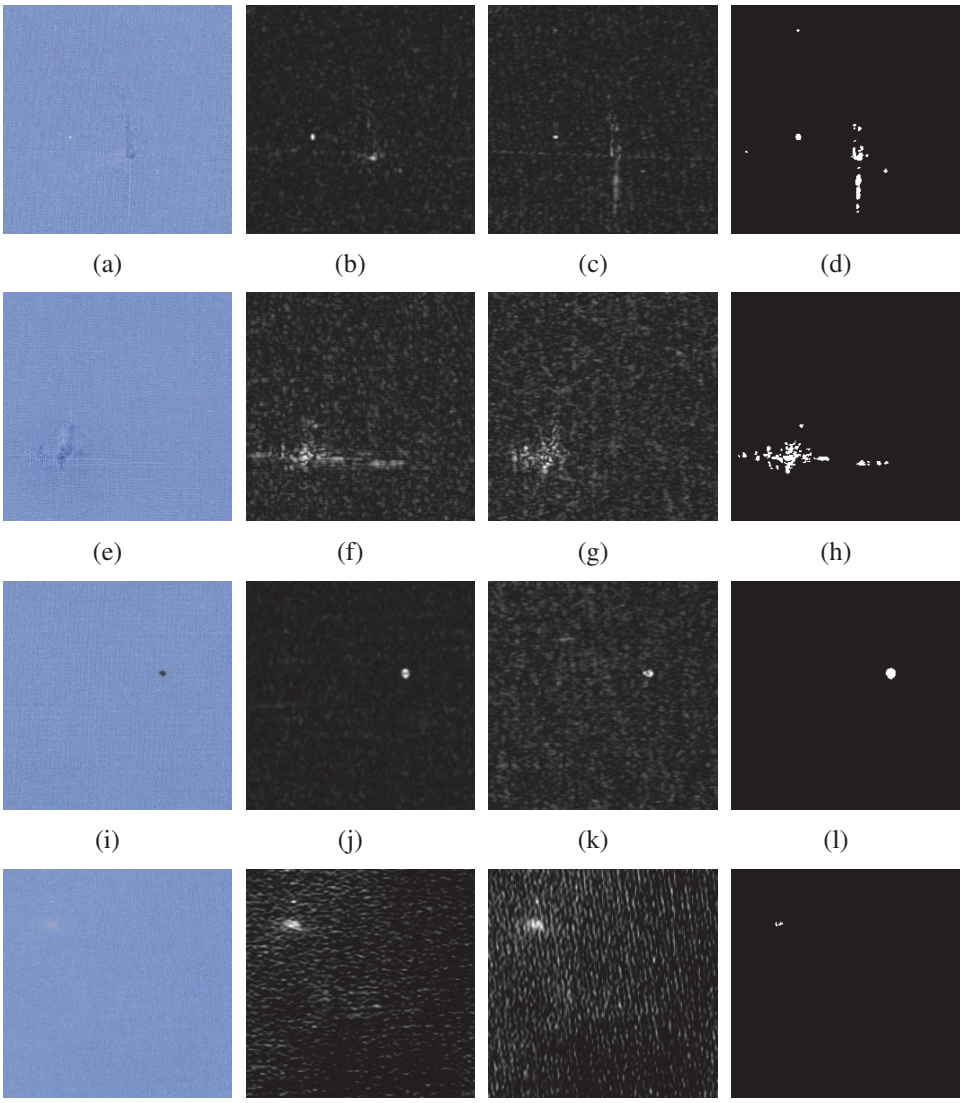

Figure 4.4: Detection results for a piece of light blue plain fabric.

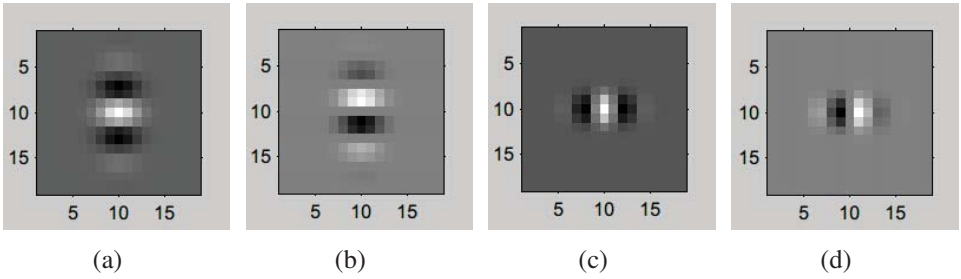

Figure 4.5: Optimal Gabor filters for the inspection of fabric samples in Fig. 4.4.

and even surface, the contrast between defects and background texture is normally high. Therefore, utilizing optimal Gabor filters as edge detectors, the proposed detection model could achieve outstanding performance in the inspection of plain fabric.

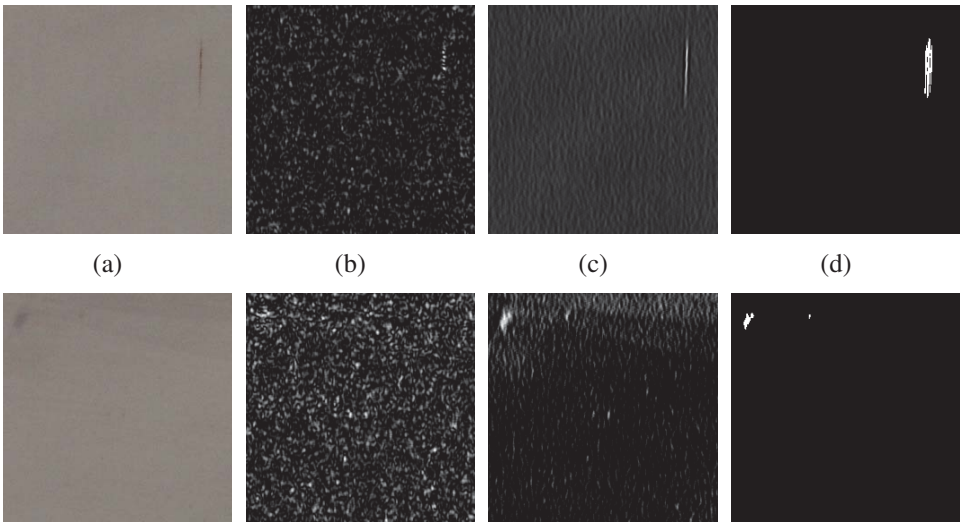

(a) (b) (c) (d)

(e) (f) (g) (h)

Figure 4.6: Detection results for a piece of white plain fabric.

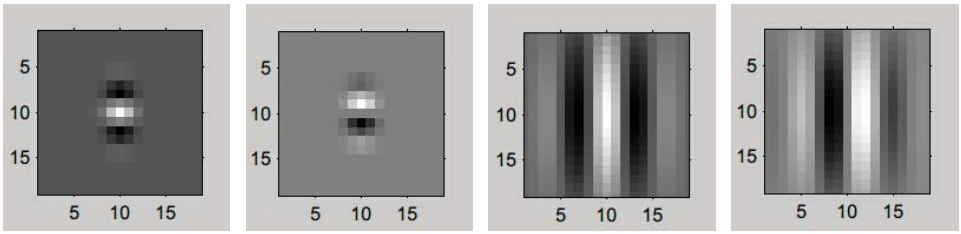

(a) (b) (c) (d)

Figure 4.7: Optimal Gabor filters for the detection of fabric samples in Fig. 4.6.

4.4.3 Comparison of Proposed Model and Other Four Popular Models

To further verify the effectiveness of the proposed model for plain fabric inspection, the detection performance of the model is compared with that of the other four popular detection approaches. The evaluations are under the same environment and based on the initial set of 91 defective and 91 non-

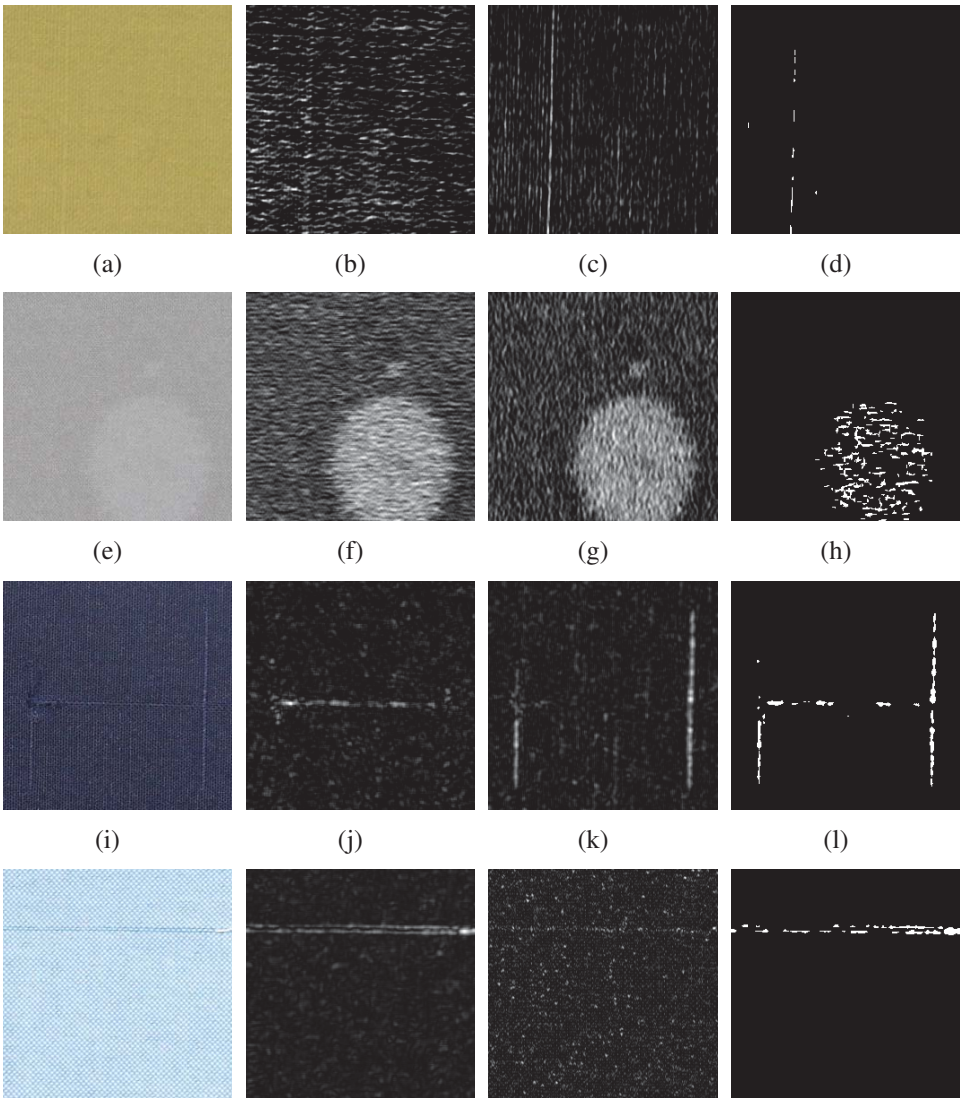

Figure 4.8: Detection results of plain fabric.

defective fabric samples. Among the four selected models, the first one is based on a Gabor filters bank, which consists of 18 Gabor filters [12]. This method is widely considered a classic fabric defect detection model. The second and the third models are based on optimized Gabor filters [77, 79]. The main difference is in their optimization algorithms. The last model selected for comparison utilizes wavelet shrinkage after Fourier analysis of test images to accentuate the features of defects [11]. This process is considered one of the latest spectral methods for fabric defect detection. Therefore, these four models are used in comparison experiments. Source codes of the approaches in [11, 79] are obtained from the author of these two references. The approaches in [12, 77] are programmed by the author in this research.

Table 4.4 shows that the detection model proposed in this research outperforms the other four popular models in all four aspects. The comparison results of time performance are summarized in Table 4.5 in terms of average operation time (AOT) consumed in processing each fabric image sample. The AOT further proves that the proposed model is the most effective and efficient for detecting plain fabric defects.

Table 4.4: Performance comparison of defect detection models

	Precision	**Sensitivity**	**Specificity**	**Accuracy**
Model in [12]	81.3%	82.2%	81.1%	81.7%
Model in [77]	84.6%	80%	85.5%	82.8%
Model in [79]	88.7%	84.9%	89.2%	87.7%
Model in [11]	78.5%	88.9%	75.4%	81.7%
Proposed model	**93.5%**	**95.6%**	**93.5%**	**94.4%**

Table 4.5: Time cost comparison of defect detection models

	AOT(s)
Model in [12]	0.24
Model in [77]	0.12
Model in [79]	0.16
Model in [11]	0.42
Proposed model	**0.07**

In Figs. 4.9 and 4.10, the second to the fifth rows are the detection results

obtained by the models in [12], [77], [79], and [11], respectively. The figures in the last row are the detection results obtained by the proposed model. The proposed detection model distinguished all defect samples and is the best one among all models in the following ways: First, the detection results in the second column are relatively close to those of the proposed model. However, the computational time is longer than that of the proposed model, because 17 more Gabor filters are utilized in [12]. Second, compared with the models in [77] and [79], the proposed model achieved better results even in detecting defects with subtle intensity changes because non-defective and defective samples are employed in the Gabor filter optimization. Moreover, as the stability of the SA optimization algorithm utilized in [79] is not high, the solutions of Gabor filter optimization usually fall in local optima. Therefore, the shapes of the detection results are usually incomplete. Finally, many false detections emerged in the results obtained by the detection model in [11]. Becasue Fourier analysis was unable to accurately distinguish the frequency components between normal fabric texture and defective texture, which resulted in poor defect segmentation and misclassification of the normal area.

In all, according to the statistical results stated in Tables 4.4 and 4.5, with the utilization of optimal Gabor filters, a relatively high defect detection rate has been ensured by the proposed detection model, which performs well in feature extraction of plain fabric defects. Moreover, comparing with the existing approaches, the detection efficiency has been significantly improved.

4.5 Summary

This chapter presents the automated and efficient defect detection model proposed for plain fabric inspection. This model has two modules, namely, Gabor filters optimization (offline) and defect detection (real-time). First,

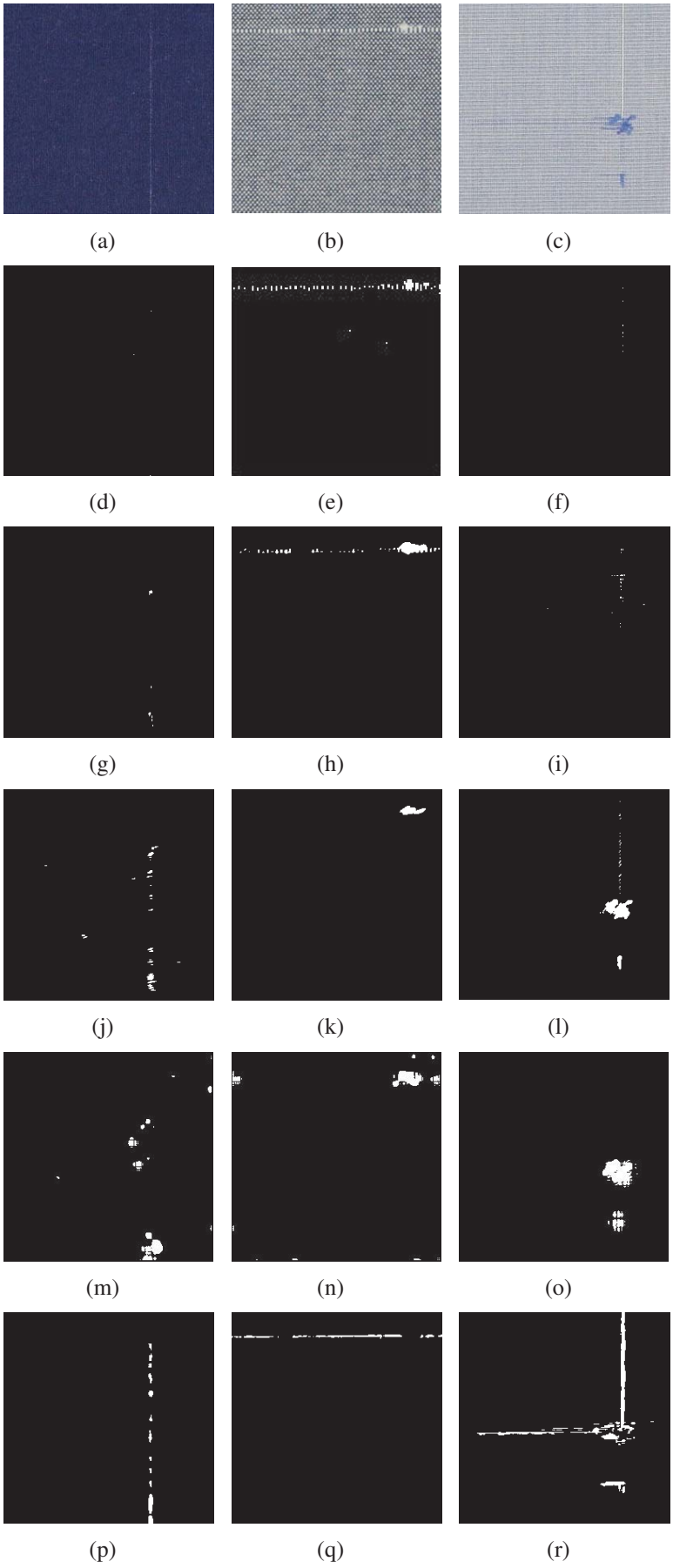

Figure 4.9: Results of comparison experiments on real fabric samples.

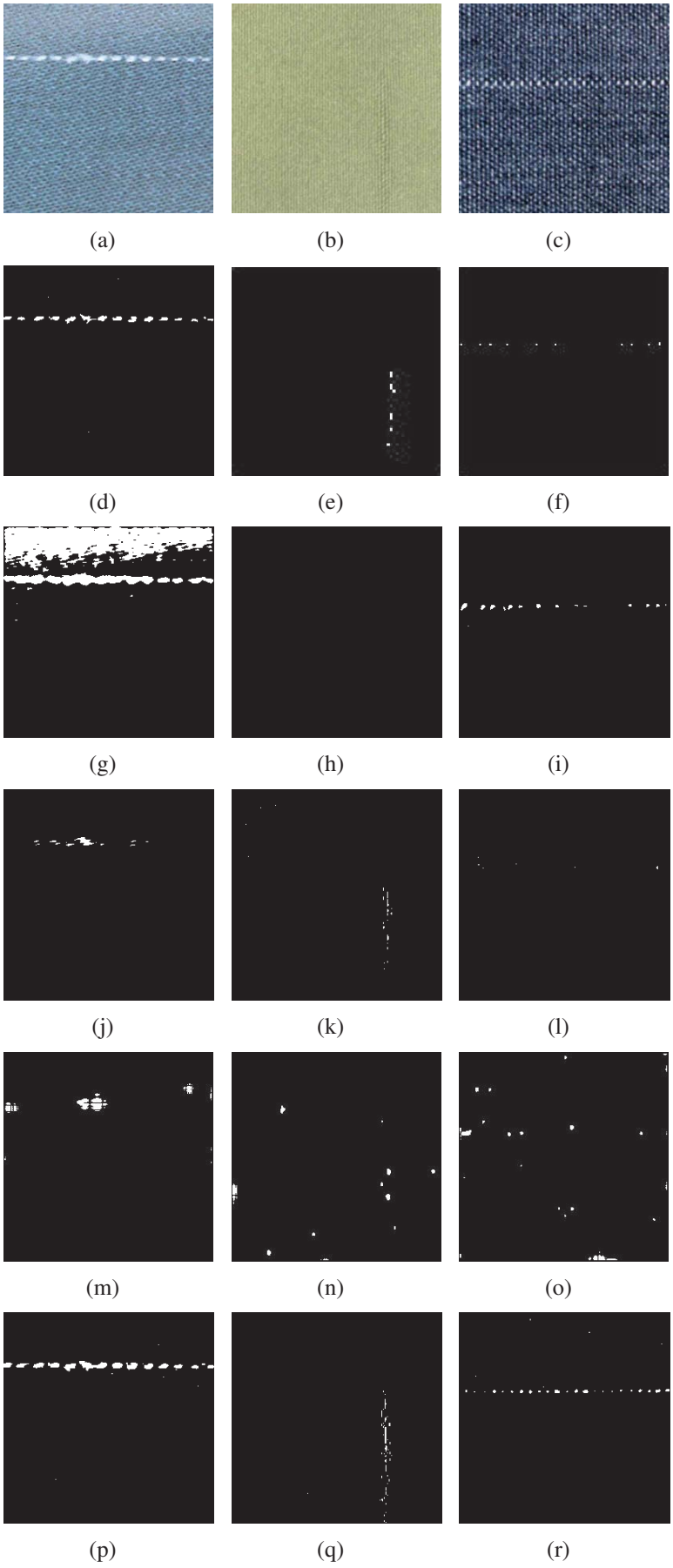

Figure 4.10: Results of comparison experiments on scanned fabric samples.

Gabor filter optimization problem is designed according to the features of defects and standard fabric texture, such that the best texture discrimination is easier to achieve. With the use of CoDE, global optimal Gabor filters, which best segment the defects from the fabric texture background, are obtained. Second, on the basis of the analysis of the orientation features of fabric defects, the real-time defect detection module, which employs only two optimal Gabor filters together with thresholding and fusion operations, is capable of successfully locating fabric defects. Therefore, the computational cost of the whole model is greatly reduced.

Extensive experiments were conducted. The performance of the proposed defect detection model is evaluated based on real fabric samples. A series of results demonstrates its effectiveness on the detection of defects of various shapes, sizes, and locations. The proposed defect detection model achieves a high successful detection rate and low false alarm rate. Comparative experiments were conducted based on four popular detection models. Detection results illustrate that the proposed defect detection model performs the best in terms of detection accuracy and efficiency.

Chapter 5

Nonlocal Sparse Representation-based Defect Detection Model for Twill Fabric Inspection

Compared with plain fabric, the weaving structure of twill fabric is more complicated. Hence, detection of twill fabric defects is more challenging. The twill fabric inspection problem will be investigated from the view of image denoising, instead of feature extraction. A novel defect detection model will be developed for twill fabric in this chapter.

5.1 Framework of Twill Fabric Inspection Model

On the basis of an observation of several defective samples of twill fabric shown in Fig. 5.1, twill fabric is associated with a texture of diagonally parallel ribs, whose orientation is variable with different weaving methods. Therefore twill defects are usually not as sharp as plain fabric defects. On

the one hand, when filtered by Gabor filters, the filtering response of rib weaving texture will cause a significant disturbance to the detection results. On the other hand, extracting the features of defects which are mixed with the weaving texture by using the existing approaches, such as statistical methods and spectral methods, is greatly difficult. Fabric defects that appear as anomalous arrayed pixels could be regarded as noise in the image. Thus, no matter structural or tonal fabric defects, defects can be treated as singular points that do not belong to the normal fabric texture. Similar to image denoising, image restoration-based model first tends to estimate non-defective versions of input images through sparse coding on the basis of a selected dictionary. Possible defects could be segmented from residual images of the inputs and their estimations.

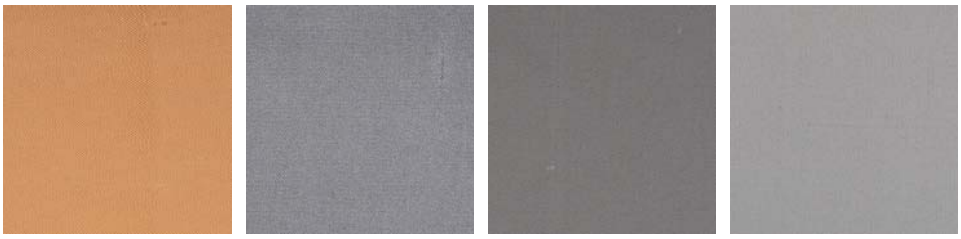

(a) (b) (c) (d)

Figure 5.1: Defective samples of twill fabric.

The selection of dictionary influences accuracy of normal fabric texture restoration, which in turn will affect the false alarm rate of the detection model. An over-complete dictionary is able to provide sufficient basic information for image restoration. Meanwhile compact sub-dictionaries reduce the instability caused by sparse coding over an over-complete dictionary and are more efficient because of high periodicity and refined structure of fabric texture. Therefore, K-means clustering and PCA are adopted to generate compact sub-dictionaries from non-defective fabric images.

Moreover, conventional sparse coding models, such as the regression model, do not perform well in eliminating local noise, and thereby detection accuracy on small defects is affected. By exploiting the rich amount of non-local

feature redundancies of images, the detection accuracy of defects that appear as small outliers in the image will be significantly improved.

On the basis of the above discussion, a defect detection model based on non-locally centralized sparse representation is developed to address the twill fabric inspection problem. First, all images are preprocessed through gray-level transformation to enhance image contrast. Then, the approximation images of the input images are constructed based on adaptive compact sub-dictionaries, which are obtained from non-defective samples. Finally, possible defects in the residual image of the input image and its approximation are segmented by solving the simple thresholding problem. A flowchart of the proposed defect detection model is given in Fig. 5.2. The entire model consists of two main modules, namely, dictionary learning, which is an offline process, and defect detection, which can be executed in real time. The details of each operation will be introduced in the following sections.

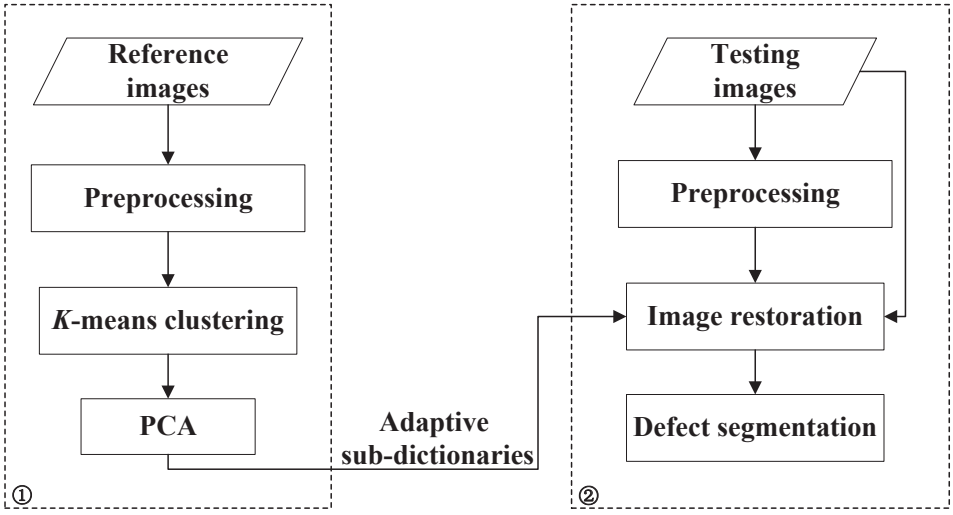

Figure 5.2: Flowchart of the twill defects detection process: ① dictionary learning; ② detection model.

5.2 Preprocessing via Gray-level Transformation

Generally, fabric texture is synthetic and quite refined because of the fine raw materials and precise weaving structure. The contrast between small defect and the background will be influenced when the detail of the fabric texture is not well presented in the digital image. As a result, the discrimination of defects and normal fabric texture is a difficult task. Moreover, as the textile material usually absorbs dust in the air, noise is hard to avoid in the image and is sometimes mixed with the defects, which could increase the omission ratio or the false alarm rate. To increase the contrast of the input images and highlight the possible fabric defects, preprocessing is introduced into the system before detection operation.

Among all contrast enhancement operations, such as log, gamma, and contrast-stretching transformation, gray-level transformation is the simplest and most straightforward one. Log transformation maps a narrow range of low gray-level intensities into a wider range output, which is useful for highlighting dark but important details. However, the method comprises the dynamic range of the images and therefore the contrast of the image as well. Gamma transformation is more versatile than log transformation, because different transformation curves could be obtained through varying its parameters. However, in a real fabric inspection environment, adjusting the Gamma transformation parameter online to adapt to different colors of fabric images is impractical. The preprocessing operation adopted in this research is contrast-stretching transformation whose function is as follows:

$$\mathbf{s} = T(\mathbf{r}) = \frac{1}{1 + (\frac{m}{\mathbf{r}})^{\varepsilon}}, \tag{5.1}$$

where $\mathbf{r}$ denotes the intensities of the input image; $\mathbf{s}$ is the corresponding intensity of the output; ε and m control the slope and the center of gravity

of the transformation function respectively. The gray-level range under m will be compressed. By contrast, the gray-level range under m will expand. Therefore, the result of the transformation function is an image of higher contrast. Normally, the value of m is set as the median value of the input gray-level intensities. In other words, the value could be adaptively selected according to different image samples, which increases the degree of freedom of preprocessing. The value of ε depends on desired gray-level range $[LL, HL]$ of the output image

$$\varepsilon_1 = \log_{\frac{m}{\min(\mathbf{r})}} \left(\frac{1}{LL-1} \right), \tag{5.2}$$

$$\varepsilon_2 = \log_{\frac{m}{\max(\mathbf{r})}} (\frac{1}{HL-1}), \tag{5.3}$$

$$\varepsilon = \lceil \min(\varepsilon_1, \varepsilon_2) \rceil . \tag{5.4}$$

Fig. 5.3 shows several examples of the preprocessing results. Defects in the original images are too subtle to notice. However, after preprocessing, the dynamic range of the image is obviously expanded. The contrast between defects and texture background is thus greatly enhanced.

5.3 Image Restoration based on Sparse Representation

The involvement of normal fabric texture information in sub-dictionaries, according to fabric structural information, requires dividing patches of non-defective fabric images into several classes by *K*-means clustering. The sub-dictionary learnt from each cluster is adaptively selected to provide the most relevant basis in the sparse representation of fabric texture. With the learned dictionary, non-locally centralized sparse representation model is adopted to

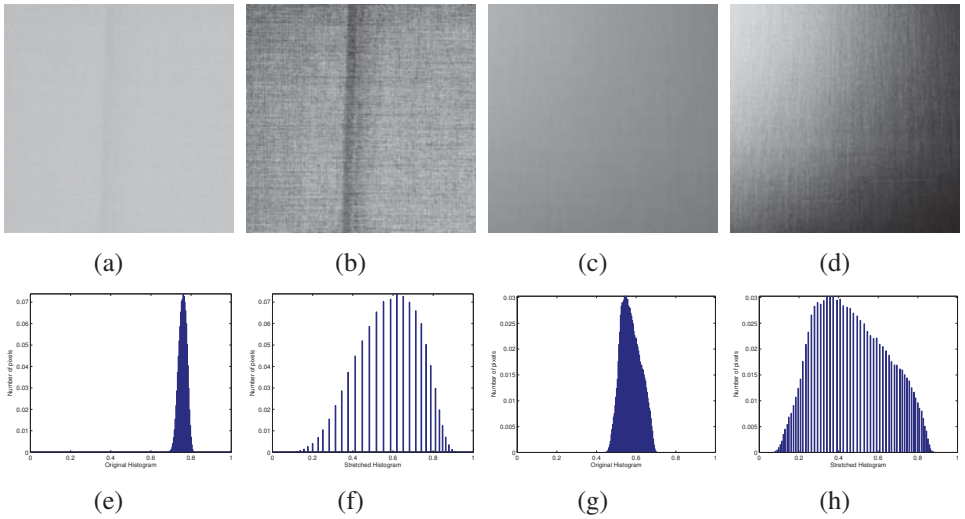

Figure 5.3: Examples of preprocessing results. (a) and (c) are the original images. (b) and (d) are the images preprocessed by contrast-stretching transformation. (e) - (h) are the corresponding histograms of the images in the first row.

find a sparse vector $\boldsymbol{\alpha} = [\alpha_1; \alpha_2; ...; \alpha_m]$, such that $\hat{\mathbf{x}} = \boldsymbol{\Phi}\boldsymbol{\alpha}$. Exploiting non-local redundancies in an image ensures that possible fabric defects could be successfully eliminated in the restored non-defective version of the input image. In the rest of this section, sparse representation of fabric texture based on learnt dictionaries is illustrated in detail.

5.3.1 Adaptive Sub-Dictionary Learning

Nowadays, the appearance of textiles changes because of the development of fabric design. Even for uniform texture fabric, texture structure could vary significantly across images, as shown in Fig. 5.4. With different weaving method, the fabric textures exhibit slight differences in their structure elements. Therefore, non-defective fabric images are divided into small patches, which could be clustered according to their structural features. Each cluster of patches represents a kind of fabric texture element. The objective of sparse representation is to find a linear combination of a small number of basic atoms to restore the signal with minimal approximation error. Thus, effective representations of testing patches are easily to obtain over sub-

dictionaries learned from each cluster of fabric image patches. Suppose that $\mathbf{x}_i = \mathbf{R}_i\mathbf{x}, i = 1, 2..., N$, is the i^{th} patch vector of image $\mathbf{x}$, where $\mathbf{R}_i$ is a matrix extracting patch $\mathbf{x}_i$ from $\mathbf{x}$. The estimation of $\mathbf{x}$ could be denoted as the average of all restored patches $\hat{\mathbf{x}}_i$, which can be formulated as the following function [112]:

$$\hat{\mathbf{x}} = \mathbf{\Phi} \circ \boldsymbol{\alpha} = \left(\sum_{i=1}^{N} \mathbf{R}_i^T \mathbf{R}_i \right)^{-1} \sum_{i=1}^{N} (\mathbf{R}_i^T \mathbf{\Phi}_{k_i} \boldsymbol{\alpha}_i), \tag{5.5}$$

where operation "$\circ$" is defined for convenience of expression; $\mathbf{\Phi}_{k_i}$ represents the k^{th} sub-dictionary, which is selected to restore the i^{th} image patch, and $\boldsymbol{\alpha}_i$ denotes the coefficient of the sparse representation of the i^{th} image patch.

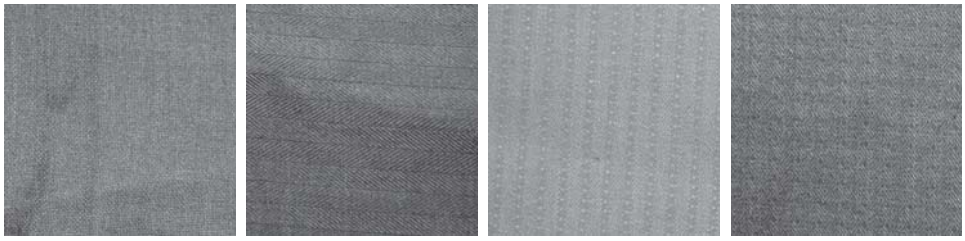

(a) (b) (c) (d)

Figure 5.4: Gray-level examples of different patterns of white woven fabric.(a) is plain weaving pattern; (b) is twill weaving pattern; (c) and (d) are jacquard weaving patterns.

To better suppress noise and block artifacts [113, 114], N overlapping image patches, denoted by $\mathbf{S} = [\mathbf{s}_1, \mathbf{s}_2, ..., \mathbf{s}_N]$, are cropped from non-defective fabric samples that are selected as reference images. Suppose that K distinctive fabric texture elements are involved in all image patches. Hence, dataset $\mathbf{S}$ can be clustered into K clusters, from each of which a sub-dictionary could be learned. Subsequently, for a given image patch, the most suitable structure basis could be selected from $\mathbf{\Phi}_k$. To obtain clusters that are associated with fabric structure texture, image clustering is conducted in the feature space. As shown in Fig. 5.4, most of the semantic information of the fabric texture is conveyed by the edges in the image. High-pass filtering is able to enhance the edges and structures in the image, as well as reduce the disturbance of

pixel intensity variations between different image samples. Therefore, the outputs of high-pass filtering are utilized as the features for the classification of non-defective image patches. Given the low computational cost and easy implementation, *K*-means algorithm is adopted to divide $\mathbf{S}^h$, which denotes the high-pass filtered patch set, into K sub-sets. The centroid of each cluster $\mathbf{S}_k^h, k = 1, 2, ..., K$ is denoted by $\boldsymbol{\mu}_k$. Consequently, the clustering result of the original image patches is denoted by $\mathbf{S}_k, k = 1, 2, ..., K$.

The next step of dictionary learning is to obtain a sub-dictionary $\boldsymbol{\Phi}_k$ from a cluster $\mathbf{S}_k$ such that $\hat{\mathbf{S}}_k = \boldsymbol{\Phi}_k \boldsymbol{\alpha}_k$. As the representation coefficient is required to be as sparse as possible, the solution of $\boldsymbol{\Phi}_k$ is usually solved by iteratively minimizing $\boldsymbol{\Phi}_k$ and $\boldsymbol{\alpha}_k$ in the following function [101]:

$$(\hat{\boldsymbol{\Phi}}_k, \hat{\boldsymbol{\alpha}_k}) = \arg\min\{\| \mathbf{S}_k - \boldsymbol{\Phi}_k \boldsymbol{\alpha}_k \|_F^2 + \lambda \| \boldsymbol{\alpha}_k \|_1\}. \tag{5.6}$$

where $\| \cdot \|_F$ is the Frobenius norm.

However, the joint optimization problem of Eq. (5.6) is time consuming. Moreover, the solution of this function is normally an over-complete dictionary, which is unsuitable for the problem of fabric image representation. On the one hand, when representing a specific type of fabric structure element, only limited elements are involved in each sub-set $\mathbf{S}_k$. On the other hand, elements in one sub-set are highly correlated with each other, such that an over-complete dictionary may cause data redundancy in sparse coding. In [115], PCA was found to be suitable for learning sub-dictionaries. PCA can extract the principal components of a set of possibly correlated data, which reveals the internal structure of the data. With regard to fabric image patches, the differences of weaving structure among a cluster are not large. Therefore, in the proposed model, PCA is applied on each cluster of image patches $\mathbf{S}_k$ to achieve a set of values of linearly uncorrelated variables that compose a compact dictionary $\boldsymbol{\Phi}_k$. A compact dictionary is sufficient for

sparse representation of an image patch and reduces the computational cost of the model. Fig. 5.5 shows examples of sub-dictionary learnt from the training dataset. The centroids of two clusters are shown in the first column. The other columns show the first several atoms in the corresponding sub-dictionaries.

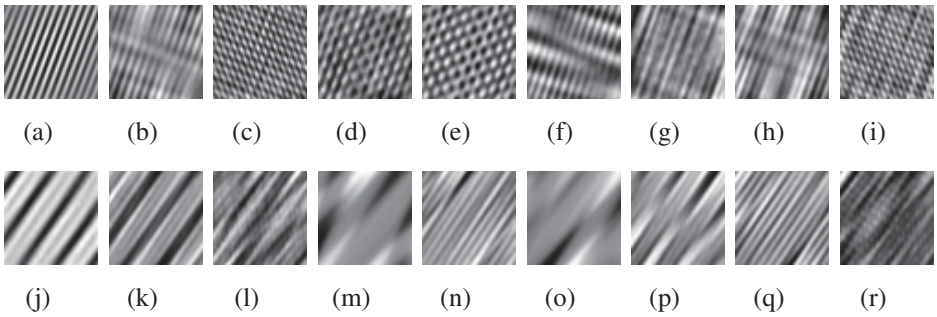

Figure 5.5: Examples of sub-dictionaries. (a) and (j) demonstrate the centroids of two sub-dictionaries after *K*-means clustering. (b) - (i) show the nearest eight atoms to the centroid of the first cluster. (k) - (r) show the nearest eight atoms to the centroid of the second cluster.

All sub-dictionaries together could be deemed as an over-complete dictionary that characterizes all the local fabric structures. Thus, instead of a universal and over-complete dictionary, a sub-dictionary is beneficial for avoiding the visual artifacts and the considerable calculation generated by sparse coding over a redundant dictionary.

The sub-dictionaries learned from clustered image patches adaptively exploited the local structure information of images. Thus, for a given local image patch, the assignment of appropriate sub-dictionary could be adaptively accomplished in the real-time model. Owing to the characteristic of fine structure of fabric texture, the average noise level of fabric images is relatively low. Therefore, the cluster attribute of a given image patch $\mathbf{y}_i$ is directly decided by the distance between its high-pass filtering output $\mathbf{y}_i^h$ and the centroid $\boldsymbol{\mu}_k$ of every cluster. The dictionary for image patch $\mathbf{x}_i$ is selected by the following function:

$$k_i = \arg\min_k \parallel \mathbf{y}_i^h - \boldsymbol{\mu}_k \parallel_2, \tag{5.7}$$

where k_i represents the sequence number of sub-dictionary for the i_th image patch.

5.3.2 Sparse Representation Model based on Nonlocal Similarities

Unlike uniform distributed and Gaussian distributed noise, the distribution of fabric defects in the image does not follow any specific rules or patterns. Fabric defects usually occupy only a small proportion of area in the image, which could be treated as outliers in the image. Moreover, the conventional regression model only performs well in removing Gaussian distributed noise. This feature makes such singular point noise removal is difficult by approximating the high quality image **x** from the observed image **y** barely on the basis of the l_1 norm constraint. As discussed in [116], over a fixed dictionary, errors may occur between sparse codes of **x** and **y**, which are defined as sparse coding noise (SCN) $\mathbf{v}_\alpha = \boldsymbol{\alpha}_y - \boldsymbol{\alpha}_x$, where $\boldsymbol{\alpha}_x = \arg\min_\alpha \| \boldsymbol{\alpha} \|_0$, s.t. $\| \mathbf{x} - \boldsymbol{\Phi}\boldsymbol{\alpha} \|_2 \leq \varepsilon$. Obviously, restoration result could be significantly improved if suppressing the SCN is introduced into the sparse representation model. Therefore, the image restoration will be based on the non-locally centralized sparse representation model [116]:

$$\begin{aligned} \boldsymbol{\alpha}_y = \arg\min_{\boldsymbol{\alpha}} \{ \| \mathbf{y} - \boldsymbol{\Phi} \circ \boldsymbol{\alpha} \|_2^2 + \lambda \sum_i \| \boldsymbol{\alpha}_i \|_1 \\ + \gamma \sum_i \| \boldsymbol{\alpha}_i - \boldsymbol{\beta}_i \|_1 \}, \end{aligned} \tag{5.8}$$

where λ denotes the regularization parameter that controls the balance between the sparse approximation of **x** and the sparsity of $\boldsymbol{\alpha}$; and $\boldsymbol{\beta}_i$ is an estimation of $\boldsymbol{\alpha}_{\mathbf{x}_i}$; γ is the regularization parameter.

Generally, parameter $\boldsymbol{\beta}$ could be obtained from the sparse coding coefficients of images that are similar to the input image. Repetitive structures found in the fabric image for any local texture feature lead to deriving $\boldsymbol{\beta}$ from the input testing image itself. Moreover, it is found in [116] that the sparse coding coefficients are correlated, instead of random distribution. Owing to the high structural periodicity of fabric texture, local and non-local redundancies appear in the images, which mean that the spatially separated patches are still likely to have similar patterns. Thus, for a given i_{th} patch, the nonlocal similar patches could be searched in a large widow centered at pixel i. Then, $\boldsymbol{\beta}_i$ is computed as the weighted average of the sparse coefficients associated with nonlocal similar patches to the i_{th} patch:

$$\boldsymbol{\beta}_i = \sum_{q \in \boldsymbol{\Omega}_i} \omega_{i,q} \boldsymbol{\alpha}_{i,q}, \tag{5.9}$$

where $\boldsymbol{\Omega}_i$ denotes a set of image patches that are similar to the i_{th} patch; and $\boldsymbol{\alpha}_{i,q}$ represents the sparse coefficients of the q_{th} patch within set $\boldsymbol{\Omega}_i$; $\omega_{i,q}$ is the corresponding weight, which is inversely proportional to the distance between $\mathbf{x}_i$ and $\mathbf{x}_{i,q}$.

For eliminating fabric defects, which are regarded as outliers in the image, the non-locally centralized sparse representation model outperforms the conventional regression model. The former brings the structure information of non-defective areas in the testing image in the restoration of the estimated image. That is to say, the estimation of the normal structure features of the testing image is not only based on the adaptively selected sub-dictionary but also on non-local feature redundancies in the testing image itself to increase image restoration accuracy and the defect detection rate.

As discussed in Section 5.3.1, for the entire training dataset, the set of K compact sub-dictionaries could still be regarded as an over-complete dictionary. When one sub-dictionary is adaptively chosen in the sparse

coding, only a small number of atoms in the over-complete dictionary are selected. As a result, regularization constraint $\| \boldsymbol{\alpha}_i \|_1$ is satisfied. Hence, the non-locally centralized sparse representation model is adjusted as follows:

$$\boldsymbol{\alpha}_y = \arg\min_{\boldsymbol{\alpha}} \left\{ \| \mathbf{y} - \boldsymbol{\Phi} \circ \boldsymbol{\alpha} \|_2^2 + \gamma \sum_i \| \boldsymbol{\alpha}_i - \boldsymbol{\beta}_i \|_1 \right\}. \tag{5.10}$$

The surrogate algorithm, which is an iterative algorithm, is adopted to solve objective function in Eq. (5.10). $\boldsymbol{\beta}$ is first initialized as $\boldsymbol{\beta}^{(-1)} = 0$, in order to obtain the initial sparse coefficients $\boldsymbol{\alpha}_y^{(0)}$. Thus, the initial estimation of $\mathbf{x}$ is solved by $\mathbf{x}^{(0)} = \boldsymbol{\Phi} \circ \boldsymbol{\alpha}_y^{(0)}$. Thereafter, by searching similar patches from $\mathbf{x}^{(0)}$, the non-local estimation $\boldsymbol{\beta}^{(0)}$ can be updated through Eq. (5.9), which improved the accuracy of sparse representation coefficients in turn. This procedure is iterated until the convergence constraint is satisfied. With optimal sparse representation coefficients $\boldsymbol{\alpha}_y$, the estimation of the non-defective fabric image $\mathbf{x}$ could be represented as $\hat{\mathbf{x}} = \boldsymbol{\Phi} \circ \boldsymbol{\alpha}_y$, because only normal fabric structure information is admitted in the sub-dictionaries learned previously. Noise is greatly reduced in the restored image, and the defective areas would not be well presented.

5.4 Defect Segmentation

Similar to template matching, defect detection based on image denoising tends to segment possible defects through comparing the inspection image with a reference image. However, instead of a fixed template fabric image, the reference image used in this research is the non-defective image which is restored according to the most relevant basis.

Ideally, the possible fabric defects regarded as noise in the inspection image could be removed in the estimated version of the input image. In the residual

image of the inspection image and its estimation, the gray-level intensity of the defective area will be greater than that of the background area. Thus, a simple thresholding operation would distinguish defective pixels from the background in the residual image after image restoration.

The thresholding limits are derived from the reference residual image of a standard non-defective sample and its estimation which is restored by the procedures in Section 5.3. Instead of setting a fixed parameter, thresholding limits could be adaptively selected for each fabric type to achieve good detection results as much as possible. Meanwhile, the adaptively selected parameter is beneficial to reduce false alarm rate because the noise and blurry effects caused by dust will weaken in the restored image. Suppose that the gray-level intensity of the reference residual image is denoted as $\mathbf{R}(x, y)$. Then upper and lower thresholding limits are:

$$\psi_{upper} = \max_{x,y \in W} |\mathbf{R}(x, y)|, \tag{5.11}$$

$$\psi_{lower} = \min_{x,y \in W} |\mathbf{R}(x, y)|, \tag{5.12}$$

where W is a window obtained by removing 10 pixels from each side of the image $\mathbf{R}(x, y)$ to avoid distortion effects caused by the borders of the image. Hence, the binary feature image $\mathbf{B}(x, y)$ could be obtained by:

$$\mathbf{B}(x, y) = \begin{cases} 1, & \text{if } \mathbf{G}(x, y) > \psi_{upper} \text{ or } \mathbf{G}(x, y) < \psi_{lower}, \\ 0, & \text{otherwise}, \end{cases} \tag{5.13}$$

where $\mathbf{G}(x, y)$ denotes the gray-level intensities of the testing residual image.

5.5 Experiment Results and Discussion

The performance of the proposed fabric inspection model is validated through two databases. The first one is TILDA, which is created by a workshop on texture analysis of Deutsche Forschungsgemeinschaft Germany [74]. Samples in this database are gray-level images. Both structural and tonal defects are included, such as holes, chafed yarn, flying yarn and dye streak. The second one is a database created by the author, which consists of 102 non-defective and 102 defective fabric samples acquired from an apparel factory in Mainland China and scanned from the fabric defect handbook [25]. The most common types of defects that always appear in the textile and apparel industries are all involved in these fabric samples, such as thick yarn, missing yarn and rope mark. First, the proposed detection model is applied on fabric databases to demonstrate its effectiveness. Then, with the same fabric samples, the performance of the proposed defect detection model is compared with the other three representative detection models, namely, detection model based on Gabor filter bank [12], Fourier and wavelet-based model [11], and adaptive sparse representation-based model [16]. Source codes of these approaches are obtained from the authors and programmed in this research.

5.5.1 Experimental Setup

Four kinds of woven fabric with a relatively coarse texture are included in the TILDA database. Within each fabric type, four classes of defect were defined. For each of the above classes, 50 images (768×512 pixels) were acquired through relocation and rotation of the textile samples. In our own database, images of the real fabric samples were captured at 1050×1050 pixels by a digital camera Canon 600D. In the experiments, the image

processing toolbox of MATLAB prototyping environment was adopted to program all the detection models. Similar to the experiments in Chapter 4, the binary feature images, which denote the detection results, were visually assessed by experienced operators. Furthermore, the performance of defect detection models was evaluated according to *precision*, *sensitivity*, *specificity* and *accuracy*, which are clearly defined in Section 4.4.1. The rate of correct detection alarm is indicated by *precision*. *Sensitivity* indicates the detection rate of all defective samples. The rate of correct classification of non-defective samples is given in terms of *specificity*. *Accuracy* manifests the rate of overall correct classification of all testing samples.

5.5.2 Performance Evaluation of the Proposed Defect Detection Model

The inspection of twill fabric was conducted in accordance with the procedures shown in Fig. 5.2. Several representative detection results are shown in Figs. 5.6 - 5.9. For each fabric type, a set of non-defective image samples were collected as the training data in the dictionary learning. The binary result images revealed that defects of various shapes, sizes, and positions could be successfully identified by the proposed detection model. Tables 5.1 and 5.2 summarize the overall experimental results by using the proposed defect detection model on TILDA and our own database, respectively.

Table 5.1: Performance of the proposed detection model on TILDA

	Precision	**Sensitivity**	**Specificity**	**Accuracy**
Performance	92.0%	97.8%	91.5%	94.6%

Table 5.2: Performance of the proposed detection model on our own database

	Precision	**Sensitivity**	**Specificity**	**Accuracy**
Performance	92.5%	96.1%	92.2%	94.1%

Fig. 5.6 shows the detection results of four types of fabric in TILDA. For

each type of defect, one representative sample was selected as demonstration. These defects are holes, stain, missing yarn, and spot. From the detection results, it is noticed that most of the defects were well detected. For the first three types of fabric, the proposed detection model accurately located the defects and outlined their shapes. However, two defects on the fourth fabric type were not well detected because the coarse fabric texture greatly influenced image restoration accuracy and thresholding selection. In all, the proposed detection model still achieved a rather high successful detection rate on TILDA. Moreover, as shown in Fig. 5.6, nearly no false detection appeared in the detection results, which revealed that the detection model has high sensitivity and robustness.

As remarked in the database, an image with resolution of 768×512 in TILDA covers only an area of 37.5 sq cm, in which the defects occupied a large proportion. Given that most of the fabric defects found in a real case might be smaller than the samples in TILDA, more real samples collected from an apparel company and scanned from the fabric defects handbook were used in the second step of experiments to further validate the effectiveness of the proposed detection model for the apparel industry. The image samples collected from the real apparel factory are of 1050×1050 and cover an A4 size area. The smallest defects on the fabric surface occupy only an area of one or two pixels approximately. Larger coverage of a testing image could result in a more efficient detection model. In accordance with the type of fabric defects, the defective samples are classified into three groups. First, defects are caused by yarn arrangement such as missing yarn, thick-yarn, and knots. Second, tonal defects include color marks and oil stains. Third, subtle defects are very small and of low contrast with respect to the background. The detection results are presented in Figs. 5.7 - 5.9.

Fig. 5.7 shows several examples of the detection results of defects related to yarn arrangement. Defects on the fabric whose weft and wrap yarns are of

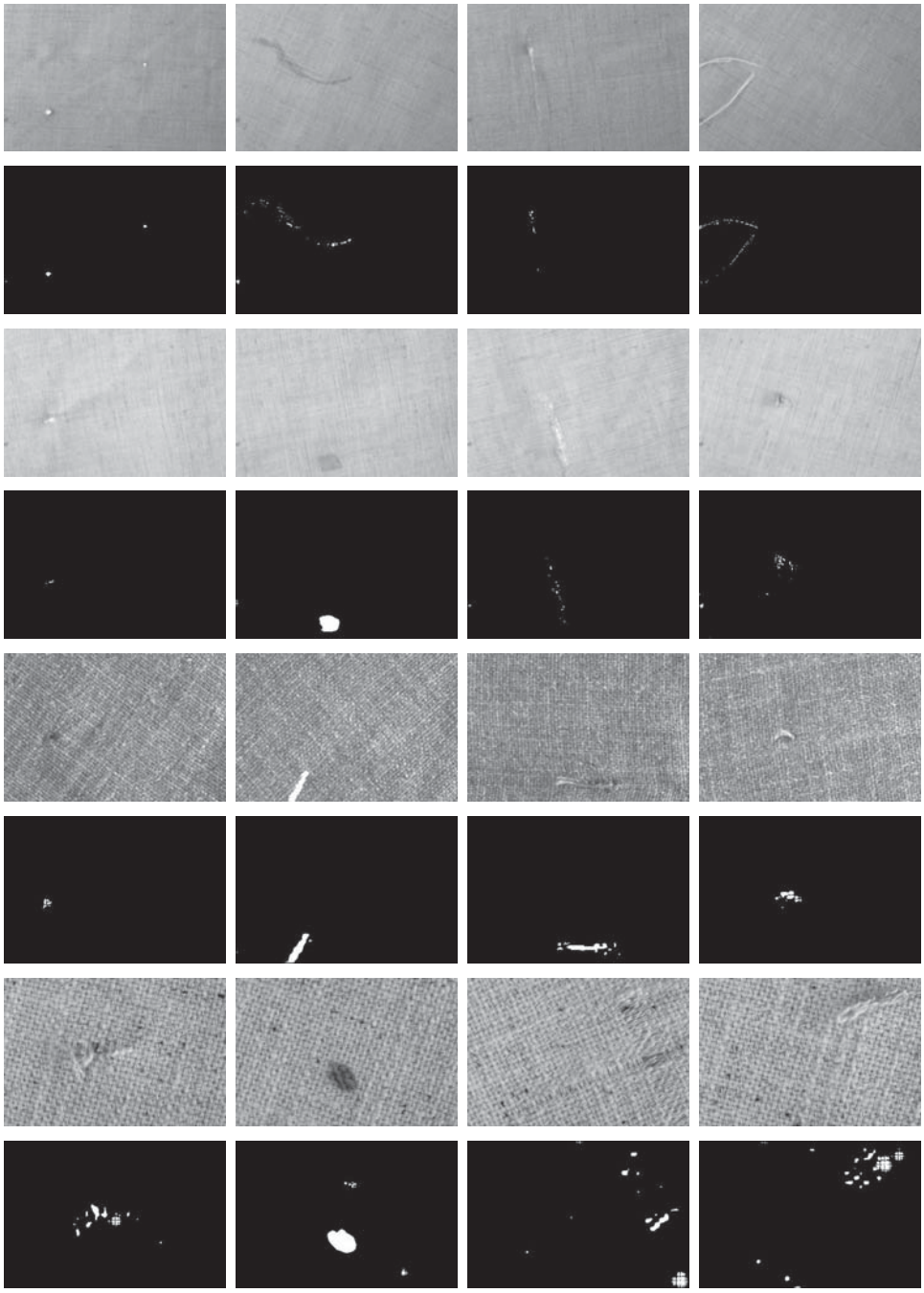

Figure 5.6: Detection results of TILDA database.

different colors are more conspicuous than others, e.g., Figs. 5.7(a) - 5.7(c). The proposed detection model successfully located the defect and outlined their accurate shape. Their fabric texture structure is slightly more complex than others; thus, false alarms appeared in their detection results, e.g., Figs. 5.7(e) and 5.7(f). Given the high density of yarn arrangement of twill fabric, the defects on such fabric are usually of low contrast, such as Figs. 5.7(i) and 5.7(j). However, the proposed detection model successfully segmented the two problems, as shown in Figs. 5.7(m) and 5.7(n).

5.5.3 Comparison of the proposed model and two representative models

To further validate the effectiveness of the proposed model in fabric defect detection, detection performance is compared with the other three representative defect detection approaches, namely, detection model based on Gabor filters bank [12], Fourier and wavelet-based model [11], and adaptive sparse representation-based model [16]. The first two are the representatives in the feature extraction-based detection approaches, which are popular in fabric defect detection applications. The last one represents the newly emerged non-feature extraction-based detection approaches, which have attracted much attention in the recent defect detection research. Source code of the approach in [11] is provided by the author of this reference, while those of the other two comparative approaches are programmed by the author in this research. The evaluations were conducted under the same environment on the basis of the real fabric sample database.

Figs. 5.10 - 5.12 present the comparison of the detection results on the database of real fabric samples . The images of defective fabric samples are shown in the first row. The detection results obtained by using Gabor filters bank [12], Fourier and wavelet-based model [11], regression-based model

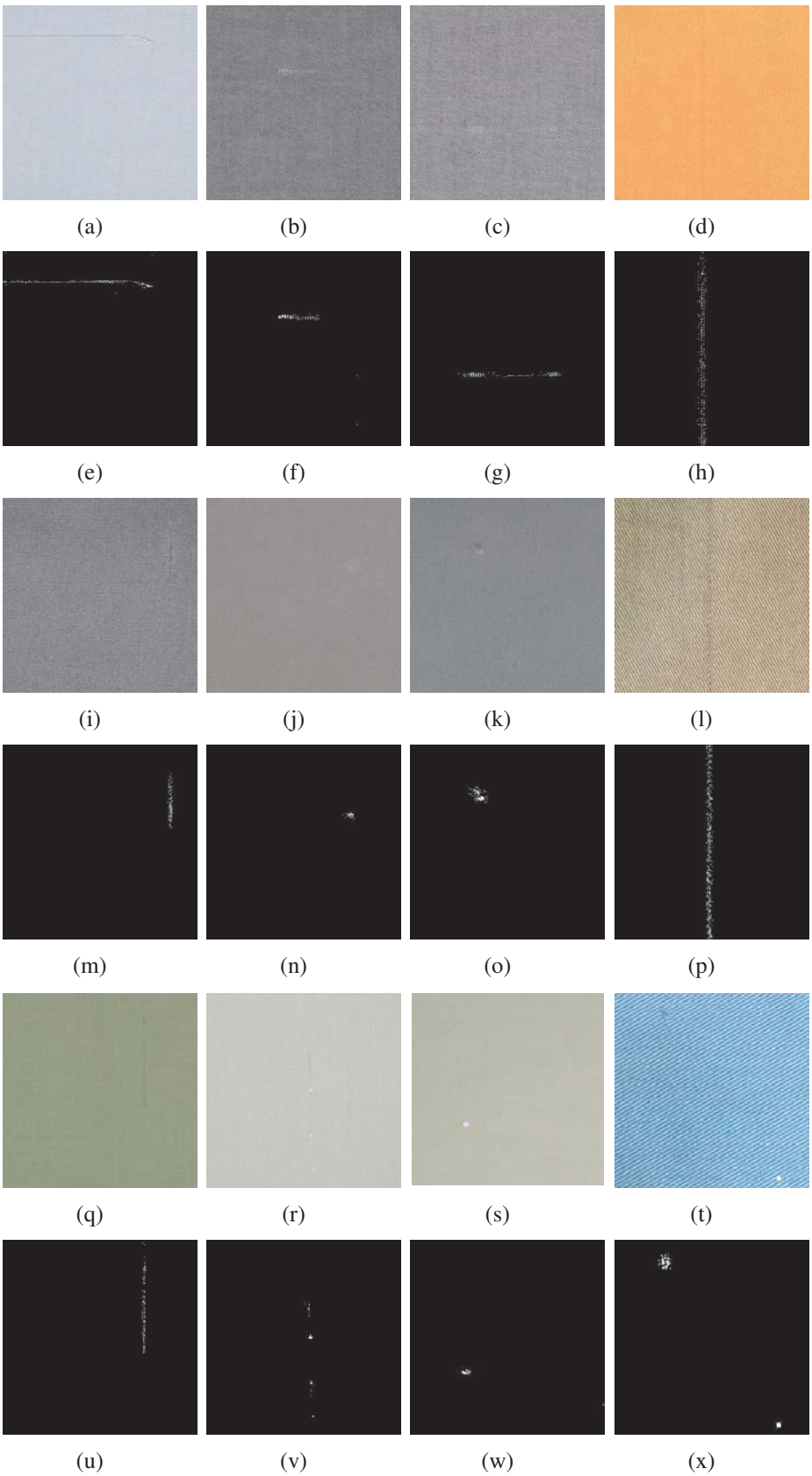

Figure 5.7: Detection results of missing yarn, thick yarn, and knots.

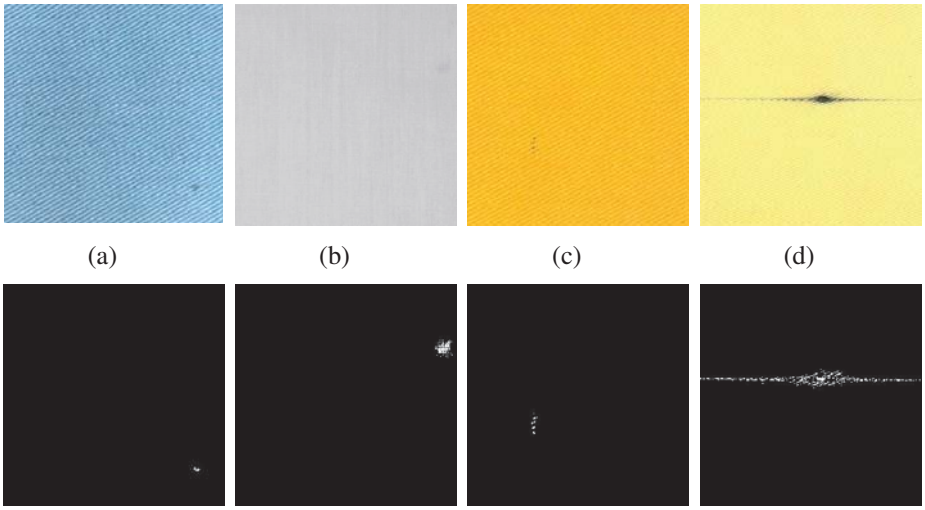

(a) (b) (c) (d)

(e) (f) (g) (h)

Figure 5.8: Detection results of stain defects.

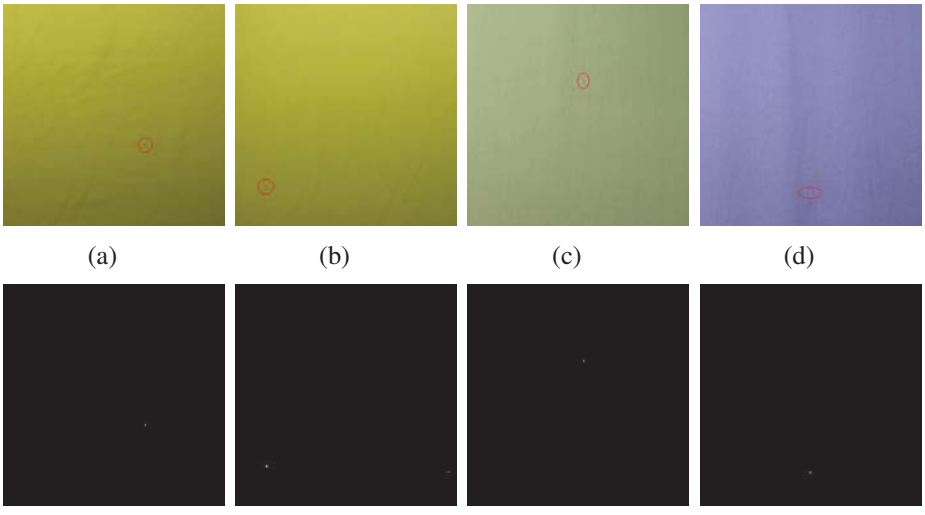

(a) (b) (c) (d)

(e) (f) (g) (h)

Figure 5.9: Detection results of tiny defects.

[16], and the proposed detection model are shown in the second, third, fourth and last rows, respectively. It is worth mentioning that the proposed detection model distinguished all defect samples, and generally outperformed the other three methods.

The detection model proposed in [12] and [11] mainly depends on the feature extraction of defects. Hence, the sensitivity of the detection model would not be satisfied when the boundaries of defects are blurry or the defects are confused with normal fabric texture. For example, in Figs. 5.10(d) and 5.11(a), although the stain defects were successfully detected by all detection models, structural defects were well located only by the proposed model.

Compared with the conventional regression-based model in [16], non-local similarities of the fabric structure information were utilized to reduce noise in the restored image in the proposed model, which in turn increased the detection rate. Therefore, even for small and subtle defects, the proposed detection model could achieve good performance, as shown in Figs. 5.10(q), 5.11(s), and 5.11(t).

The comparative detection results on several tiny defects are demonstrated in Fig. 5.12. It is noticed that the three representative detection models failed to detect most of the defects when the defects were hard to visually distinguish. Moreover, uneven illumination in Figs. 5.12(b) and 5.12(c) resulted in lots of false alarms in the detection results with the use of the detection model in [16]. However, the utilization of features of non-local image patches makes the proposed defect detection model immune to uneven illumination. Table 5.3 summarizes the performance comparison of the four detection models, which revealed that the detection rate of the proposed detection model is high than that of the other three models, and that a good balance between defect detection rate and false alarm rate is ensured.

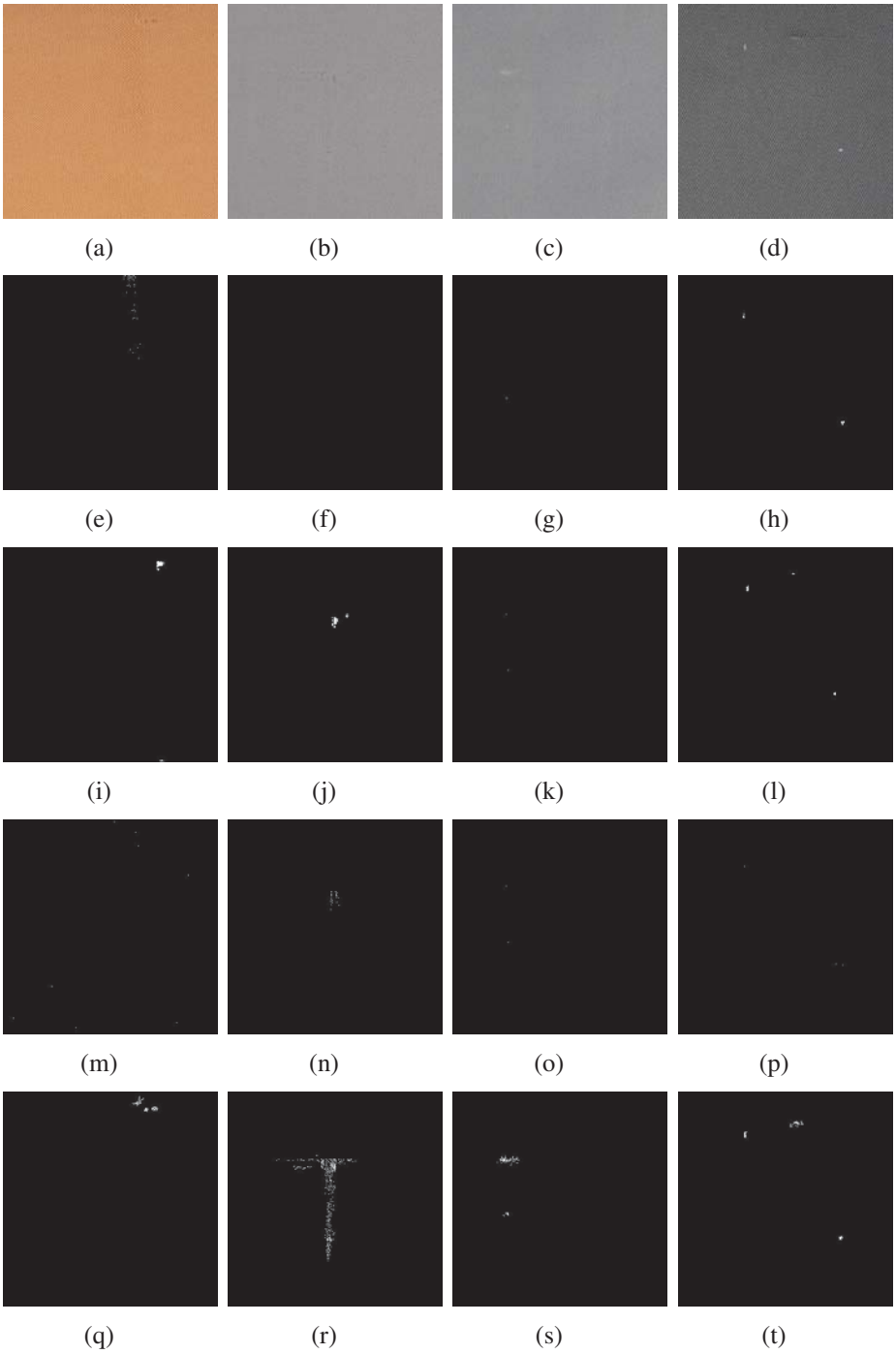

Figure 5.10: Results of comparison experiments on real fabric samples.

Table 5.3: Performance comparison of defect detection models

	Precision	**Sensitivity**	**Specificity**	**Accuracy**
Model in [12]	79.3%	81.2%	83.1%	82.2%
Model in [11]	82.7%	88.2%	79.1%	83.5%
Model in [16]	**93.3%**	82.3%	**94.1%**	88.2%
Proposed model	92.5%	**96.1%**	92.2%	**94.1%**

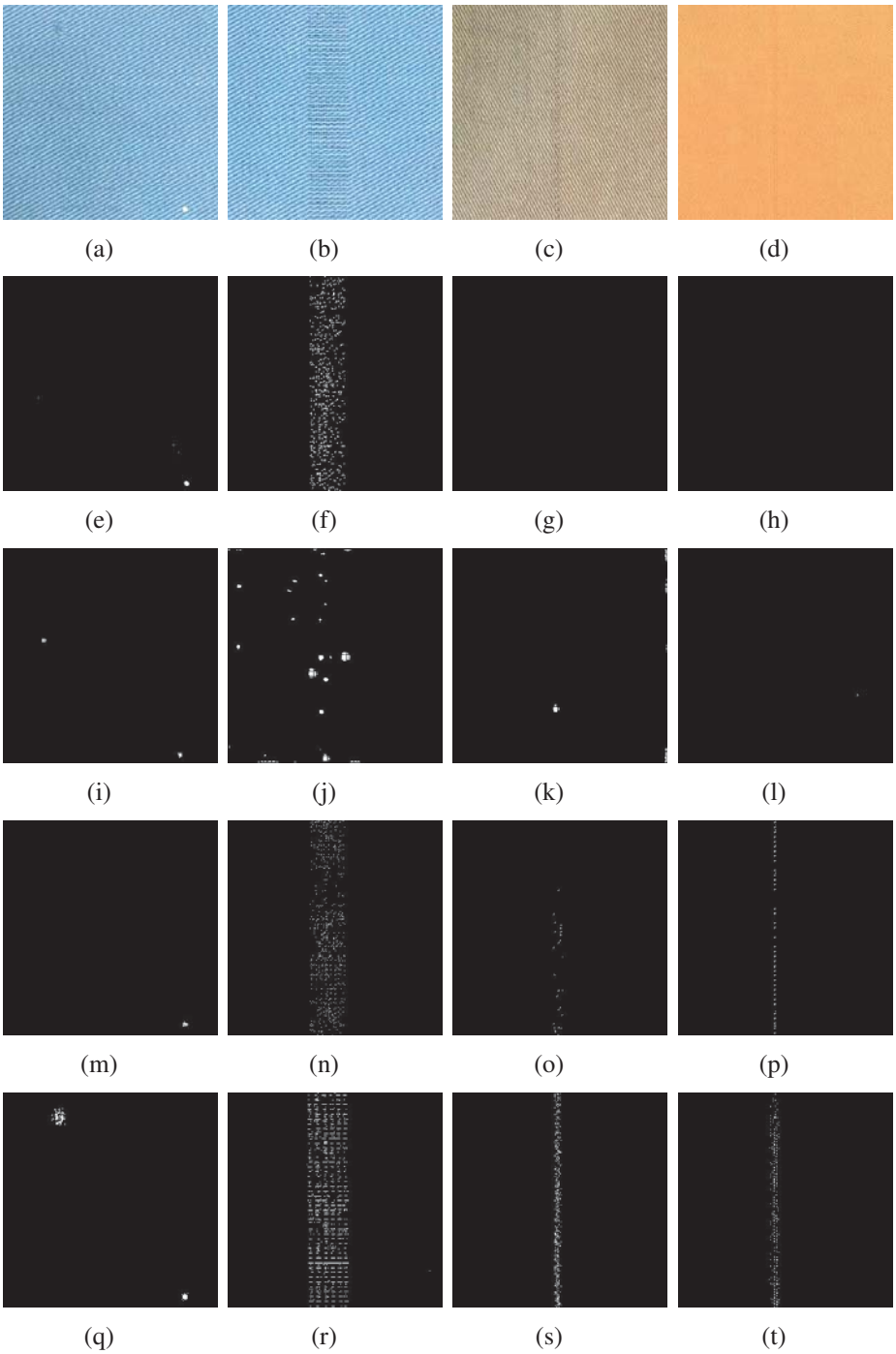

Figure 5.11: Results of comparison experiments on scanned fabric samples.

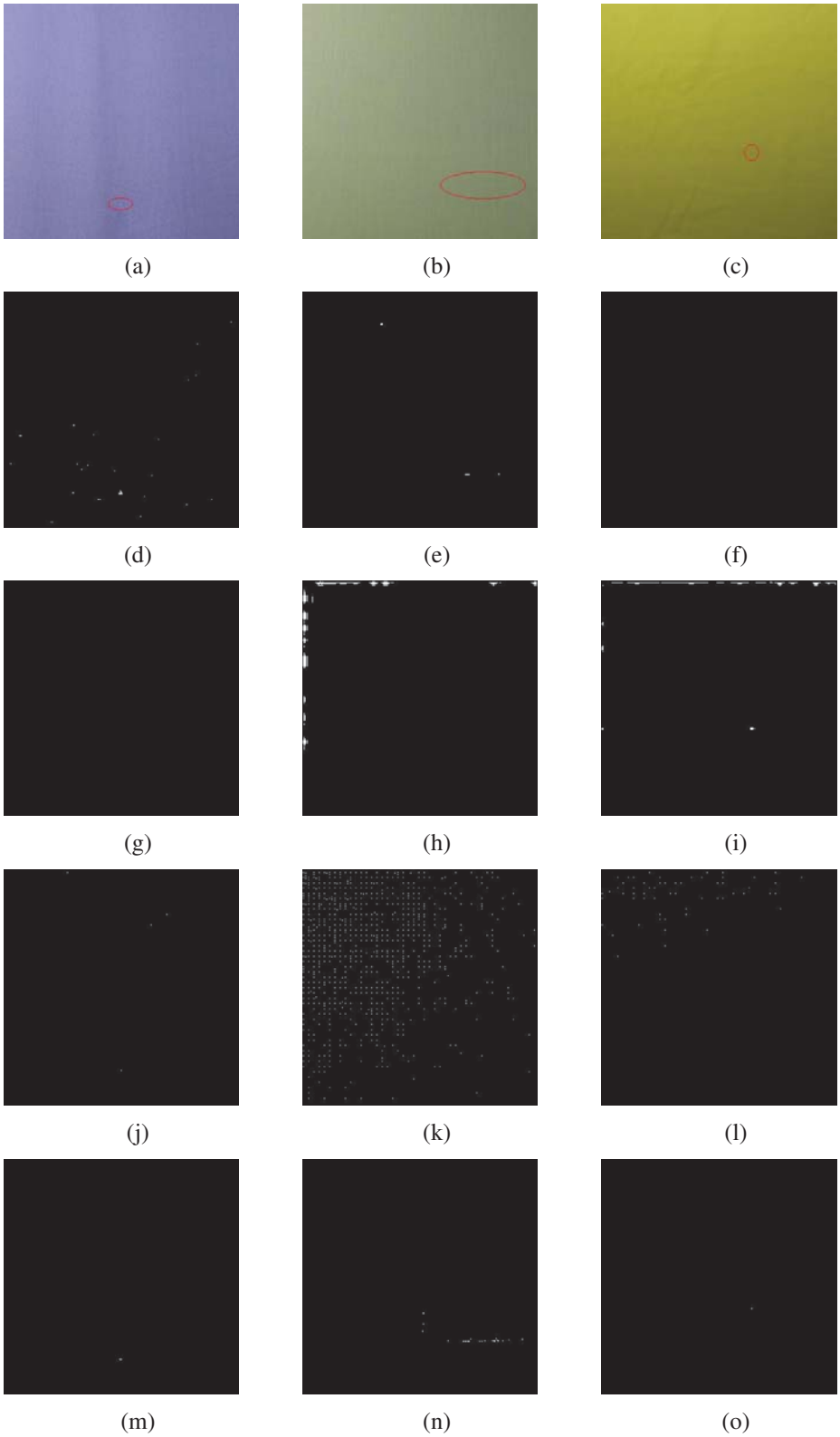

Figure 5.12: Results of comparison experiments on tiny defects.

5.6 Summary

In this chapter, a non-locally centralized sparse representation-based detection model was developed to solve the intelligent inspection problem of twill fabric. The proposed model is mainly based on two modules, which are dictionary learning (offline) and defect detection through image restoration (real-time). First, the compact sub-dictionaries learned from non-defective samples could be adaptively selected in sparse coding to provide the most relaxant fabric structure information for image restoration. Then, by adopting the non-locally centralized sparse representation model, non-local similarities of the fabric structure information are exploited to improve the image restoration effect, thereby increasing the defect detection rate. This method is more effective in detecting small defects because image restoration is a pixel-based operation, which is sensitive to small aberrations.

Extensive experiments were conducted to validate the performance of the proposed model. The TILDA database and real fabric samples were used to evaluate the performance of the proposed detection model. The effectiveness of the proposed model on various types of defects was verified by observations of the amount of detection results. Further experiments that compared the proposed model with three representative detection models manifest that the proposed detection model had a higher successful detection rate and lower false alarm rate than the other models.

Chapter 6

A Hybrid Defect Detection Model for Striped Fabric Inspection

Different from plain and twill fabric in solid color, the image of striped fabric consists of basic repeat unit and weaving texture, in which there lies two groups of defects: pattern variants and common fabric defects. Therefore, a hybrid defect detection model is developed to detect both types of defects successfully.

6.1 The Framework of Twill Fabric Inspection Model

Fig. 6.1 shows a few image samples of non-defective and defective striped fabric. As discussed in Chapter 1, besides the common fabric defects, variations of repeat pattern, which are regarded as pattern defects, greatly impair fabric quality as well. For example, Fig. 6.1(c) shows a skewed stripe pattern that is a typical type of pattern defect normally caused by restarting a weaving machine. The variance of striped fabric is significantly larger

than a fabric in solid color; thus, small variations of weaving texture do not cause perceivable changes to the statistical features of the entire image. For example, part of the common fabric defect in Fig. 6.1(d) is covered by a stripe pattern, which makes it considerably difficult to detect the defects directly by approaches based on feature extraction, such as statistical, model-based and spectral methods. Moreover, instead of the weaving texture, the repeated stripe pattern is the principal component in the images of a striped fabric. Approaches based on sparse representation are also incompatible in pattern fabric inspection, because the detail loss of repeated pattern in the restored image causes numerous false alarms in defect detection. Therefore, reducing the interference brought by stripe patterns in detecting defects is a key issue in the design of striped fabric inspection model.

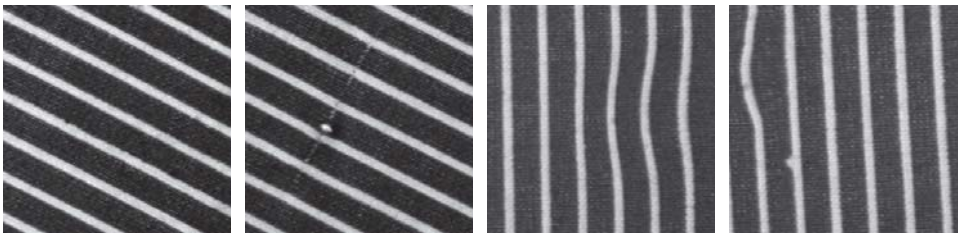

(a) (b) (c) (d)

Figure 6.1: Several image samples of a striped fabric.

Direct Gabor filtering fails to extract the features of defects, because the edge of stripe pattern will have a relative large response in the filtered image, which will increase the false alarm rate of the defect detection. However, the freedom in the selection of orientation and frequency of a Gabor filter provides the possibility to remain the response of object that we are interested in the filtered image. A Gabor filter which is designed to enhance the response of horizontal lines, will accordingly restrain the response of vertical lines. Therefore, a Gabor filter can be optimized to eliminate the normal stripe pattern in the first step of striped fabric inspection, so that the features of pattern variants and common defects can be kept. Thereafter, the filtered image can be regarded as uniform fabric, and the remaining defects can be

considered as noise, because the filtered boundaries of the defects are not as sharp as the original. Therefore, image restoration techniques can be utilized to detect the defects in the second step of inspection. Due to the filtering effect, the non-defective texture will simultaneously be slightly changed when eliminating stripe pattern. Dictionary learnt from referencing images will influence the image restoration accuracy. Therefore, non-local self-similarities of the inspection image are utilized to restore the non-defective filtering response and then highlight the defects.

On the basis of the above discussion, a hybrid defect detection model, consisting of optimal Gabor filtering and sparse representation, is developed to solve the issues in striped fabric inspection. Before the commencement of real-time inspection, evolutionary algorithm-based Gabor filter optimization is carried out offline to obtain the optimal solution that could significantly eliminate the filtering response of stripe patterns. After optimal Gabor filtering in the first step of inspection, the output feature images of inspection fabric and non-defective reference fabric are transmitted to the second step of inspection which is based on image restoration. The filtering response of non-defective texture is restored by the non-local self-similarities of the inspection filtered image. Finally, pattern defects and common defects are segmented by simple thresholding operation from the residual image of the restored and the original feature images. A flowchart of the proposed hybrid defect detection model is shown in Fig. 6.2. The details of each operation is introduced in the following sections.

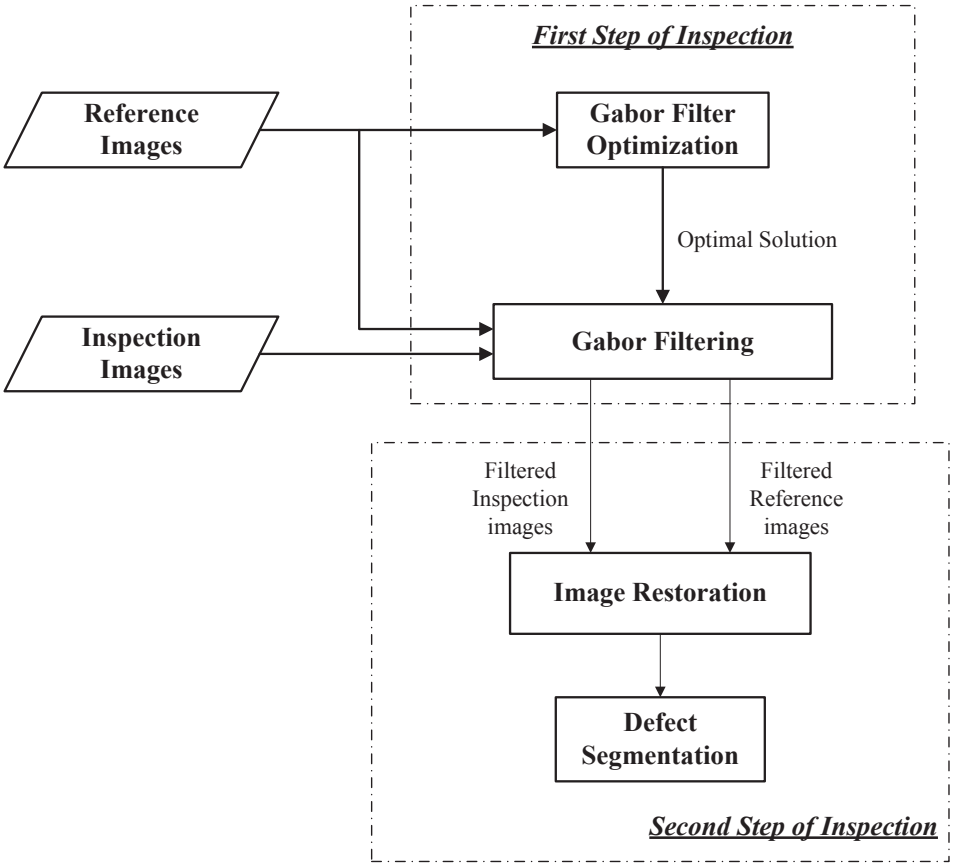

Figure 6.2: Flowchart of the striped fabric inspection process.

6.2 Step One: Optimal Gabor Filtering based on CoDE

Fig. 6.3 shows the corresponding feature images of a defective striped fabric sample filtered respectively by two optimal Gabor filters formulated by sinusoidal function in different orientations. As mentioned in Chapter 3, imaginary part of Gabor filters which are formulated with sinusoidal function perform well in detecting edges that are in the same direction as them [66]. The response of objects in perpendicular direction are reduced simultaneously; thus, a Gabor filter bank that essentially covers the frequency domain is effective in detecting defects on a smooth surface (for example, plain fabric) [12]. Therefore, the Gabor filter (formulated as Eq. (3.6)) is optimized perpendicularly to the stripe to eliminate the structure of repeated pattern. Only the samples of non-defective striped fabric are utilized as the reference images in the Gabor filter optimization.

Fig. 6.3 shows that the prominent feature of the original striped fabric image is its salient gradient. Based on Figs. 6.3(b) and 6.3(e), the edge structure of stripe is enhanced in the feature image by a synclastic Gabor filter, and most of the structural information of defects are lost. Conversely, the edge structure is significantly eliminated in the feature image filtered by a perpendicular Gabor filter, and the defects become considerable clearer (See Figs. 6.3(c) and 6.3(f)). The corresponding histograms suggest that an image has more pixels under high gray-level intensities when the stripe pattern is more salient. Thus, minimizing the mathematical expectation of the histogram of the edge image extracted from the filtered feature image by *Sobel* mask should be the primary objective in the Gabor filter optimization to reduce the disturbance caused by the stripe pattern. Suppose that the feature image $\boldsymbol{F}$ is of $M \times N$ pixels with 8-bit gray levels. The objective S can be formulated as

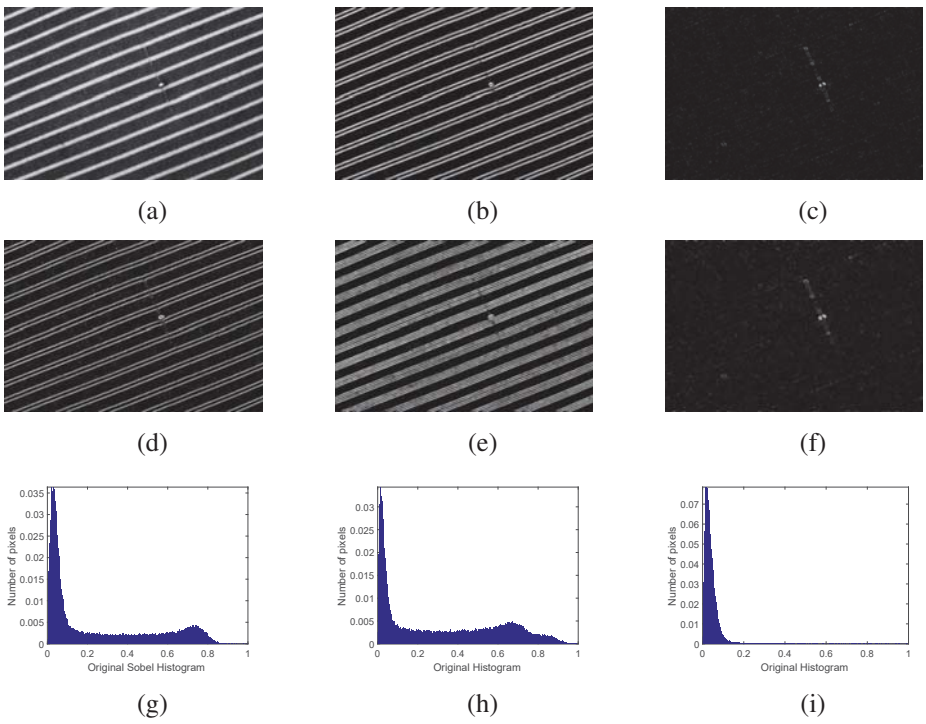

Figure 6.3: Comparison of Gabor filtering result: 6.3(a) is the original defective image; 6.3(b) is the filtering result through a synclastic Gabor filter; 6.3(c) is the filtering result through a perpendicular Gabor filter; 6.3(d) - 6.3(f) are the gradient maps of the figures in the first row extracted by *Sobel*; 6.3(g) - 6.3(i) are the corresponding histograms of the gradient maps.

$$S = \sum_{i=0}^{255} i \frac{q_i}{M \times N}, \tag{6.1}$$

where i denotes the value of gray levels, and q_i is the number of pixels under $i_t h$ gray level in the edge image extracted from $\boldsymbol{F}$. This objective ensures that the abrupt intensity changes at the edge of the stripe pattern is significantly eliminated. Furthermore, the variance of the filtered feature image denoted by σ should be as small as possible to ensure that the texture of the original fabric sample is as uniform as possible after Gabor filtering. This condition is beneficial for the robustness of defect detection. Therefore, the final objective function adopted in the Gabor optimization is

$$\text{maximize} \quad J = \sigma \times \sum_{i=0}^{255} i \frac{q_i}{M \times N}. \tag{6.2}$$

Based on the analysis of optimization method in Section 4.2, CoDE, one of the powerful evolutionary algorithm, is adopted as the optimization algorithm in obtaining the optimal set of parameters of Gabor filter. As stated in Section 6.1, only one Gabor filter can eliminate the filtering response of edges in the striped fabric; the orientation parameter θ is designed perpendicularly to the stripe pattern. Hence, three Gabor parameters should be optimized: the central frequency of Gabor filter f_0; and the frequency bandwidth B and shape factor of Gabor filter λ, which jointly determine the smoothing parameters σ_x and σ_y.

The specific optimization process is described as follows:

(1) Representation: The first step of the optimization process is to encode solutions into decision vectors which are of three dimensions: f_0, B, and λ.

(2) Population initialization: The initial chromosomes are assigned with real numbers at the beginning while rounding down to discrete in evaluating

the objective function to apply CoDE, which is a continuous evolutionary algorithm.

(3) Mutation, crossover, and selection: Optimization proceeds into mutation and crossover after the initialization process. CoDE has three selected strategies of trial vector generation and three parameter settings. Three candidate trial vectors U_{i1}, U_{i2} and U_{i3} are obtained using the three trial vector generation strategies "rand/1/bin", "rand/2/bin", and "current-to-rand/1" for the current individual X_i in every generation. The control parameter setting is randomly chosen (See Eqs. (4.5) - (4.7)).

The evolution process does not stop until predefined criteria are met. Fig. 6.4 shows several striped fabric samples and the corresponding filtered results of Gabor filters that are optimized through the previous procedures. The stripe patterns are successfully eliminated while keeping the response of basic weaving texture and defects. The pattern defects deviate from the orientation of the original stripe pattern; thus, they are also retained in the feature image.

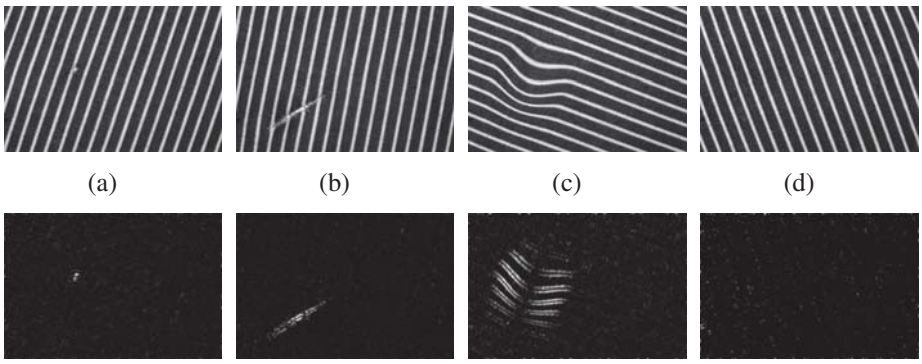

Figure 6.4: Filtering results of striped fabric by optimal Gabor filters perpendicular to the stripe pattern.

6.3 Step Two: Image Restoration-Based Defect Detection

The interference of stripe edge structure is significantly reduced after the Gabor filtering in the first step of inspection to make the inspection approaches for basic weaving texture detect the remaining defects effectively. Fig. 6.4 demonstrates that the filtering response of the basic weaving texture in the background is not as uniform as that of the plain fabric. Therefore, approach based on optimal Gabor filter cannot be applied in this step. Moreover, defect boundaries are slightly weakened. Therefore, image restoration-based detection approach, which does not rely on feature extraction, is adopted to find the defects from the Gabor-filtered images.

6.3.1 Image Restoration Based on Non-local Self-similarities

The structural information of the basic weaving texture in the filtered image is changed compared with the original fabric images. The comparison of Figs. 6.4(e) and 6.4(f) shows that the regularity of background texture between similar types of fabric is significantly smaller. Therefore, it is difficult to learn an effective dictionary for texture representation of the filtered image. However, for a given image patch, its estimation can be obtained based on its non-local self-similarities [117]; thus, regarded as random noise, fabric defects in the filtered feature image can be successfully removed.

Suppose that the feature image $\mathbf{F}$ is divided into K overlapping patches, $\mathbf{F}_i = \mathbf{R}_i\mathbf{F}, i = 1, 2..., K$, is the i^{th} patch vector of image $\mathbf{F}$, where $\mathbf{R}_i$ is a matrix extracting patch $\mathbf{F}_i$ from $\mathbf{F}$. The fused image $\mathbf{F}$ through all image patches can be formulated as

$$\hat{\mathbf{F}} = \left(\sum_{i=1}^{N} \mathbf{R}_i^T \mathbf{R}_i \right)^{-1} \sum_{i=1}^{N} (\mathbf{R}_i^T \mathbf{F}_i). \tag{6.3}$$

A set of patches that are of similar intensity distribution in a certain range can be searched for each patch $\mathbf{F}_i$. Patch $\mathbf{F}_i^q$ is selected as a similar patch to $\mathbf{F}_i$ if the Euclidean distance between them is less than the predefined threshold. The weighted average of the first L closest patches can be used to restore patch $\mathbf{F}_i$:

$$\mathbf{F}_i^{'} = \sum_{q=1}^{L} b_i^q \mathbf{F}_i^q, \tag{6.4}$$

where $\mathbf{F}_i^{'}$ is the new estimated image patch of $\mathbf{F}_i$; the weight b_i^q is set to be inversely proportional to the distance between patches $\mathbf{F}_i$ and $\mathbf{F}_i^q$:

$$b_i^q = exp(- \parallel \mathbf{F}_i - \mathbf{F}_i^q \parallel_2^2 / h)/\omega, \tag{6.5}$$

where h is a preset scalar and ω is a normalization factor.

Each image patch can still be restored from the local and non-local redundancies of the inspection image itself without a standard texture dictionary, which is beneficial for increasing the detection sensitivity on small defects. Compared with the conventional regression model [16] and non-locally centralized sparse coding model applied in Chapter 5, the image restoration based non-local self-similarities outperforms in terms of computational cost. Thereafter, the new image $\mathbf{F}^{'}$ can be synthesized by Eq. 6.3. The non-defective pixels are similar to the pixels of the original feature image in the newly restored image, whereas the restoration error in estimating the defective pixels is quite larger.

6.3.2 Defect Segmentation

The defective pixels, which are regarded as noise, are replaced by non-defective texture in the newly restored image. Thus, the defective area can be highlighted in the residual image by comparing the restored image with the original filtered image. A simple thresholding operation following image subtraction can segment the defects from the background of the residual image.

The threshold limits are derived from the reference residual image of a non-defective sample and its estimation that is restored by the the non-local self-similarities in the image, for each specific type of striped fabric. Suppose that the gray-level intensity of the reference residual image is denoted as $\mathbf{F}_r(x, y)$. Subsequently, the upper and lower threshold limits are

$$\psi_{upper} = \max_{x,y \in W} |\mathbf{F}_r(x, y)|, \tag{6.6}$$

$$\psi_{lower} = \min_{x,y \in W} |\mathbf{F}_r(x, y)|, \tag{6.7}$$

where W is a window centered at the feature image obtained by removing 10 pixels from each side of the image $\mathbf{F}_r(x, y)$. Hence, the binary feature image $\mathbf{B}(x, y)$ can be obtained by

$$\mathbf{B}(x, y) = \begin{cases} 1, & \text{if } \mathbf{R}(x, y) > \psi_{upper} \text{ or } \mathbf{R}(x, y) < \psi_{lower}, \\ 0, & \text{otherwise}, \end{cases} \tag{6.8}$$

where $\mathbf{R}(x, y)$ denotes the gray-level of the testing residual image.

6.4 Experiment Results and Discussion

The experiments are conducted on the samples of striped fabric selected from TILDA database, in which 50 non-defective samples and 300 defective samples are included, to validate the effectiveness of the proposed defect detection model. In the database, pattern defects include compactor crease and pattern variants caused by mechanical fault; and common defects include chafed yarn, flying yarn and color mark. The detection results of both pattern defects and common fabric defects are demonstrated and analyzed.

The experiment setup is the same with those in Chapters 4 and 5. Image samples in TILDA are of 768×512 pixels. The image processing toolbox of MATLAB prototyping environment is adopted to program all the detection models. The performance of defect detection models is evaluated by *precision*, *sensitivity*, *specificity* and *accuracy*, which are clearly defined in Section 4.4.1.

6.4.1 Performance Evaluation of the Proposed Defect Detection Model

The inspection of striped fabric is conducted according to the procedures shown in Fig. 6.2. Figs. 6.5 - 6.6 demonstrate several representative detection results using the proposed defect detection model. A non-defective sample is selected as the reference to optimize the Gabor filter at the beginning of the inspection of each type of fabric. Images in the second column, which well be restored in the second step of inspection, show the optimal filtering response in the first step of inspection. The binary image in the third column shows the final detection results. Table 6.1 summarizes overall experimental results using the proposed defect detection model.

Table 6.1: Performance of the proposed detection model on striped fabric samples of TILDA

	Precision	**Sensitivity**	**Specificity**	**Accuracy**
Performance	94.7%	90.0%	70.0%	87.1%

Fig. 6.5 demonstrates the detection results of pattern defects. The first three samples are the variations of repeated stripe pattern usually caused by restart of the weaving machine or a malfunction in the weaving tensor. The last three samples are caused by fabric crease. All these defects are successfully detected. The edges of the incorrectly arranged stripe are not eliminated in the filtered images in the first step, because these misarranged stripes deviate from the standard orientation of repeated patterns. Subsequently, the defects were are segmented from the background based on the restored filtering response of the non-defective fabric texture.

The detection results of several common defects on the striped fabric are shown in Fig. 6.6. The first three are structural defects related to weaving texture. Part of the first defect is of considerable low contrast, which is almost drowned in the texture of image background. The defect can be highlighted using the proposed detection model with the Gabor filter optimized through the procedures stated in Section 6.2 while suppressing the stripe pattern. Moreover, the second defect is on the side of the edge of the stripe pattern and is enhanced in the filtered feature image. The least two are tonal defects that only alter the local intensity value of the fabric but not the weaving structure. Particularly, the proposed detection model has detected the defect in the upper-right corner of the last image that overlaps the stripe pattern, which further verifies that the proposed detection model is sensitive to most types of fabric defects.

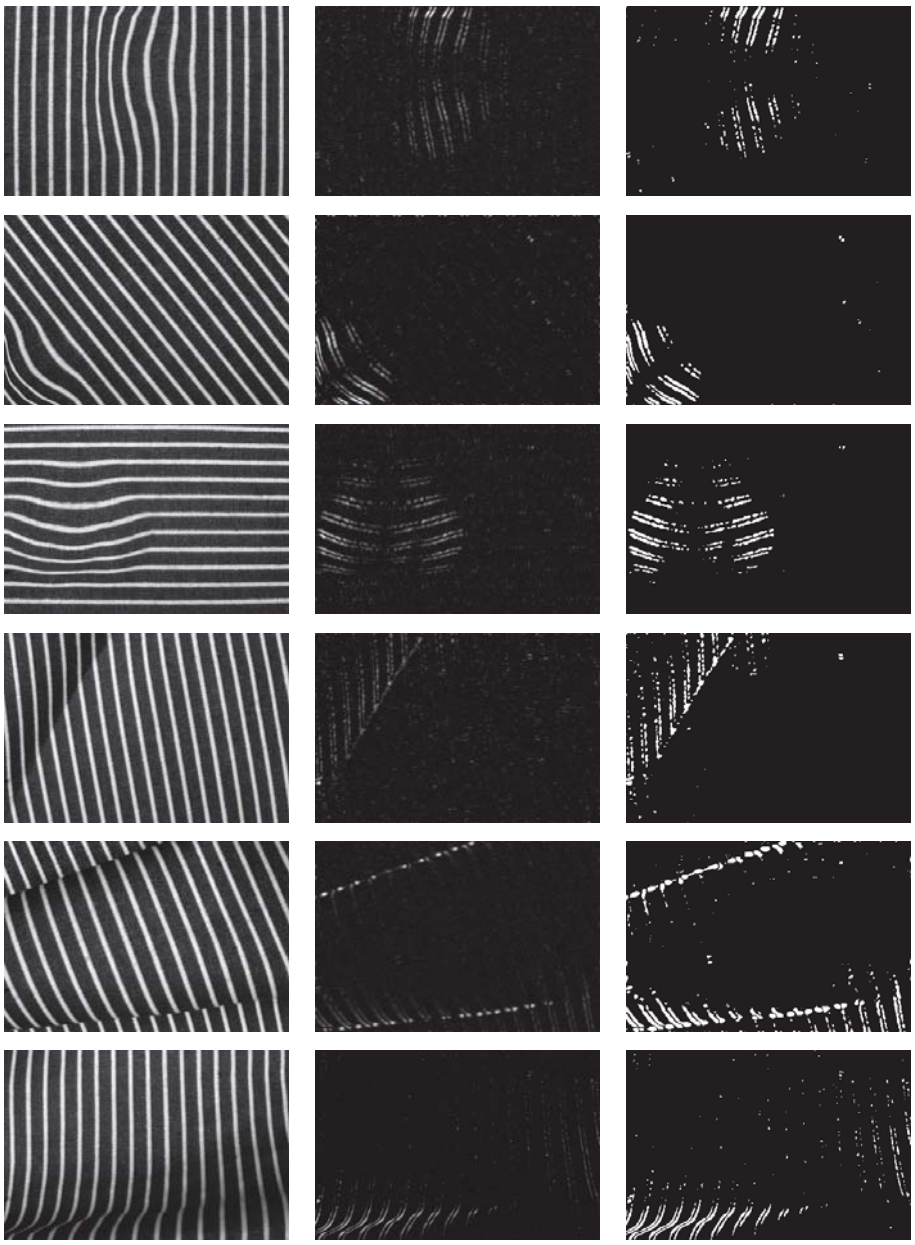

Figure 6.5: Detection results of pattern defects on striped fabric.

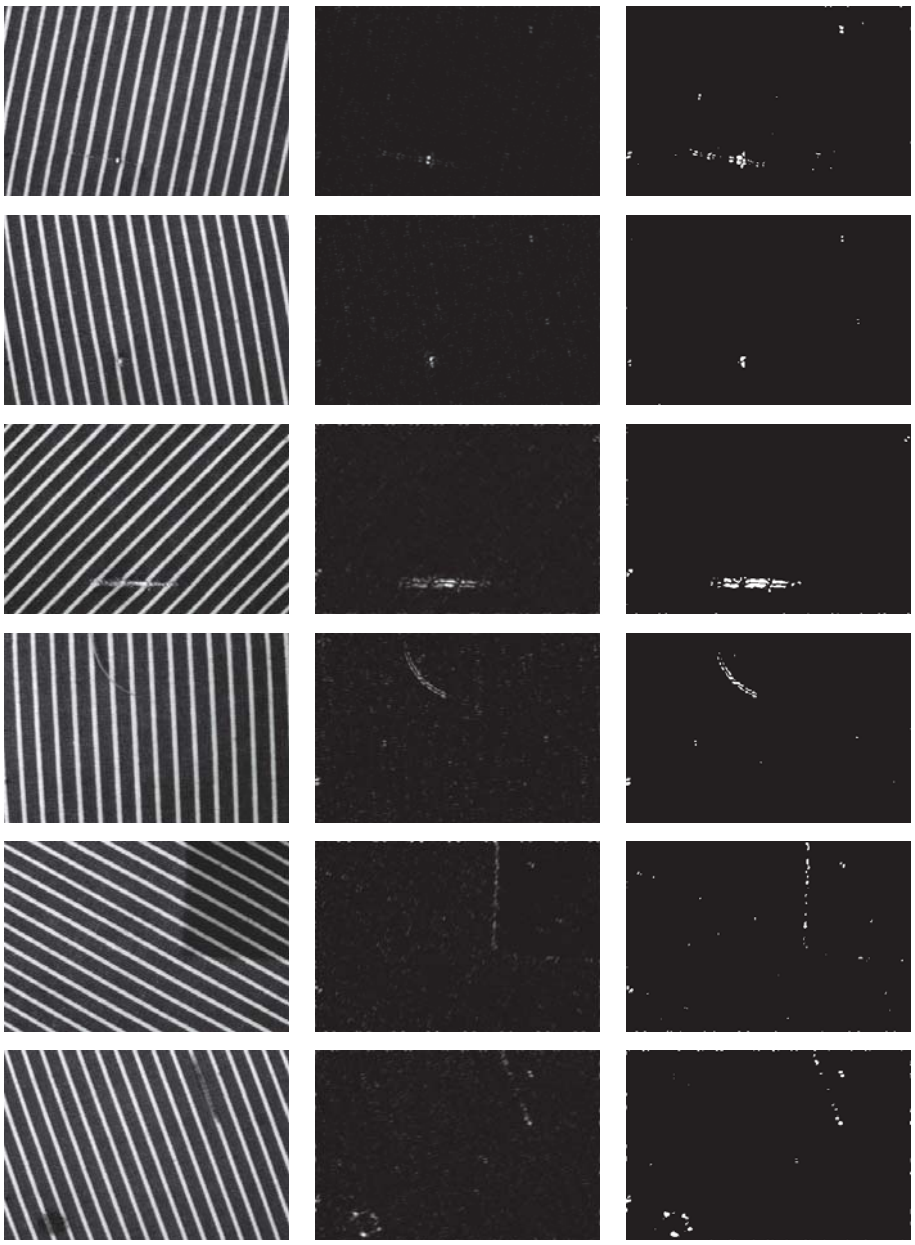

Figure 6.6: Detection results of common fabric defects on striped fabric.

6.5 Summary

In this chapter, with the use of Gabor filtering and image restoration techniques, a hybrid defect detection model is developed for the inspection of striped fabric. The proposed model can detect both pattern defects and common fabric defects in two steps. First, a Gabor filter was optimized to minimize the image gradient for each type of fabric, eliminating the repeated stripe pattern in the filtered feature image. The feature image with remaining defects are subject to image restoration, which is the second step of the inspection. Only non-local self-similarities are utilized to estimate the filtering response of non-defective texture in the image restoration, which is beneficial in increasing restoration accuracy. Finally, the defects are segmented from the residual image of the restored and original filtered images.

The performance of the hybrid defect detection model is evaluated by extensive experiments with the samples of striped fabric in TILDA database. The experimental results on misarranged and crease defects indicate that the proposed detection model is effective on any directional pattern defects because of the selective orientation of Gabor filters. Accurate detection results on common fabric defects also prove that the proposed model performs well in detecting most types of fabric defects while reducing the interference of stripe pattern.

Chapter 7

Conclusions and Future Work

This chapter starts with the conclusion of this research followed by its contributions and limitations as well as suggestions for future work.

7.1 Conclusions

This research addresses the problem in automatic fabric inspection in the textile and apparel industry, using computer vision techniques. The specific fabric inspection model was designed for different types of fabric according to their weaving structure characteristics for the first time. For plain, twill, and striped fabrics, three defect detection models were developed to solve most types of the common fabric defects and pattern defects, improving the overall performance of fabric inspection in the textile and apparel industry.

A defect detection model based on optimal Gabor filters has been proposed for plain fabric inspection in Chapter 4. The basic criss-cross plain weaving structure leads to a smooth surface of plain fabric; thus, only two Gabor filters were optimized by CoDE to extract the features of plain defects in horizontal and vertical, respectively. Both non-defective and typical defect samples

were involved in the optimization of Gabor filters in this research. The mathematical function of optimization objective was designed to maximize the difference between the filtering response of non-defective and defective fabric textures. Plain defects could be easily segmented from the normal fabric texture filtered by the optimal Gabor filters by simple thresholding operation. Extensive experiments demonstrated that the proposed detection model perform well in terms of high detection sensitivity and efficiency.

In Chapter 5, a detection model based on sparse representation has been developed to address the inspection. Approaches based on feature extraction failed to achieve high detection accuracy because of the complex twill weaving structure and the blurry boundaries of twill defects. Therefore, image restoration techniques are utilized to detect twill defects as randomly distributed noise in this research. Owing to the sparsity of fabric defects, non-defective texture of the inspection image is estimated through non-locally sparse representation; thus, the defect can be labeled in the residual image of the inspection image and its estimation. Adaptive sub-dictionaries, which could provide non-defective texture information, are learnt from reference images by K-means algorithms and PCA in the offline stage. The experiment results revealed that the proposed detection model is particularly sensitive to small-sized defects.

A hybrid fabric inspection model has been developed in Chapter 6 to detect defects on striped fabric. The proposed hybrid detection model provides a two-step solution to detect pattern defects and common fabric defects. The performance of detection approaches for fabric in solid color were not satisfied in the inspection of striped fabric because of the complex texture of stripe pattern. Therefore, a Gabor filter is optimized to suppress the filtering response of the stripe pattern in the first step of the proposed model. The mathematical function of optimization objective was designed to minimize the gradient intensity and the variance of the filtered image;

thus, the feature image of the striped fabric could be treated as a fabric in solid color after optimal Gabor filtering. Image restoration based on non-local self-similarities and thresholding operation were applied to segment the remaining defects, thereby increasing detection accuracy. The experiment results indicated that the proposed detection model detected any directional pattern defects effectively because of the selective orientation of Gabor filters; the proposed model also identified most types of fabric defects while reducing the interference of stripe pattern.

7.2 Contributions of this Research

This research enriches our understanding of automatic fabric defect detection from both academic and industrial perspectives.

7.2.1 Contributions to Woven Fabric Inspection for the Textile and Apparel Industries

In this research, an intelligent defect detection solution is proposed to address the inspection problem of plain, twill, and striped fabrics in the textile and apparel industries. In the proposed solution, computer vision techniques are used to fulfill the fabric defect detection automatically, which could overcome the limitations of the current human inspection system. The labor cost is significantly reduced by integrating the proposed defect detection solution into the traditional fabric inspection machine. Meanwhile, without the human intervention, detection accuracy and efficiency are enhanced as well.

Given that the requirements of automatic fabric inspections vary with the different types of fabric in the textile and apparel industries, the woven fabric inspection problem is investigated on the basis of specific analysis

of different fabric weaving structures for the first time. The three proposed defect detection models for plain, twill, and striped fabrics are proven to be generally superior to several representatives of the existing models, in terms of detection accuracy, robustness, and efficiency.

7.2.2 Contributions to Automatic Plain Fabric Defect Detection

Owing to the smooth characteristic of plain fabric surface, defects in plain fabric are easy to notice, and therefore, the requirements of detection accuracy and efficiency are high in the industrial applications. The proposed detection model for plain fabric, which is based on optimal Gabor filters, has greatly reduced the computational cost and increased the successful detection rate by directly extracting the features of plain fabric defects.

Considering the shape and orientation characteristics of plain fabric defects, the only two Gabor filters optimized by CoDE could avoid data redundancies caused by Gabor filter bank in the feature extraction of defects. In addition, the proposed model could obtain the best extraction of defects because of the capacity of global optimization of CoDE, and thereby increasing the detection accuracy. In all, the high detection accuracy and efficiency of the proposed detection make it satisfied in the real-time industrial applications.

7.2.3 Contributions to Automatic Twill Fabric Defect Detection

The weaving structure of twill fabric is considerably more complex than plain fabric, which makes the defects smaller and more inconspicuous. Moreover, the interference caused by ribs-like twill texture influences the stability of

fabric inspection. With defects regarded as random distributed noise on the surface of twill fabric, the detection model presented in this research has improved detection robustness and sensitivity, especially on small and blurry defects in complex texture.

By exploiting the cross-correlation of fabric structures, compact sub-dictionaries learnt from non-defective reference images are beneficial for increasing detection efficiency and reducing the false alarm rate. In addition, compared with feature extraction-based approaches, image restoration based on non-locally centralized sparse representation has greatly improved the detection performance on tiny defects.

7.2.4 Contributions to Automatic Striped Fabric Defect Detection

Striped fabric is one of the typical patterned fabrics, which is widely used in our daily lives, such as business shirt and pants. However, specific defect detection approaches have not yet been proposed for striped fabric. Most of the existing approaches failed in striped fabric inspection because of the salient intensity changes of the image and the similarities between the stripe pattern and fabric defects. In this research, the newly proposed hybrid striped inspection model could detect not only common fabric defects but also pattern defects in two steps.

Owing to the frequency selectivity of Gabor filters, an optimal Gabor filter has first obtained to reduce the response of stripe patterns, while remaining the features of defects. Hence, detection robustness has been significantly improved by eliminating interferences caused by stripe patterns. Considering the filtered image as a fabric in solid color, image restoration based on nonlocal self-similarities in the second step could enhance the detection rate

of the remaining defects.

7.3 Limitations and Future Work

This research can facilitate the development of automatic fabric inspection for textile and apparel industry. However, this research still has limitations, which can be an avenue for future research.

In this research, the three proposed defect detection models partly depend on the abrupt intensity changes on the edge of defects, and the contrast between defects and fabric image background with the samples of 2D fabric image. This limitation results in difficulties in outlining defect shapes accurately. The Gabor filters are good edge detector; however, they are insensitive to color mark defects in the proposed plain fabric inspection model, because tonality at the edge of a defect gradually changes. In the proposed twill fabric inspection model, non-local similarities are utilized in image restoration to increase restoration accuracy. However, this model also relies on the intensity changes in labeling defects as noise. The features of defective texture are likely to remain in the restored image if the original intensities are similar with its surrounding pixels, thus influencing the accuracy of the following defect segmentation. The structure of fabric texture is significantly fine that any fabric defects will cause disturbances to the arrangement of yarns at that location. The defect should be easily found by examining yarn arrangement if the image of a fabric sample is acquired at a large resolution. Therefore, the solution for fabric inspection based on yarn arrangement should be investigated in the future.

As shown in the experiments in this research, the defective fabric samples are limited. TILDA is the only public fabric texture database that is utilized as testing data in most of the current studies. However, only four types of fabric

are included in this database, and the size of defects are comparatively large that it does not conform to the actual situation in factories. Therefore, more defective samples were acquired from an apparel factory in Mainland China. However, the samples only consist of the most frequently encountered types of defects, such as slub, broken end, thick yarn, flying yarn and holes. The effectiveness of the proposed detection model on some types of defect, such as color smear, dragging end and dye streak, cannot be verified. Therefore, collecting more defective samples and constructing a more comprehensive fabric defect database should be accomplished in the future work. It is very necessary to expand the application of the proposed detection model on more types of fabric, especially fabric with complex texture.

7.4 Related Publications

The author demonstrated the originality of this research through the following publications:

[1] L. Tong, W. K. Wong, and C. K. Kwong. Fabric defect detection for apparel industry: A nonlocal sparse representation approach. *IEEE Access*, vol. 5, no. 1, pp. 5947-5964, Dec. 2017.

[2] L. Tong, W. K. Wong, and C. K. Kwong. Differential evolution-based optimal Gabor filter model for fabric inspection. *Neurocomputing*, vol. 173, no. 3, pp. 1386-1401, Jan. 2016.

Bibliography

[1] Henry Y. T. Ngan, Grantham K. H. Pang, and Nelson H. C. Yung. Automated fabric defect detection–a review. *Image and Vision Computing*, 29(7):442–458, 2011.

[2] Wikipidia. Plain weave. `https://en.wikipedia.org/wiki/Plain_weave`.

[3] Chi-ho Chan and Grantham KH Pang. Fabric defect detection by fourier analysis. *IEEE Transactions on Industry Applications*, 36(5):1267–1276, 2000.

[4] Che-Seung Cho, Byeong-Mook Chung, and Moo-Jin Park. Development of real-time vision-based fabric inspection system. *IEEE Transactions on Industrial Electronics*, 52(4):1073–1079, 2005.

[5] Christos Anagnostopoulos, D Vergados, Eleftherios Kayafas, Vassilis Loumos, and G Stassinopoulos. A computer vision approach for textile quality control. *The Journal of Visualization and Computer Animation*, 12(1):31–44, 2001.

[6] Ville Tirronen, Ferrante Neri, Tommi Kärkkäinen, Kirsi Majava, and Tuomo Rossi. An enhanced memetic differential evolution in filter design for defect detection in paper production. *Evolutionary Computation*, 16(4):529–555, 2008.

[7] Jong Pil Yun, SungHoo Choi, Jong-Wook Kim, and Sang Woo Kim.

Automatic detection of cracks in raw steel block using Gabor filter optimized by univariate dynamic encoding algorithm for searches (udeas). *NDT & E International*, 42(5):389–397, 2009.

[8] A Latif-Amet, Aysin Ertüzün, and Aytül Erçil. An efficient method for texture defect detection: sub-band domain co-occurrence matrices. *Image and Vision Computing*, 18(6):543–553, 2000.

[9] Manuel FM Costa, Francisco Rodrigues, Joao Guedes, and Jorge Lopes. Automated evaluation of patterned fabrics for defect detection. In *Education and Training in Optics and Photonics (ETOP'99)*, pages 403–407. International Society for Optics and Photonics, 2000.

[10] Henry YT Ngan, Grantham KH Pang, SP Yung, and Michael K Ng. Defect detection on patterned jacquard fabric. In *32nd Applied Imagery Pattern Recognition Workshop, 2003. Proceedings*, pages 163–168. IEEE, 2003.

[11] Guang-Hua Hu, Qing-Hui Wang, and Guo-Hui Zhang. Unsupervised defect detection in textiles based on Fourier analysis and wavelet shrinkage. *Applied Optics*, 54(10):2963–2980, 2015.

[12] Ajay Kumar and Grantham KH Pang. Defect detection in textured materials using Gabor filters. *IEEE Transactions on Industry Applications*, 38(2):425–440, 2002.

[13] Adriana Bodnarova, Mohammed Bennamoun, and Shane Latham. Optimal Gabor filters for textile flaw detection. *Pattern Recognition*, 35(12):2973–2991, 2002.

[14] Jayanta K Chandra, Pradipta K Banerjee, and Asit K Datta. Neural network trained morphological processing for the detection of defects in woven fabric. *The Journal of The Textile Institute*, 101(8):699–706, 2010.

[15] Hİ Çelik, LC Dülger, and M Topalbekiroğlu. Development of a machine vision system: real-time fabric defect detection and classification with neural networks. *The Journal of The Textile Institute*, 105(6):575–585, 2014.

[16] Jian Zhou and Jun Wang. Fabric defect detection using adaptive dictionaries. *Textile Research Journal*, pages 1846–1859, 2013.

[17] Jian Zhou, Dimitri Semenovich, Arcot Sowmya, and Jun Wang. Dictionary learning framework for fabric defect detection. *The Journal of The Textile Institute*, 105(3):223–234, 2014.

[18] Qiuping Zhu, Minyuan Wu, Jie Li, and Dexiang Deng. Fabric defect detection via small scale over-complete basis set. *Textile Research Journal*, 84(15):1634–1649, 2014.

[19] Henry YT Ngan, Grantham KH Pang, and Nelson HC Yung. Motif-based defect detection for patterned fabric. *Pattern Recognition*, 41(6):1878–1894, 2008.

[20] Henry YT Ngan, Grantham KH Pang, and Nelson HC Yung. Ellipsoidal decision regions for motif-based patterned fabric defect detection. *Pattern Recognition*, 43(6):2132–2144, 2010.

[21] Ajay Kumar. Computer-vision-based fabric defect detection: a survey. *IEEE Transactions on Industrial Electronics*, 55(1):348–363, 2008.

[22] Radovan Stojanovic, Panagiotis Mitropulos, Christos Koulamas, Yorgos Karayiannis, Stavros Koubias, and George Papadopoulos. Real-time vision-based system for textile fabric inspection. *Real-Time Imaging*, 7(6):507–518, 2001.

[23] Bithika Mallik-Goswami and Asit K Datta. Detecting defects in fabric with laser-based morphological image processing. *Textile Research Journal*, 70(9):758–762, 2000.

[24] Kai-Ling Mak, P Peng, and KFC Yiu. Fabric defect detection using morphological filters. *Image and Vision Computing*, 27(10):1585–1592, 2009.

[25] S. C. Graniteville. *Manual of standard fabric defects in the textile industry*. Graniteville Company, 1975.

[26] Mahmoud Abdel Aziz, Ali S Haggag, and Mohammed S Sayed. Fabric defect detection algorithm using morphological processing and DCT. In *2013 1st International Conference on Communications, Signal Processing, and their Applications (ICCSPA)*, pages 1–4. IEEE, 2013.

[27] H İbrahim Çelik, L Canan Dülger, Mehmet Topalbekiroğlu, et al. Fabric defect detection using linear filtering and morphological operations. *Indian Journal of Fibre & Textile Research (IJFTR)*, 39(3):254–259, 2014.

[28] Vikrant Tiwari and Gaurav Sharma. Automatic fabric fault detection using morphological operations on bit plane. *International Journal of Computer Science and Network Security (IJCSNS)*, 15(10):30, 2015.

[29] John Bollinger. *Bollinger on Bollinger bands*. McGraw Hill Professional, 2001.

[30] Henry YT Ngan and Grantham KH Pang. Novel method for patterned fabric inspection using Bollinger bands. *Optical Engineering*, 45(8):087202–087202, 2006.

[31] Henry YT Ngan and Grantham KH Pang. Robust defect detection in plain and twill fabric using directional Bollinger bands. *Optical Engineering*, 54(7):073106–073106, 2015.

[32] Michael Unser. Sum and difference histograms for texture classification. *IEEE Transactions on Pattern Analysis and Machine Intelligence*, (1):118–125, 1986.

[33] M Alper Selver, Vural Avşar, and Hakan Özdemir. Textural fabric defect detection using statistical texture transformations and gradient search. *The Journal of The Textile Institute*, 105(9):998–1007, 2014.

[34] Jie Zhang, Ruru Pan, Weidong Gao, and Dandan Zhu. Automatic inspection of yarn-dyed fabric density by mathematical statistics of sub-images. *The Journal of The Textile Institute*, 106(8):823–834, 2015.

[35] Bidyut Baran Chaudhuri and Nirupam Sarkar. Texture segmentation using fractal dimension. *IEEE Transactions on Pattern Analysis and Machine Intelligence*, 17(1):72–77, 1995.

[36] Aura Conci and Claudia Belmiro Proença. A fractal image analysis system for fabric inspection based on a box-counting method. *Computer Networks and ISDN Systems*, 30(20):1887–1895, 1998.

[37] Shih-Hsuan Chiu, Shen Chou, Jiun-Jian Liaw, and Che-Yen Wen. Textural defect segmentation using a Fourier-domain maximum likelihood estimation method. *Textile Research Journal*, 72(3):253–258, 2002.

[38] Hong-gang Bu, Jun Wang, and Xiu-bao Huang. Fabric defect detection based on multiple fractal features and support vector data description. *Engineering Applications of Artificial Intelligence*, 22(2):224–235, 2009.

[39] Madasu Hanmandlu, Dilip Choudhury, and Sujata Dash. Detection of defects in fabrics using topothesy fractal dimension features. *Signal, Image and Video Processing*, 9(7):1521–1530, 2015.

[40] Richard W Conners, Charles W Mcmillin, Kingyao Lin, and Ramon E Vasquez-Espinosa. Identifying and locating surface defects in wood:

Part of an automated lumber processing system. *IEEE Transactions on Pattern Analysis and Machine Intelligence*, (6):573–583, 1983.

[41] Jagdish Lal Raheja, Sunil Kumar, and Ankit Chaudhary. Fabric defect detection based on GLCM and Gabor filter: a comparison. *Optik-international Journal for Light and Electron Optics*, 124(23):6469–6474, 2013.

[42] Dandan Zhu, Ruru Pan, Weidong Gao, and Jie Zhang. Yarn-dyed fabric defect detection based on autocorrelation function and glcm. *Autex Research Journal*, 15(3):226–232, 2015.

[43] Dmitry Chetverikov. Pattern regularity as a visual key. *Image and Vision Computing*, 18(12):975–985, 2000.

[44] M Bennamoun and A Bodnarova. Automatic visual inspection and flaw detection in textile materials: Past, present and future. In *IEEE International Conference on Systems, Man, and Cybernetics, 1998.*, volume 5, pages 4340–4343. IEEE, 1998.

[45] Umer Farooq, Tim King, PH Gaskell, and N Kapur. Machine vision using image data feedback for fault detection in complex deformable webs. *Transactions of the Institute of Measurement and Control*, 26(2):119–137, 2004.

[46] Michael K Ng, Henry YT Ngan, Xiaoming Yuan, and Wenxing Zhang. Patterned fabric inspection and visualization by the method of image decomposition. *IEEE Transactions on Automation Science and Enginering*, 11:943–947, 2014.

[47] SH Hajimowlana, R Muscedere, GA Jullien, and JW Roberts. 1D autoregressive modeling for defect detection in web inspection systems. In *Midwest Symposium on Circuits and Systems, 1998. Proceedings*, pages 318–321. IEEE, 1998.

[48] Olivier Alata and Clarisse Ramananjarasoa. Unsupervised textured image segmentation using 2D quarter plane autoregressive model with four prediction supports. *Pattern Recognition Letters*, 26(8):1069–1081, 2005.

[49] Serhat Ozdemir and A Ercil. Markov random fields and karhunen-loève transforms for defect inspection of textile products. In *IEEE Conference on Emerging Technologies and Factory Automation, 1996. EFTA'96. Proceedings*, volume 2, pages 697–703. IEEE, 1996.

[50] Guang-Hua Hu, Guo-Hui Zhang, and Qing-Hui Wang. Automated defect detection in textured materials using wavelet-domain hidden markov models. *Optical Engineering*, 53(9):093107–093107, 2014.

[51] C Castellini, F Francini, G Longobardi, B Tiribilli, and P Sansoni. On-line textile quality control using optical Fourier transforms. *Optics and Lasers in Engineering*, 24(1):19–32, 1996.

[52] Du-Ming Tsai and Bo Hsiao. Automatic surface inspection using wavelet reconstruction. *Pattern Recognition*, 34(6):1285–1305, 2001.

[53] Adriana Bodnarova, Mohammed Bennamoun, and Shane J Latham. A constrained minimisation approach to optimise Gabor filters for detecting flaws in woven textiles. In *2000 IEEE International Conference on Acoustics, Speech, and Signal Processing, 2000. ICASSP'00. Proceedings*, volume 6, pages 3606–3609. IEEE, 2000.

[54] Rusen Meylani, Aysin Ertüzün, and Aytül Erçil. Texture defect detection using the adaptive two-dimensional lattice filter. In *International Conference on Image Processing, 1996. Proceedings*, pages 165–168, 1996.

[55] PeiFeng Zeng and T Hirata. On-loom fabric inspection using multi-scale differentiation filtering. In *37th IAS Annual Meeting, Conference*

Record of the Industry Applications Conference, 2002, volume 1, pages 320–326. IEEE, 2002.

[56] D-M Tsai and C-Y Hsieh. Automated surface inspection for directional textures. *Image and Vision Computing*, 18(1):49–62, 1999.

[57] Kyung-Jin Choi, Young-Hyun Lee, Jong-Woo Moon, Chong-Kug Park, and Fumio Harashima. Development of an automatic stencil inspection system using modified hough transform and fuzzy logic. *IEEE Transactions on Industrial Electronics*, 54(1):604–611, 2007.

[58] V Jayashree and Shaila Subbaraman. Identification of twill grey fabric defects using DC suppressed Fourier power spectrum sum features. *Textile Research Journal*, pages 1485–1497, 2012.

[59] Ajay Kumar and Grantham Pang. Identification of surface defects in textured materials using wavelet packets. In *Thirty-Sixth IAS Annual Meeting, Conference Record of the 2001 IEEE Industry Applications Conference, 2001*, volume 1, pages 247–251. IEEE, 2001.

[60] Du-Ming Tsai and Cheng-Huei Chiang. Automatic band selection for wavelet reconstruction in the application of defect detection. *Image and Vision Computing*, 21(5):413–431, 2003.

[61] Xuezhi Yang, Grantham Pang, and Nelson Yung. Discriminative training approaches to fabric defect classification based on wavelet transform. *Pattern Recognition*, 37(5):889–899, 2004.

[62] Zhijie Wen, Junjie Cao, Xiuping Liu, and Shihui Ying. Fabric defects detection using adaptive wavelets. *International Journal of Clothing Science and Technology*, 26(3):202–211, 2014.

[63] Shengqi Guan and Zhaoyuan Gao. Fabric defect image segmentation based on the visual attention mechanism of the wavelet domain. *Textile Research Journal*, 84(10):1018–1033, 2014.

[64] Anne M Treisman and Garry Gelade. A feature-integration theory of attention. *Cognitive Psychology*, 12(1):97–136, 1980.

[65] John G Daugman. Uncertainty relation for resolution in space, spatial frequency, and orientation optimized by two-dimensional visual cortical filters. *JOSA A*, 2(7):1160–1169, 1985.

[66] Rajiv Mehrotra, Kameswara Rao Namuduri, and Nagarajan Ranganathan. Gabor filter-based edge detection. *Pattern Recognition*, 25(12):1479–1494, 1992.

[67] Linlin Shen and Songhao Zheng. Hyperspectral face recognition using 3D Gabor wavelets. In *21st International Conference on Pattern Recognition (ICPR), 2012*, pages 1574–1577. IEEE, 2012.

[68] David A Clausi and M Ed Jernigan. Designing Gabor filters for optimal texture separability. *Pattern Recognition*, 33(11):1835–1849, 2000.

[69] Wei-Yu Han and Jen-Chun Lee. Palm vein recognition using adaptive Gabor filter. *Expert Systems with Applications*, 39(18):13225–13234, 2012.

[70] Linlin Shen, Ziyi Dai, Sen Jia, Meng Yang, Zhihui Lai, and Shiqi Yu. Band selection for Gabor feature based hyperspectral palmprint recognition. In *2015 International Conference on Biometrics (ICB)*, pages 416–421. IEEE, 2015.

[71] Philippe Vautrot, Noël Bonnet, and Michel Herbin. Comparative study of different spatial/spatial-frequency methods (Gabor filters, wavelets, wavelets packets) for texture segmentation/classification. In *International Conference on Image Processing, 1996. Proceedings*, volume 3, pages 145–148. IEEE, 1996.

[72] Weitao Li, Kezhi Mao, Hong Zhang, and Tianyou Chai. Selection of Gabor filters for improved texture feature extraction. In *2010 IEEE*

International Conference on Image Processing, pages 361–364. IEEE, 2010.

[73] Lucia Bissi, Giuseppe Baruffa, Pisana Placidi, Elisa Ricci, Andrea Scorzoni, and Paolo Valigi. Automated defect detection in uniform and structured fabrics using Gabor filters and PCA. *Journal of Visual Communication and Image Representation*, 24(7):838–845, 2013.

[74] Deutsche Forschungsgemeinschaft Germany. Tilda textile texture-database. `http://lmb.informatik.uni-freiburg.de/resources/datasets/tilda.en.html`. Version 1.0, 1996.

[75] D-M Tsai and C-P Lin. Fast defect detection in textured surfaces using 1D Gabor filters. *The International Journal of Advanced Manufacturing Technology*, 20(9):664–675, 2002.

[76] Kai Ling Mak and P Peng. An automated inspection system for textile fabrics based on Gabor filters. *Robotics and Computer-Integrated Manufacturing*, 24(3):359–369, 2008.

[77] Kai-Ling Mak, Pai Peng, and Ka-Fai Cedric Yiu. Fabric defect detection using multi-level tuned-matched Gabor filters. *Journal of Industrial and management optimization*, 2012.

[78] Cui Mao, Arunkumar Gururajan, Hamed Sari-Sarraf, and Eric Hequet. Machine vision scheme for stain-release evaluation using gabor filters with optimized coefficients. *Machine Vision and Applications*, 23(2):349–361, 2012.

[79] Guang-Hua Hu. Optimal ring Gabor filter design for texture defect detection using a simulated annealing algorithm. In *2014 International Conference on Information Science, Electronics and Electrical Engineering (ISEEE)*, volume 2, pages 860–864. IEEE, 2014.

[80] D-M Tsa and S-K Wu. Automated surface inspection using Gabor filters. *The International Journal of Advanced Manufacturing Technology*, 16(7):474–482, 2000.

[81] Chang-Chiun Huang and I-Chun Chen. Neural-fuzzy classification for fabric defects. *Textile Research Journal*, 71(3):220–224, 2001.

[82] Ajay Kumar. Neural network based detection of local textile defects. *Pattern Recognition*, 36(7):1645–1659, 2003.

[83] AS Tolba. Neighborhood-preserving cross correlation for automated visual inspection of fine-structured textile fabrics. *Textile Research Journal*, 81(19):2033–2042, 2011.

[84] Tao Qu, Lian Zou, Qinglin Zhang, Xi Chen, and Cien Fan. Defect detection on the fabric with complex texture via dual-scale over-complete dictionary. *The Journal of The Textile Institute*, 107(6):743–756, 2016.

[85] Jian Zhou and Jun Wang. Unsupervised fabric defect segmentation using local patch approximation. *The Journal of The Textile Institute*, 107(6):800–809, 2016.

[86] Liping Zhao and James O Coplien. Symmetry in class and type hierarchy. In *Proceedings of the Fortieth International Conference on Tools Pacific: Objects for Internet, Mobile and Embedded Applications*, pages 181–189. Australian Computer Society, Inc., 2002.

[87] Hagit Zabrodsky, Shmuel Peleg, and David Avnir. Symmetry as a continuous feature. *IEEE Transactions on Pattern Analysis and Machine Intelligence*, 17(12):1154–1166, 1995.

[88] Yanxi Liu, Robert T Collins, and Yanghai Tsin. A computational model for periodic pattern perception based on frieze and wallpaper groups.

IEEE Transactions on Mattern Analysis and Machine Intelligence, 26(3):354–371, 2004.

[89] Henry YT Ngan, Grantham KH Pang, and Nelson HC Yung. Performance evaluation for motif-based patterned texture defect detection. *IEEE Transactions on Automation Science and Engineering*, 7(1):58–72, 2010.

[90] Henry YT Ngan, Grantham KH Pang, SP Yung, and Michael K Ng. Wavelet based methods on patterned fabric defect detection. *Pattern Recognition*, 38(4):559–576, 2005.

[91] Stephane G Mallat. A theory for multiresolution signal decomposition: the wavelet representation. *IEEE Transactions on Pattern Analysis and Machine Intelligence*, 11(7):674–693, 1989.

[92] Ma Li and Richard C Staunton. Optimum Gabor filter design and local binary patterns for texture segmentation. *Pattern Recognition Letters*, 29(5):664–672, 2008.

[93] Junfeng Jing, Huanhuan Zhang, Jing Wang, Pengfei Li, and Jianyuan Jia. Fabric defect detection using Gabor filters and defect classification based on LBP and Tamura method. *Journal of The Textile Institute*, 104(1):18–27, 2013.

[94] Dennis Gabor. Theory of communication. part 1: The analysis of information. *Journal of the Institution of Electrical Engineers-Part III: Radio and Communication Engineering*, 93(26):429–441, 1946.

[95] David P Casasent and John S Smokelin. Neural net design of macro Gabor wavelet filters for distortion-invariant object detection in clutter. *Optical Engineering*, 33(7):2264–2271, 1994.

[96] Bangalore S Manjunath and Wei-Ying Ma. Texture features for

browsing and retrieval of image data. *IEEE Transactions on Pattern Analysis and Machine Intelligence*, 18(8):837–842, 1996.

[97] Bruno A Olshausen et al. Emergence of simple-cell receptive field properties by learning a sparse code for natural images. *Nature*, 381(6583):607–609, 1996.

[98] Julien Mairal, Michael Elad, and Guillermo Sapiro. Sparse representation for color image restoration. *IEEE Transactions on Image Processing*, 17(1):53–69, 2008.

[99] John Wright, Allen Y Yang, Arvind Ganesh, S Shankar Sastry, and Yi Ma. Robust face recognition via sparse representation. *IEEE Transactions on Pattern Analysis and Machine Intelligence*, 31(2):210–227, 2009.

[100] Chia-Po Wei, Yu-Wei Chao, Yi-Ren Yeh, and Yu-Chiang Frank Wang. Locality-sensitive dictionary learning for sparse representation based classification. *Pattern Recognition*, 46(5):1277–1287, 2013.

[101] Joel A Tropp and Stephen J Wright. Computational methods for sparse solution of linear inverse problems. *Proceedings of the IEEE*, 98(6):948–958, 2010.

[102] Stéphane G Mallat and Zhifeng Zhang. Matching pursuits with time-frequency dictionaries. *IEEE Transactions on Signal Processing*, 41(12):3397–3415, 1993.

[103] Yagyensh Chandra Pati, Ramin Rezaiifar, and PS Krishnaprasad. Orthogonal matching pursuit: Recursive function approximation with applications to wavelet decomposition. In *1993 Conference Record of The Twenty-Seventh Asilomar Conference on Signals, Systems and Computers, 1993.*, pages 40–44. IEEE, 1993.

[104] Scott Shaobing Chen, David L Donoho, and Michael A Saunders. Atomic decomposition by basis pursuit. *SIAM Review*, 43(1):129–159, 2001.

[105] Michal Aharon, Michael Elad, and Alfred Bruckstein. K-SVD: An algorithm for designing overcomplete dictionaries for sparse representation. *IEEE Transactions on Signal Processing*, 54(11):4311–4322, 2006.

[106] Ron Rubinstein, Michael Zibulevsky, and Michael Elad. Double sparsity: Learning sparse dictionaries for sparse signal approximation. *IEEE Transactions on Signal Processing*, 58(3):1553–1564, 2010.

[107] Kjersti Engan, Sven Ole Aase, and J Hakon Husoy. Method of optimal directions for frame design. In *1999 IEEE International Conference on Acoustics, Speech, and Signal Processing, 1999. Proceedings*, volume 5, pages 2443–2446. IEEE, 1999.

[108] Ajay Kumar and Grantham Pang. Fabric defect segmentation using multichannel blob detectors. *Optical Engineering*, 39(12):3176–3190, 2000.

[109] Institut für Textilmaschinenbau und Textilindustrieder ETH. *Catalogue of types of fabric defects in grey goods*. Schlieren, Schweiz: International Textile Service, Switzerland, 2 edition, 1989.

[110] Francesco Bianconi and Antonio Fernández. Evaluation of the effects of Gabor filter parameters on texture classification. *Pattern Recognition*, 40(12):3325–3335, 2007.

[111] Yong Wang, Zixing Cai, and Qingfu Zhang. Differential evolution with composite trial vector generation strategies and control parameters. *IEEE Transactions on Evolutionary Computation*, 15(1):55–66, 2011.

[112] Michael Elad and Michal Aharon. Image denoising via sparse and redundant representations over learned dictionaries. *IEEE Transactions on Image Processing*, 15(12):3736–3745, 2006.

[113] Marius Lysaker and Xue-Cheng Tai. Iterative image restoration combining total variation minimization and a second-order functional. *International Journal of Computer Vision*, 66(1):5–18, 2006.

[114] Julien Mairal, Francis Bach, Jean Ponce, Guillermo Sapiro, and Andrew Zisserman. Non-local sparse models for image restoration. In *2009 IEEE 12th International Conference on Computer Vision*, pages 2272–2279. IEEE, 2009.

[115] Weisheng Dong, Lei Zhang, Guangming Shi, and Xiaolin Wu. Image deblurring and super-resolution by adaptive sparse domain selection and adaptive regularization. *IEEE Transactions on Image Processing*, 20(7):1838–1857, 2011.

[116] Weisheng Dong, Lei Zhang, Guangming Shi, and Xin Li. Nonlocally centralized sparse representation for image restoration. *IEEE Transactions on Image Processing*, 22(4):1620–1630, 2013.

[117] Jielin Jiang, Jian Yang, Yan Cui, Wai Keung Wong, and Zhihui Lai. Sparse nonlocal priors based two-phase approach for mixed noise removal. *Signal Processing*, 116:101–111, 2015.